Stochastic Finite Element Based Reliability Analysis of Steel Fiber Reinforced Concrete (SFRC) Corbels

University of Gaziantep

Ph.D. Thesis

in

Civil Engineering

Supervisor

Prof. Dr. Abdulkadir ÇEVİK

By

Mehmet Eren GÜLŞAN

September 2015

T.C.
REPUBLIC OF TURKEY
UNIVERSITY OF GAZİANTEP
GRADUATE SCHOOL OF NATURAL & APPLIED SCIENCES
CIVIL ENGINEERING DEPARTMENT

Name of the thesis:Stochastic Finite Element Based Reliability Analysis of Steel Fiber Reinforced Concrete (SFRC) Corbels

Name of the student: Mehmet Eren GÜLŞAN

Exam date: September 10, 2015

Approval of the Graduate School of Natural and Applied Sciences

Prof. Dr. Metin BEDİR
Director

I certify that this thesis satisfies all the requirements as a thesis for the degree of Doctor of Philosophy

Prof. Dr. Mustafa GÜNAL
Head of Department

This is to certify that we have read this thesis and that in our consensus/majority opinion it is fully adequate, in scope and quality, as a thesis for the degree of Doctor of Philosophy.

Prof. Dr. Abdulkadir ÇEVİK
Supervisor

Examining Committee Members:	Signature
Prof. Dr. İbrahim Halil GÜZELBEY	………………….
Prof. Dr. Mustafa ÖZAKÇA	………………….
Prof. Dr. Abdulkadir ÇEVİK	………………….
Assoc. Prof. Dr. Mahmut BİLGEHAN	………………….
Assoc. Prof. Dr. Mehmet Cemal GENEŞ	………………….

I declare that all information in this document has been obtained and presented in accordance with academic rules and ethical conduct. I also declare that, as required by these rules and conduct, I have fully cited and referenced all material and results that are not original to this work.

Mehmet Eren GÜLŞAN

ABSTRACT

STOCHASTIC FINITE ELEMENT BASED RELIABILITY ANALYSIS OF STEEL FIBER REINFORCED CONCRETE (SFRC) CORBELS

GULSAN, Mehmet Eren
Ph.D. in Civil Engineering
Supervisor: Prof. Dr. Abdulkadir CEVIK
September 2015
145 pages

Corbels are significant structural elements in construction sector and it is critical connection region between beams and columns or walls, especially in industrial buildings. Therefore its mechanical behavior directly influences the safety of the related structure. Use of steel fiber as secondary reinforcement in reinforced concrete corbels is a good option to achieve ductility without any loss in load carrying capacity. This thesis investigates mechanical behavior of steel fiber reinforced concrete (SFRC) corbels. A detailed research was carried out on SFRC corbels. Experimental, Finite Element (FE), Stochastic and Reliability analyses of SFRC corbels were carried out for the thesis studies. As a result of experimental and finite element analyses, mechanical outputs of SFRC corbels were interpreted and rules were proposed for the prediction of failure mode and crack pattern of SFRC corbels. Moreover, suitable probability distribution function, resistance factor and statistical parameters (bias factor and coefficient of variation value) were proposed as a result of stochastic and reliability analyses. A numerical formulation was proposed for the prediction of load carrying capacity of SFRC corbels in the content of thesis studies. Numerical model exhibit good fit with the results from the literature and parametric studies implemented on the model shows that it can be used for the ultimate load capacity of SFRC corbels safely.

Keywords: Steel Fiber Reinforced Concrete, Corbels, Load Carrying Capacity, Ductility, Uncertainty, Stochastic Analysis, Reliability Analysis.

ÖZET

ÇELİK LİF KATKILI BETONARME KISA KONSOLLARIN STOKASTİK SONLU ELEMANLAR YÖNTEMİNE DAYALI GÜVENİLİRLİK ANALİZİ

GÜLŞAN, Mehmet Eren
Doktora Tezi, İnşaat Mühendisliği
Tez Yöneticisi: Prof. Dr. Abdulkadir ÇEVIK
Eylül 2015
145 sayfa

Kısa konsollar yapı sektöründeki önemli yapı elemanlarındandır ve özellikle endüstriyel yapılarda kirişler ve kolonlar ya da duvarlar arasındaki kritik bağlantı bölgesini oluşturmaktadır. Bundan dolayı kısa konsolun mekanik davranışı bulunduğu yapının güvenliğini doğrudan etkilemektedir. Çelik liflerin betonarme kısa konsollarda ikincil donatı olarak kullanımı yük taşıma kapasitesi kaybı olmadan sünekliği sağlaması açısından güzel bir seçenektir. Bu tez çelik lif katkılı betonarme kısa konsolların mekanik davranışını araştırmaktadır. Bu kapsamda, kısa konsollar için detaylı bir araştırma yürütülmüştür. Tez çalışmaları için çelik lif katkılı kısa konsolların Deneysel, Sonlu Elemanlar (SE), Stokastik ve Güvenilirlik analizleri gerçekleştirilmiştir. Deneysel ve sonlu elemanlar analizleri sonucunda çıkan sonuçlar irdelenmiş ve çelik katkılı kısa konsolların kırılma modları ve çatlak oluşum türlerinin tahmini konusunda kurallar önerilmiştir. Ayrıca, stokastik ve güvenilirlik analizleri sonucunda çelik katkılı kısa konsollar için uygun olasılık dağılımı fonksiyonu, dayanım faktörü ve istatistiksel parametreler (hata faktörü ve değişkenlik katsayısı) önerilmiştir. Tez çalışmaları kapsamında, çelik lif katkılı kısa konsolların yük taşıma kapasitesinin hesabı için sayısal bir formül önerilmiştir. Önerilen model literatürdeki ilgili sonuçlarla iyi bir uyum göstermektedir ve model üzerinde gerçekleştirilen parametrik çalışma modelin çelik lif katkılı kısa konsolların yük taşıma kapasitesi tahmininde güvenli bir şekilde kullanılabileceğini göstermektedir.

Anahtar Kelimeler: Çelik Lif Katkılı Beton, Kısa Konsollar, Yük Taşıma Kapasitesi, Süneklik, Belirsizlik, Stokastik Analiz, Güvenilirlik Analizi.

ACKNOWLEDGEMENTS

I would like to express my special gratitudes to my supervisor Prof. Dr. Abdulkadir ÇEVİK. I would like to thank him for his significant guidances and helps to develop me as a both researcher and also lecturer scientist.

I would also like to thank my committee member, Prof. Dr. İbrahim H. Güzelbey, Prof. Dr. Mustafa ÖZAKÇA for their important comments and suggestions.

I would also like to express sincere thanks to all lecturers of Mechanical Division of Civil Engineering Department of Gaziantep University, Dr. Mustafa ÖZAKÇA, Dr. Abdulkadir ÇEVİK, Dr. Nildem TAYŞİ, Dr. Tolga GÖĞÜŞ and Dr. Talha EKMEKYAPAR for their helps and understandings during my thesis works.

I would also like to thank all people who helped me during my experimental works. I might not complete my experimental works without their devoted support.

Sincere thanks to Gaziantep University Scientific Research Projects Unit, some parts of this dissertation was supported by the support of them.

A special thanks to my family. I am very grateful to them for their understandings, supports, patience and encouragements during my education life.

TABLE OF CONTENTS

LIST OF FIGURES

Page

LIST OF TABLES

Page

LIST OF SYMBOLS

a	Shear span of corbels
A_s	Cross sectional area of main reinforcement
b	Width of corbels
d	Effective depth for corbels
h	Height of corbels
f_c	Cylindrical compressive strength of concrete
f_{ct}	Splitting tensile strength of concrete
f_{cu}	Cubic compressive strength of concrete
f_y	Yield strength of main reinforcement
v_f %	Steel fiber percentage amount
ε	Strain in corresponding direction
σ	Stress in corresponding direction
E_c	Modulus of elasticity of concrete
G_f	Fracture energy of concrete
D	Dead load
L	Live load
R	Resistance of a structural element

S External load on a structural element

T Total load

V Load carrying capacities of corbels

ρ Reinforcement ratio

ϕ Resistance factor

s Standard deviation

λ Bias factor

β Reliability index

μ Arithmetic mean

CHAPTER 1

INTRODUCTION

1.1 General

The use of precast reinforced concrete elements for the construction of buildings and bridges has become more common during the last decades. Corbels are an example of such structural elements, and they are used to transfer loads from beams or slabs to columns or walls. Brackets or corbels either hang out from a column or a structural wall or is the overhanging portion of a beam (Fig. 1.1). The shear span ratio of the corbel is equal to or less than 1 ($a/d \leq 1$). Corbels can be provided to support rails, which transmit heavy loads from moving cranes in heavy – duty factory workshops. Corbels are also constructed at the cantilevered end of girders in double cantilever balanced reinforced concrete bridges to support the end spans of the bridge. There may be between one and four corbels at one position along the height of a column, depending on the design and location of the column in the building.

Figure 1.1 Typical Corbels Constructed in Industrial Building (Waschbeton, 2013)

1.2 Steel Fiber Reinforced Concrete (SFRC)

Steel fiber reinforced concrete (SFRC) is concrete made of hydraulic cement containing fine or fine and coarse aggregate and discontinuous discrete steel fibers (Fig. 1.2). In tension, SFRC fails only after the steel fiber breaks or is pulled out of the cement matrix shows a typical fractured surface of SFRC. Steel fibers intended for reinforcing concrete are defined as short, discrete lengths of steel having an aspect ratio (ratio of length to diameter) from about 20 to 100, with any of several cross-sections, and that are sufficiently small to be randomly dispersed in an unhardened concrete mixture using usual mixing procedures (ACI 544.1R-96 Report, 2002).

Figure 1.2 Hooked End Steel Fibers (Bekaert, 2014)

The addition of steel fibers provides a number of significant behavioral enhancements to concrete. In compression, steel fibers do not significantly affect the ascending curve of the compressive stress-strain response, but they cause the descending post-peak response curve to decline in a shallower fashion than the curve of plain concrete, resulting in an increased ductility and toughness (Fanella and Naaman, 1985). The peak compressive strength is not significantly affected; experiments have observed a maximum strength gain of only 15% (Fanella and Naaman, 1985; ACI 544.1R-96 Report, 2002; Thomas and Ramaswamy, 2007). However, the peak strain increases perceptibly with the addition of steel fibers.

The addition of steel fibers has a much more noticeable effect on the tensile behavior of the composite. In typical fiber volume contents the material exhibits strain-softening behavior; however, the degradation in load-carrying capacity is slower than that of plain concrete. This results in the composite having greater ductility and energy absorption capabilities than plain concrete. In addition, because the fibers bridge the cracks in the composite and aid in the transfer of forces across the cracks, crack widths are less than those of plain concrete. If reinforcing bars are present, multiple cracks can form, even for a strain-softening material. There will be more cracks at a shorter spacing and smaller widths than the equivalent structure constructed from plain concrete (Deluce, 2011).

1.3 Research Significance

Use of steel fiber in reinforced concrete corbels provides considerable advantages. Previous studies related with corbels have concluded that reinforced concrete corbels, which include only steel fibers as secondary reinforcement, have almost the same load carrying capacity with ones in which horizontal stirrups are used against shear failure. Use of steel fiber facilitates the fabrication of corbels because of easier placement of it as compared to placement of horizontal stirrups. It is also more economical as compared to traditional corbel production since the workmanship and material costs about reinforcement preparation were reduced dramatically. Steel fibers allow corbels to experience large deflections after achieving ultimate load without a dramatic loss in load carrying capacity or demonstrating a sudden and brittle failure (Fattuhi and Hughes, 1989b).

Significant advantages of steel fiber reinforced concrete corbels require a detailed information and research as there is no sufficient information about design rule and mechanical behavior of SFRC corbels. Moreover, the orientation of steel fiber affects the mechanical properties of concrete significantly and this leads to uncertainties in various mechanical properties of SFRC. Therefore, detailed research on steel fiber reinforced concrete corbels is required to overcome the lack in this field.

1.4 Objectives and Aim of the Study

Use of steel fiber reinforced concrete in various types of structural elements has been widely studied so far. However, use of them in construction sector has not become popular, yet, particularly in Turkey, because there is no sufficient information about design consideration of SFRC structural elements in design codes.

Corbels are important structural elements and used frequently in construction of precast and industrial structures. Since corbels are not huge structural elements, use of steel fibers instead of horizontal stirrups provides considerable advantages for easier production and successful concreting process. It can also provide mechanical advantages as ductility to the corbel. Therefore, use of SFRC for the production of corbels is considered and detailed research on SFRC corbels was aimed in this thesis. Objectives of the dissertation can be listed as follows:

- To provide finite element modeling of steel fiber reinforced concrete corbels and to make parametric studies on failure modes and crack pattern of SFRC corbels via finite element method.

- To propose predictions for failure type of SFRC corbels.

- To investigate the effect of several variables (tensile strength, steel fiber percentage, etc.) on behavior and capacity of SFRC corbels.

- To clarify the uncertainties in the load carrying capacity of SFRC corbels and to model the uncertainty in SFRC corbels via stochastic and reliability analyses.

- To develop a general model for the ultimate load capacity of SFRC corbels valid for all range of concrete strength classes (small, medium, high).

1.5 Layout of the Thesis

The thesis is arranged in the order of experimental analysis, finite element (FE) analysis, stochastic analysis and reliability analysis for steel fiber reinforced concrete (SFRC) corbels.

In Chapter 2, literature review for SFRC corbels was presented. Earlier investigations about SFRC corbels were specified. Force mechanism and encountered failure modes were also described in this chapter.

In Chapter 3, experimental research carried out on SFRC corbels was denoted. Experimental results were interpreted and effect of several parameters on mechanical behavior of SFRC corbels was investigated.

Finite element (FE) analyses of SFRC corbels were described in Chapter 4 of the dissertation. Analysis results were compared with corresponding experimental results. Furthermore, rules were expressed for the prediction of failure modes of SFRC corbels at the end of this chapter.

In Chapter 5, reliability and stochastic analysis of SFRC corbels were mentioned. Uncertainties about load carrying capacities of SFRC corbels are explained. Several statistical and design parameters were proposed for ultimate load capacity of them.

A numerical formulation was proposed for load carrying capacity of SFRC corbels. Modeling process was detailed in Chapter 6. Generalization capability of proposed model was also investigated in the chapter by outputs of parametric studies.

Conclusions resulted from the thesis studies were stated in Chapter 7. Studies implemented during the thesis were summarized in this chapter. Recommended future works can be found at the end of the chapter.

CHAPTER 2

LITERATURE SURVEY

2.1 Introduction

Although the structural behavior of FRC elements depends on the mechanical properties of the composite, fibers can be considered as reinforcement spread out all over the depth of a member. The addition of steel fibers to the concrete allows for a substantial increase of the shear strength. The effectiveness of fiber reinforcement to increase shear resistance, is dependent on several factors, including matrix properties, fiber properties (material properties, aspect ratio, and shape), fiber content, and bond stress versus slip response of fibers.

In the literature, it is shown that FRC can substitute, at least partially, transverse reinforcement. For this reason, some authors emphasize the usefulness of fibers for industrial applications. Minimum transverse reinforcement requirement can be met by using fibers in sufficient amount and with minimum performance in terms of toughness. Thus, fibers can effectively replace the minimum amount of transverse reinforcement satisfying the minimum shear reinforcement criteria in structural design codes (Asensio, 2012).

The addition of steel fibers is known to improve the apparent bond between steel and concrete, and the compressive, tensile, flexural, impact, and toughness properties of the concrete. Also, during the testing of conventionally reinforced or pre-stressed concrete beams, it was found that the replacement of stirrups with steel fibers, or the addition of steel fibers, provided effective reinforcement against shear failure. Results from limited tests reported recently have indicated that concrete corbels reinforced with main tension bars and steel fibers were of comparable strength to corbels reinforced with main tension bars and stirrups (Fattuhi, 1987).

2.2 Previous Studies about Steel Fiber Reinforced Concrete (SFRC) Corbels

Several experimental studies have been carried out about the analysis of steel fiber reinforced corbels so far. One of these studies was implemented by Fattuhi (1987). In his study, Fattuhi aimed to determine the extent of improvement in the shear properties of concrete corbels reinforced with steel fibers and subjected to vertical loading only. The efficiency of the steel fibers was also examined when the corbel's shear span to depth ratio and fiber content were varied. It was found from the investigation that the first crack and ultimate strength and toughness of concrete corbels were considerably improved by the addition of steel fibers and the efficiency of the steel fibers at ultimate loads increased with a decrease in the shear span to depth ratio.

Hughes and Fattuhi (1989a) investigated the performance of steel and polypropylene fibers on mechanical response of reinforced concrete corbels and they found that steel and polypropylene fibers increase the shear strength and ductility of reinforced concrete corbels.

Ductility of reinforced concrete corbels containing either steel fibers or stirrups were researched by Fattuhi and Hughes (1989b). They found that the addition of fibers or stirrups improved the load carrying capacity and ductility of corbels. However, corbels reinforced with steel fibers failed in the most gradual and ductile manner.

In another study related with SFRC corbels, Fattuhi and Hughes (1989c) investigated the transformation of the mode of failure from being sudden and catastrophic to a more gradual and ductile mode. Earlier results showed that when an adequate volume of steel fibers was added to concrete, an almost elastic-plastic behavior was recorded, and the mode of failure changed from being diagonal splitting to flexure. Therefore, the purpose of the study was to provide further information on the safety aspect and to investigate the strength and ductility of corbels reinforced with different volumes of main bars and tested at different shear span to depth ratios. As result of the investigation, it was confirmed that the maximum strength and ductility of reinforced concrete corbels are improved considerably by the addition of steel fibers and showed that the improvement in ductility depends on the volume of main bars and the shear span to depth ratio.

Reinforced concrete corbels were produced and experimented also by Abdul-Wahab (1989). He compared his experimental results with proposed formulations about load carrying capacity of SFRC corbels and he extracted the restrictions and insufficiencies of each considered formula of SFRC corbels.

Column load effect on SFRC corbels was investigated by Fattuhi (1990a). The results of his studies showed that loading the column segment of the specimen or one side corbel did not appear to have any significant effect on the load carrying capacity of the failed (the other side) corbel. However, in general, the presence of column load delayed the occurrence of the early (first) crack.

An experimental study was carried out by Fattuhi (1990b) to determine the most important parameters which influence the strength of SFRC corbels and to find a more general equation for the ultimate load capacity of the corbels. His study provided additional data useful in the development of more general design criteria for determining the strength of fiber reinforced concrete corbels subjected to vertical loading only.

Moreover, in another comprehensive study, Fattuhi (1994a) investigated the flexural strength of SFRC corbels where flexural and truss models were used in an attempt to predict the load carrying capacities of corbels failing in flexure. It was extracted from the experiments that it is possible to change the mode of failure from being diagonal splitting or shear to flexure. However, this change in mode of failure depends on the volumes of main bars and fibers, and on the shear span to depth ratio. Also, the size of crack width in corbels tends to vary inversely with the volume of steel fibers, under a specific applied load.

Ultimate load investigations of SFRC corbels for the geometrical configuration different from his previous studies (trapezoidal corbel configuration) were investigated by Fattuhi (1994b). Experimental studies showed that the addition of steel fibers improved the strength and ductility of corbels. On the other hand, there was no apparent effect of fiber length to corbel depth ratio on fiber efficiency, and consequently on strength of corbels.

Fattuhi (1994c) carried out experimental studies on high strength reinforced concrete corbels reinforced with main bars and/or steel fibers, monofilament polypropylene fibers, plastic meshes. He observed the improvements in the load carrying capacity and ductility of corbels.

Kumar (2004) proposed an analytical model to estimate the shear strength of steel fiber reinforced concrete corbels without shear reinforcement under vertical loads.

Flexural behavior of reinforced concrete corbels containing steel fibers or wrapped with FRP sheets were studied by Campione et al. (2005). They carried out some experiments about SFRC corbels and proposed an analytical expression to estimate the bearing capacity of corbels.

Experiments were investigated by Campione et al. (2007) to investigate the flexural behavior of fibrous reinforced corbels and to propose simple analytical expressions to determine their bearing capacity, at the same time taking into account the shear contribution due to steel reinforcements and fibers.

Ridha (2008) carried out finite element analyses of high strength steel fiber reinforced concrete trapezoidal corbels. He used the three dimensional 20-node brick elements and specific material models proposed in the literature to model high strength corbels. He compared the finite element results with experimental studies implemented by Muhammad (1998) and obtained good agreement with the load-displacement behavior of the corresponding corbels.

A strut and tie model was proposed to determine the flexural response of steel fiber reinforced concrete corbels by Campione (2009a). His model was suitable for the determination of loads, and corresponding displacements, associated with the first cracking, yielding of main reinforcement and failure of the concrete strut.

Campione (2009b) proposed an analytical model to obtain load-deflection curves of steel fiber reinforced concrete corbels under the combined effect of vertical and horizontal loads by taking into account the concrete class (normal or high strength), steel fiber percentage and amount of main reinforcement and horizontal stirrups. He validated his model by the comparison of experimental studies had been resulted before and outputs of the model. He also compared the model results with finite element modeling results.

Yang et al. (2009) investigated the mechanical response of high strength steel fiber reinforced concrete corbels by the use of different amount of fibers and two anchorage types (welding to transverse bar and headed). They proved that usage of steel fibers improve important mechanical properties (load carrying capacity, stiffness, ductility and crack width) of high strength corbels. They also proved that headed bars anchorage type gives better results about load carrying capacities and ductility of high strength SFRC corbels as compared to welding to transverse bar anchorage type. A similar study on normal strength concrete was also carried out by Alaamer (2004).

Kumar and Barai (2010) proposed artificial neural network (ANN) based model for the prediction of steel fiber reinforced concrete corbels without stirrups.

Influence of steel fibers and headed bars on the serviceability of high strength concrete corbels was investigated with experiments on the trapezoidal shaped corbels by Yang et al. (2012). Abdel Hafez et al. (2012) worked the shear strength of high strength steel fiber reinforced concrete corbels. They produced 17 corbels by altering various parameters that are important for load carrying capacity of corbels and extracted the most important factors that affect the shear behavior of high strength SFRC corbels. They also compared the load carrying capacities resulted from their experiments with the proposed models on load carrying capacity of corbels. According to their studies it was found that the model proposed by Campione et al. (2007) gives the most appropriate values for load carrying capacities of high strength SFRC corbels.

Haido (2012) searched the performance of trapezoidal steel fiber reinforced concrete corbels by the development of nine-noded Lagrangian elements and the proposed new expression for nonlinear material behavior of steel fiber reinforced concrete.

2.3 Developed Forces in a Typical Corbel

The resistance mechanism in a corbel can be shown by a force polygon, which consists of T (tension tie), C (compressive strut) and P (applied force), (Figure 2.1).

The tensile force “T” should be taken care of by the reinforcement placed near the top face of the corbel. The magnitude of “T” depends on the inclination of the compression strut. Due to very small a/d ratio, the force P is directly transferred to the support by the compression support C. Therefore, in corbels the tension force “T” at the top remains almost constant along the shear span “a”. This means that the top reinforcement taking care of “T” should be anchored properly, beyond the face of the column and beyond the point of load application (Ersoy et al., 2006).

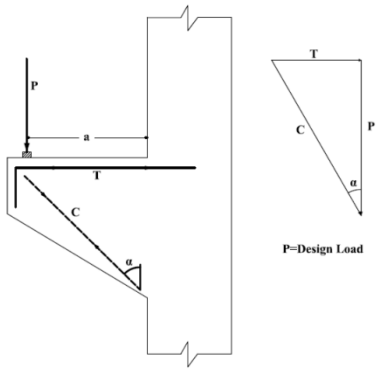

Figure 2.1 Force Analysis in a Typical Corbel

2.4 Failure Modes in a Typical Corbel

Three types of failure modes are mostly encountered in reinforced concrete (RC) and steel fiber reinforced concrete (SFRC) corbels. These failure modes can be listed as; flexural, shear (diagonal and constrained) and, diagonal splitting failure modes.

Diagonal splitting failure mode is generally observed in reinforced concrete corbels in which the main reinforcement does not reach to yielding point yet. This type of failure is very sudden and brittle and can cause hazardous results. This type of failure is shown in Fig. 2.2.

Flexural crack mode can appear in both reinforced concrete and steel fiber reinforced concrete corbels. In flexural mode main reinforcement yields before concrete fails. Since concrete is weak in tension, cracks form near the column-beam joint. The behavior in this failure mode is ductile. Therefore, sudden failure is prevented in this failure mode. (Fig. 2.3).

In shear failure mode, diagonal cracks are generally formed near the support region. However, the corbel is not divided into two parts as in the case of diagonal splitting failure mode (Fig. 2.4). This failure mode is not as ductile as flexural mode and is not as sudden and brittle as diagonal splitting mode. Its damage depends on the compressive strength of concrete, reinforcement ratio and steel fiber amount.

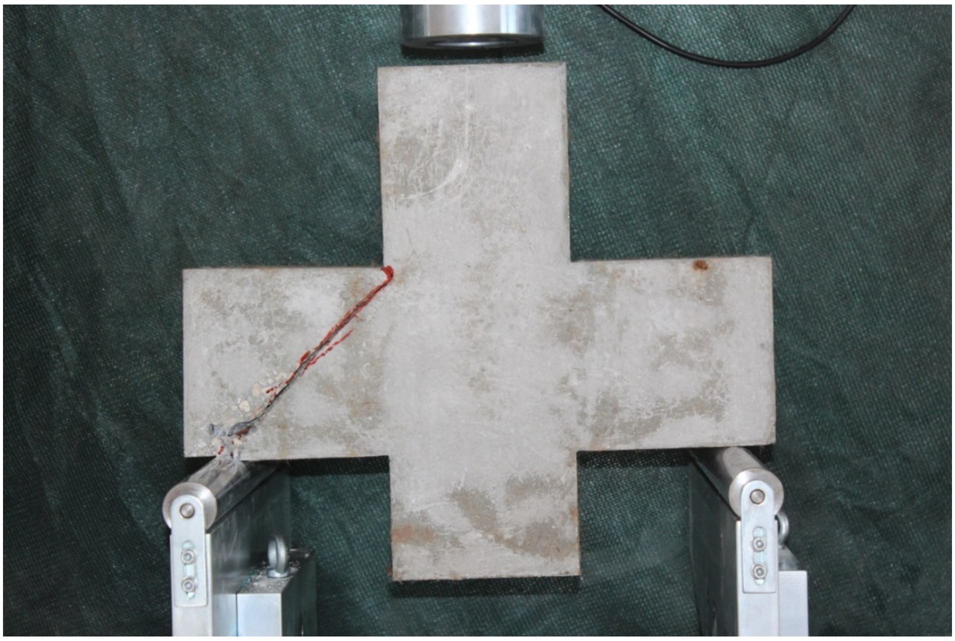

Figure 2.2 Diagonal Splitting Failure Mode

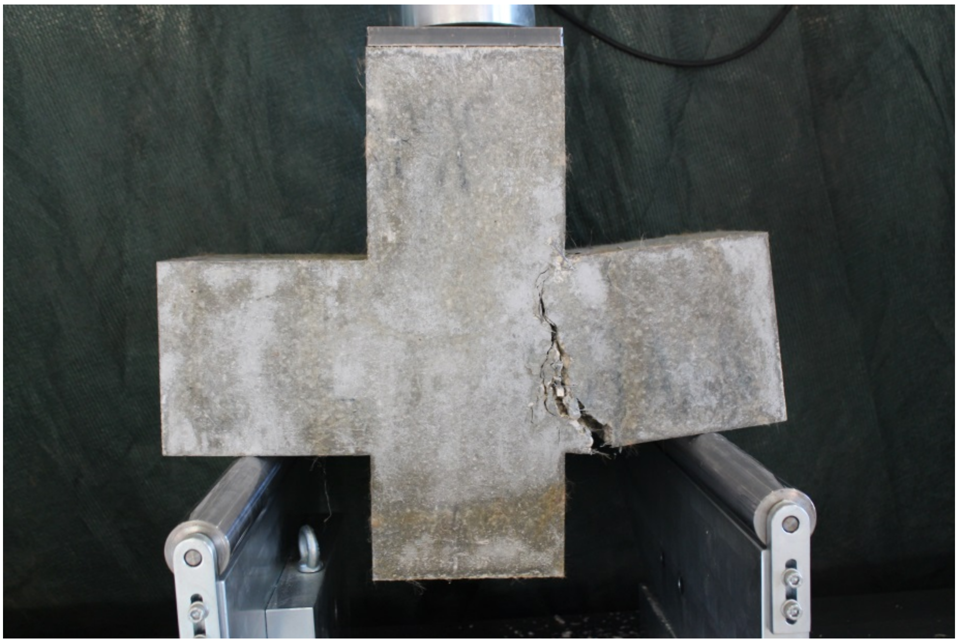

Figure 2.3 Flexural Failure Mode in a Corbel


Figure 2.4 Shear Failure Mode in a Corbel

2.5 Conclusion

Use of steel fibers provides considerable advantages for reinforced concrete corbels. For instance, it can change the failure mode from diagonal splitting to flexural mode and it can prevent the sudden failure in the corbel even if the failure mode is shear. Moreover, addition of steel fiber increases the load carrying capacity and ductility of reinforced concrete corbels. Significant benefits of steel fiber used in corbels require detailed research about the steel fiber reinforced concrete corbels.

Some researchers carried out experimental studies on normal strength and high strength reinforced concrete corbels. They investigated various mechanical properties (load carrying capacity, ductility, failure mode) of SFRC corbels. They also proposed some models in order to estimate the load carrying capacity of SFRC corbels. However, reliability analysis has to be made for SFRC corbels to use the proposed models to achieve safety. It is also important to note that stochastic analysis is required to achieve a complete reliability analysis since SFRC corbels have many uncertainties. These uncertainties can be originated from material and geometrical aspects. Therefore, detailed stochastic and reliability analyses are required to provide certain design and statistical parameters about SFRC corbels and to universalize the use of SFRC corbels in construction sector. On the other hand, elucidating the uncertainties in the load carrying capacities and failure modes of SFRC corbels will encourage the engineers and designers about the use of SFRC corbels in their projects. Therefore, reliability and stochastic analyses of SFRC corbels were carried out in this thesis and the lack information about design issues of SFRC corbels is tried to overcome.

Although some researchers carried out experimental works to observe mechanical outputs of SFRC corbels, extra experimental data are required to provide certain information about load carrying capacity of SFRC corbels. Therefore, experimental studies were carried out on reinforced concrete and steel fiber reinforced concrete corbels in this thesis studies and a new database about load carrying capacity of reinforced concrete and steel fiber reinforced concrete corbels were added to the literature.

CHAPTER 3

EXPERIMENTAL STUDIES ON RC AND SFRC CORBELS

3.1 Introduction

For the experimental part of the thesis, 24 corbels were prepared. Various parameters were changed to observe the mechanical behavior of related corbels. Variables were compressive strength, reinforcement ratio, steel fiber ratio and shear span to effective depth ratio.

Two values were considered for cubic compressive strength of corbels which were nearly 30 MPa and 50 MPa. Two reinforcement ratios whose values are 0.838% (2-ϕ10) and 1.206% (2-ϕ12) were used. For steel fiber ratio, three values were considered: No steel fiber (0%), 1% and 1.5% steel fiber ratios (as volumetric). Selected shear span to effective depth ratio values were 0.8 and 1.04. Therefore, shear span to total height ratios were calculated as 0.67 and 0.867.

3.2 Mix Design for Reinforced Concrete and Steel Fiber Reinforced Concrete

In the concrete mix design, coarse aggregate (crushed gravel and maximum size is 10 mm), fine aggregate (fine sand and size interval is 0-4 mm), cement and water whose weight ratios are 2.78 : 1.5 : 1 : 0.48, respectively were used for the concrete class of 50 MPa. 42.5R Portland cement was used for the production. Hooked end type steel fibers (ZP 305 type of Bekaert-Dramix steel fibers) were used for the preparation of SFRC corbels. Length and diameter of the steel fiber is 30 mm and 0.55 mm, respectively (aspect ratio is 54.5). Since steel fiber reduces the workability of the concrete, superplasticizer was added to mix with an amount of 0.45% of the cement weight. Amounts of ingredients are given for 1 m^3 concrete in Table 3.1.

Table 3.1 Ingredient Amounts for the Production of 1 m^3 Concrete (f_{cu} is 50 MPa)

Coarse Agg. (kg)	Fine Agg. (kg)	Cement (kg)	Water (kg)	w/c ratio	Steel fiber (kg)
1110	600	400	190	0.48	78,4 (1%) 117,6 (1.5%)

For the production of the other concrete class (f_{cu} is 30 MPa), same ingredients and same weight ratios were used except water/cement ratio (w/c) and cement type. 0.55 was selected as w/c ratio and 32.5R Portland cement was used. Related amounts of ingredients are shown in Table 3.2.

Table 3.2 Ingredient Amounts for the Production of 1 m^3 Concrete (f_{cu} is 30 MPa)

Coarse Agg. (kg)	Fine Agg. (kg)	Cement (kg)	Water (kg)	w/c ratio	Steel fiber (kg)
1110	600	400	220	0.55	78,4 (1%) 117,6 (1.5%)

3.3 Preparation of Corbels

Firstly, formworks were prepared for SFRC corbels. Special attention was given to formworks for initial set-up to remove them easily after concreting process. For each corbel, reinforcement was prepared and placed into the formworks. A typical reinforcement configuration is shown in Fig. 3.1.

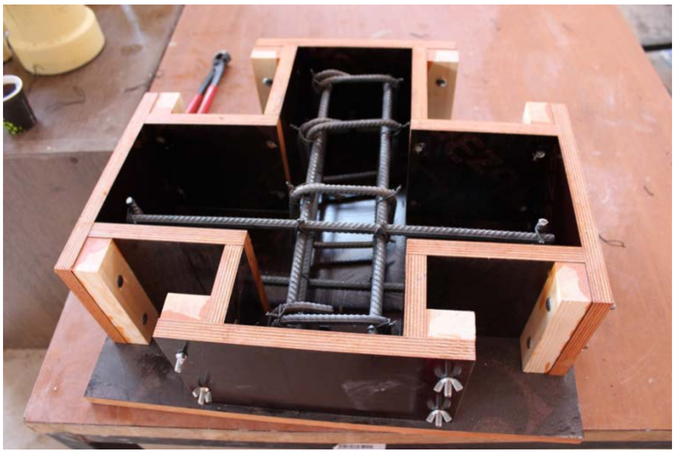

Figure 3.1 Formwork and Reinforcement Configuration for Experimented Corbels

Reinforcement configuration was prepared with 8 mm, 10 mm and 12 mm steel bars. Four 10 mm steel bars were used for the longitudinal bar of column part of the corbel (4-ϕ10). 2-ϕ10 and 2-ϕ12 steel bars were prepared for main reinforcement of corbels. To represent the real situation, stirrups were produced from 4-ϕ8 bars (Fig. 3.1). Two main reinforcements were connected to each other by small straight bars to provide the stability of the reinforcements. Therefore, they can work together during loading process. To achieve effective concreting process, spacers were placed in the specific regions of the formwork. Depth of the main reinforcement from the bottom of the corbel changes between 22 and 30 mm (average depth is nearly 25 mm). Average yield strengths for reinforcements were found to be 491 MPa, 560 MPa and 510 MPa, and average ultimate strength values found to be 614 MPa, 678 MPa and 620 MPa, for 8 mm, 10 mm and 12 mm steel bars, respectively.

Before concreting process, all of the corbel formworks and sample formworks were lubricated by special formwork grease. Concreting process was implemented by 0.05 m^3 capacity concrete mixer. A piece of steel fiber reinforced concrete immediately after concreting process is shown in Fig. 3.2. A vibrating table was prepared and used to place the concrete into the formworks effectively and to prevent air voids inside the concrete. After concreting of the formworks, all of them were finished and flattened by trowels.

Figure 3.2 Steel Fiber Reinforced Concrete in Concreting Process

Six 10mm x 20mm cylinder sample and three 10mm x 10mm cube samples were prepared for two corbels (Fig. 3.3). Three of the cylinders were taken to measure the splitting tensile strength of the concrete; other three cylinders were taken to measure the compressive strength of the concrete. Three cube samples were prepared to measure the cubic compressive strength of the concrete. Six cylinder and three cube samples and two corbel specimens were produced as a result of one concreting batch.

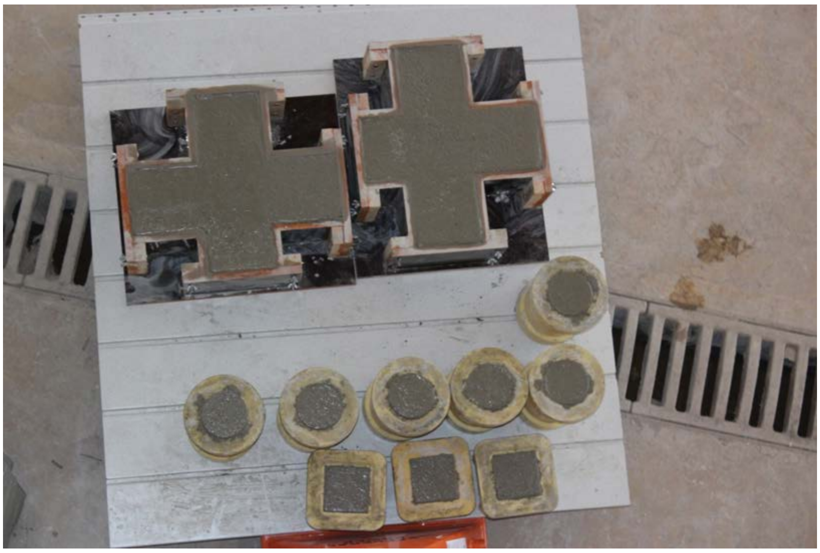

Figure 3.3 Corbels and Corresponding Cylinder and Cube Samples after Concreting Process

The formworks were removed one day after the concreting process and the corbels were covered with a special textile for curing process. Corbels and corresponding samples were watered during 28 days to reach the target strength (Fig. 3.4). The corbels and samples were tested in a loading frame after 28 days.

Figure 3.4 Curing Process for Corbel Samples

Name designation of the samples which were prepared for testing is listed in Table 3.3. In this list, first term represents the cubic compressive strength, second term represents steel fiber ratio, third term stands for the diameter of the main reinforcement and the last one stands for the shear span of the corbel.

Table 3.3 Designation and Properties of Experimented Corbels

Designation	Cubic Compressive Strength (f_{cu}) (MPa)	Steel Fiber Ratio (v_f) (%)	Diameter of Main Reinforcement (ϕ) (mm)	Shear Span (a) (mm)
50-0-10-100	50	0	10	100
50-0-10-130	50	0	10	130
50-0-12-100	50	0	12	100
50-0-12-130	50	0	12	130
50-1-10-100	50	1	10	100
50-1-10-130	50	1	10	130
50-1-12-100	50	1	12	100
50-1-12-130	50	1	12	130
50-1.5-10-100	50	1.5	10	100
50-1.5-10-130	50	1.5	10	130
50-1.5-12-100	50	1.5	12	100
50-1.5-12-130	50	1.5	12	130
30-0-10-100	30	0	10	100
30-0-10-130	30	0	10	130
30-0-12-100	30	0	12	100
30-0-12-130	30	0	12	130
30-1-10-100	30	1	10	100
30-1-10-130	30	1	10	130
30-1-12-100	30	1	12	100
30-1-12-130	30	1	12	130
30-1.5-10-100	30	1.5	10	100
30-1.5-10-130	30	1.5	10	130
30-1.5-12-100	30	1.5	12	100
30-1.5-12-130	30	1.5	12	130

3.4 Testing Procedure

Corbels were tested with a 500 kN capacity loading frame. Corresponding samples were also tested to measure the compressive strength and tensile strength. Compressive strength and tensile strengths were tested in a 2000 kN capacity concrete press machine. Geometry of experimented corbels is shown in Fig. 3.5.

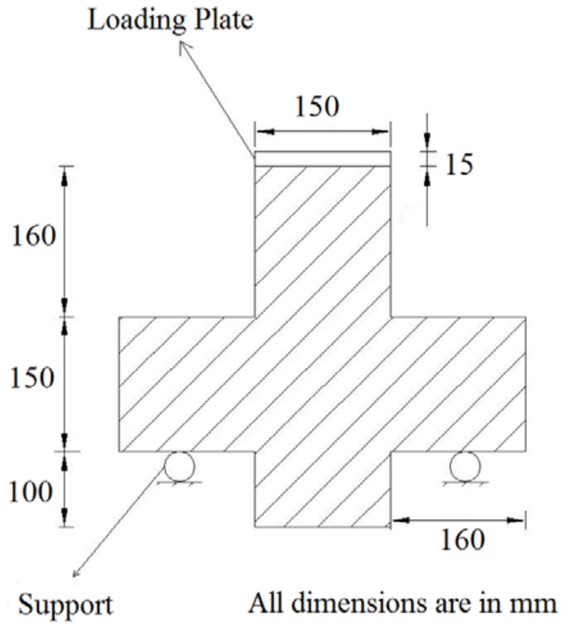

Figure 3.5 Dimensions of Experimented Corbels

The thickness of corbels is 150 mm. That is, cross sections of both column and corbels are 150mm x 150 mm square section.

Load was transferred from the loading frame to the corbel by the 15 mm thickness loading plate. Loading plate was produced from a transmission steel to transfer the load effectively. While one of the roller supports allows to rotation in the transverse direction, the other is not.

Corbel loading tests were carried out as displacement controlled mode. Therefore, post-peak behavior of corbels could be observed and load-displacement curve could be obtained. Corbels were loaded monotonically. The loading rate of corbels is 0.3 mm/minute. A typical implemented corbel test is shown in Fig. 3.6.

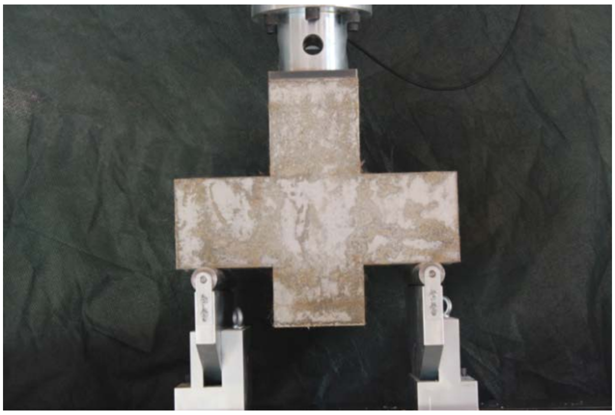
Figure 3.6 Test Configuration and Set-up for Corbels

3.5 Results of Corbel Tests

3.5.1 Load Carrying Capacities

Results of load carrying capacities of experimented corbels are listed in Table 3.4. Measurements of tensile strengths (f_{ct}), cylindrical compressive strengths (f_c), effective depth (d) and reinforcement ratio (A_s/bh) are also listed in the same table. Resulting crack patterns of corbels at failure load are shown in Appendix B (Figs. B.1-B.24).

Table 3.4 Measured Outputs of Experimented Corbels

Name	Cylindrical compressive strength (f_c) (MPa)	Splitting tensile strength (f_t) (MPa)	Eff. depth (d) (mm)	Reinforcement ratio (ρ %)	Ultimate load per corbel (kN)
50-0-10-100	39	2.8	122	0.858	65.91
50-0-10-130	39	2.8	123	0.851	55.52
50-0-12-100	38.5	2.8	124	1.216	68.06
50-0-12-130	38.5	2.8	128	1.178	57.65
50-1-10-100	40	3.7	120	0.873	110.58
50-1-10-130	40	3.7	124	0.845	78.8
50-1-12-100	38	3.6	122	1.236	121.78
50-1-12-130	38	3.6	122	1.236	89.18
50-1.5-10-100	42.5	4.5	123	0.851	125.13
50-1.5-10-130	42.5	4.5	125	0.838	86.59
50-1.5-12-100	42.5	4.2	124	1.216	127.54
50-1.5-12-130	42.5	4.2	125	1.206	89.13
30-0-10-100	24	1.9	124	0.845	57.22
30-0-10-130	24	1.9	123	0.851	37.57
30-0-12-100	25	2	124	1.216	63.53
30-0-12-130	25	2	125	1.206	48.65
30-1-10-100	22.3	2.5	124	0.851	71
30-1-10-130	22.3	2.5	124	0.851	52.6
30-1-12-100	22.3	2.3	124	1.216	73.4
30-1-12-130	22.3	2.3	127	1.187	56.15
30-1.5-10-100	25.5	3.1	122	0.858	79.67
30-1.5-10-130	25.5	3.1	123	0.851	58.35
30-1.5-12-100	25.5	3.1	127	1.187	87.01
30-1.5-12-130	25.5	3.1	124	1.216	59.79

3.5.2 Interpretation of Experimental Results

As a result of experiments, the following conclusions can be drawn:

3.5.2.1 Effect of compressive strength of concrete

Load carrying capacities of RC and SFRC corbels increase with the increment in the compressive strength of the concrete (Figs. 3.7-3.10). This increment is also indirectly related with increment of tensile strength with the compressive strength. However, it is also important to note that the rate of increment is increased when the steel fiber percentage increases since the rate of increment of tensile strength becomes higher as the fiber percentage increases for the same compressive strength. As a result, compressive strength of concrete is effective on the load carrying capacity of corbels. However, its effect is also connected with tensile strength of the concrete.

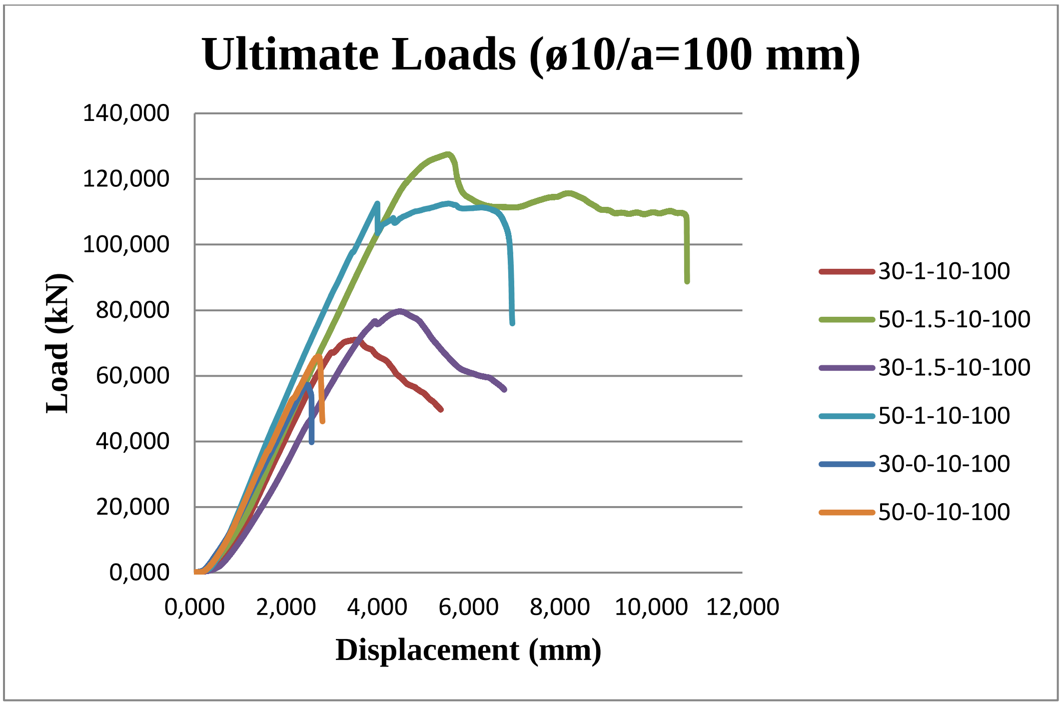

Figure 3.7 Load Carrying Capacities of Experimented Corbels
(bar diameter: 10 mm and shear span:100 mm)

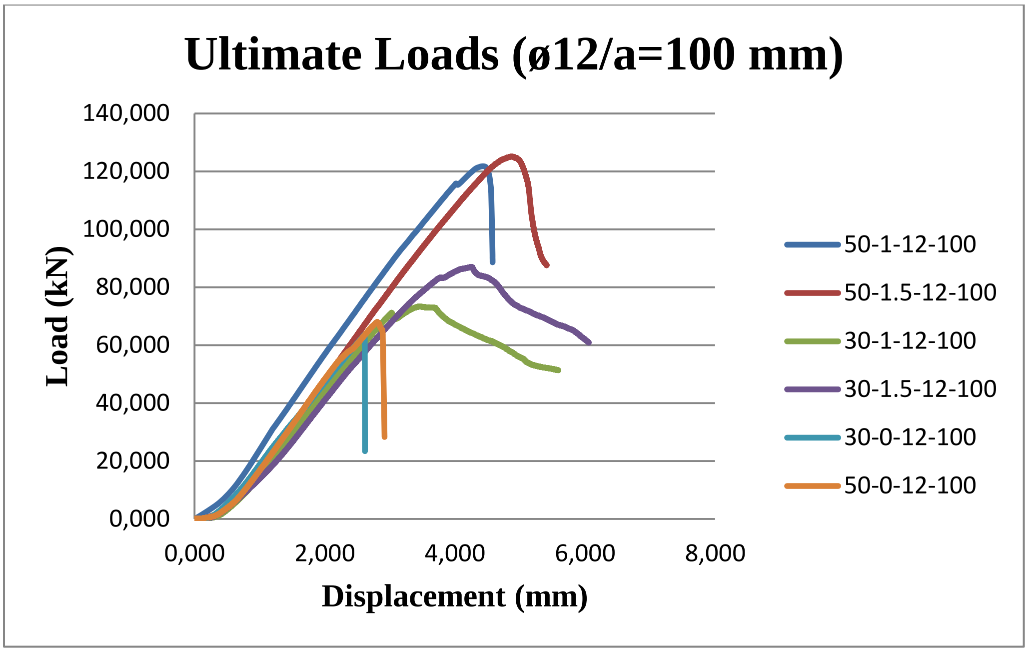

Figure 3.8 Load Carrying Capacities of Experimented Corbels
(bar diameter: 12 mm and shear span:100 mm)

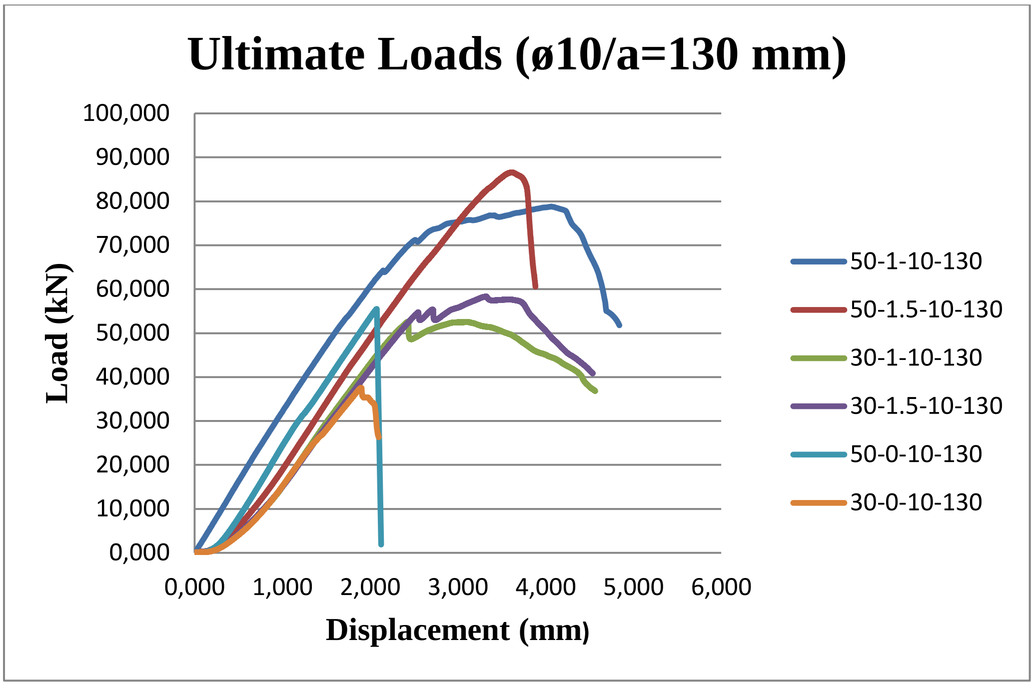

Figure 3.9 Load Carrying Capacities of Experimented Corbels
(bar diameter: 10 mm and shear span:130 mm)

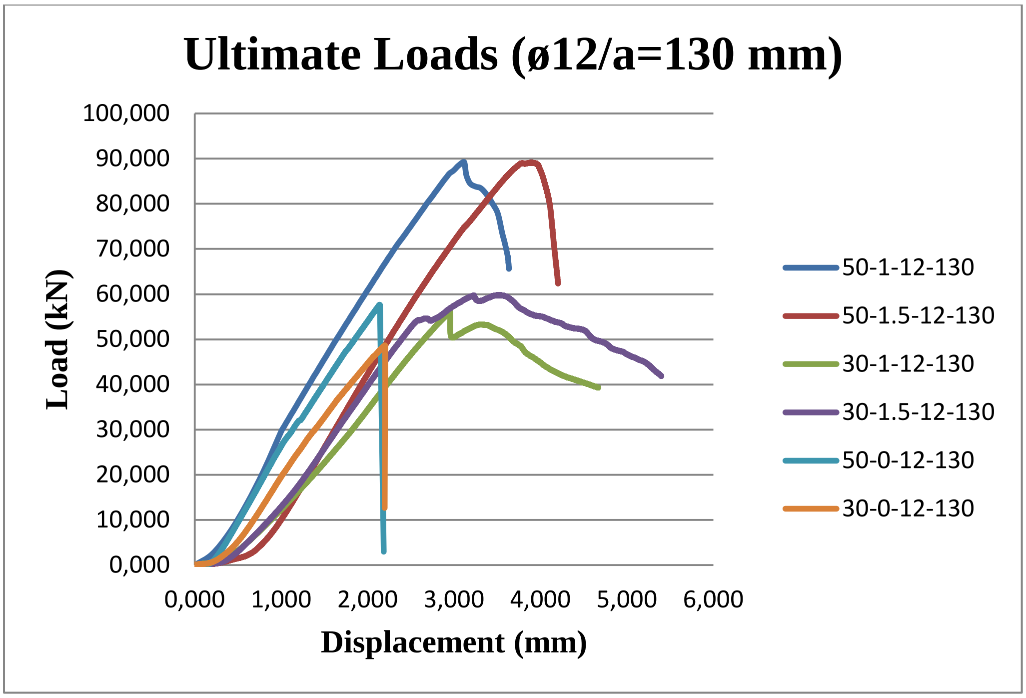

Figure 3.10 Load Carrying Capacities of Experimented Corbels
(bar diameter: 12 mm and shear span:130 mm)

3.5.2.2 Effect of steel fiber percentage (v_f %)

Effect of steel fiber percentage (v_f %) is directly related with splitting tensile strength of concrete. Whenever the steel fiber percentage increases the tensile strength of the concrete, the increment in the load carrying capacity of corbels can be observed clearly (Figs. 3.11-3.18). The increment in the capacity is pronounced more as compared to the sample without steel fiber to the same sample with steel fiber. However, a general conclusion can be made that the load carrying capacity of a corbel is increased with steel fiber percentage increment.

Another important advantage of addition of steel fiber is that it increases the ductility of corbels significantly. It is can be observed clearly from Fig. 3.11 that transition from the reinforced concrete corbel to steel fiber reinforced concrete corbel under same conditions increases the deformation capability of related corbels without a dramatic loss in the load carrying capacity. This is a desirable mechanical behavior for a structural element since ductility is considerable phenomena to provide safety, serviceability and functionality of a structural element.

The increase in the load carrying capacity of SFRC corbels becomes smaller as the steel fiber percentage increases (Figs. 3.11-3.18). This situation can be explained with the sudden increment in the tensile strength and ductility of the concrete when the steel fiber is added to plain concrete.

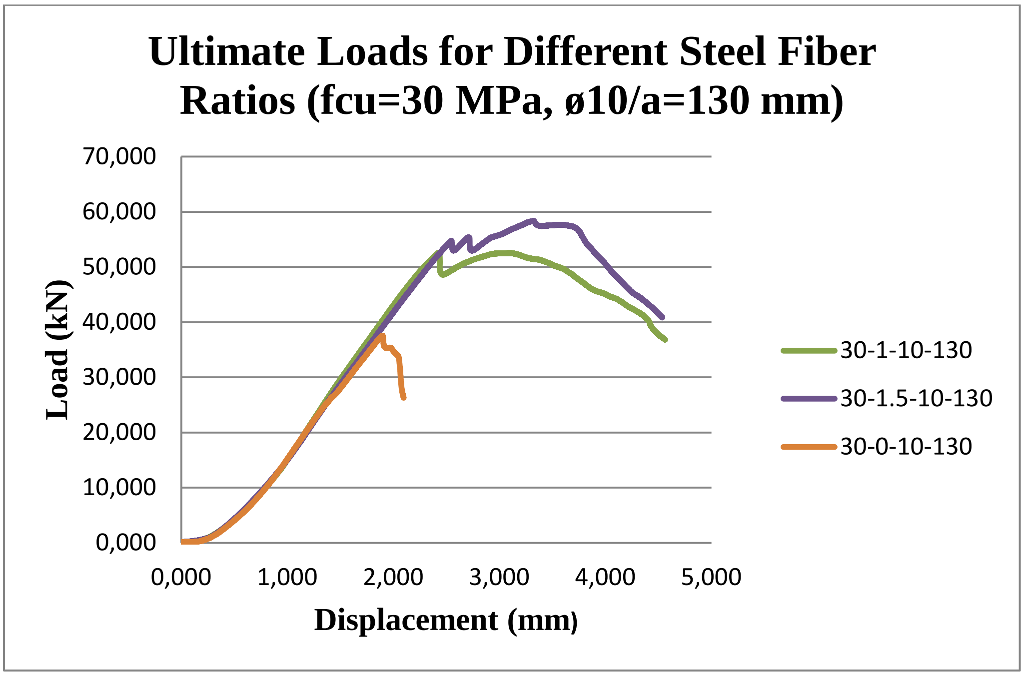

Figure 3.11 Ultimate Loads under Different Steel Fiber Amounts (f_{cu}=30MPa, ϕ10, a=130 mm)

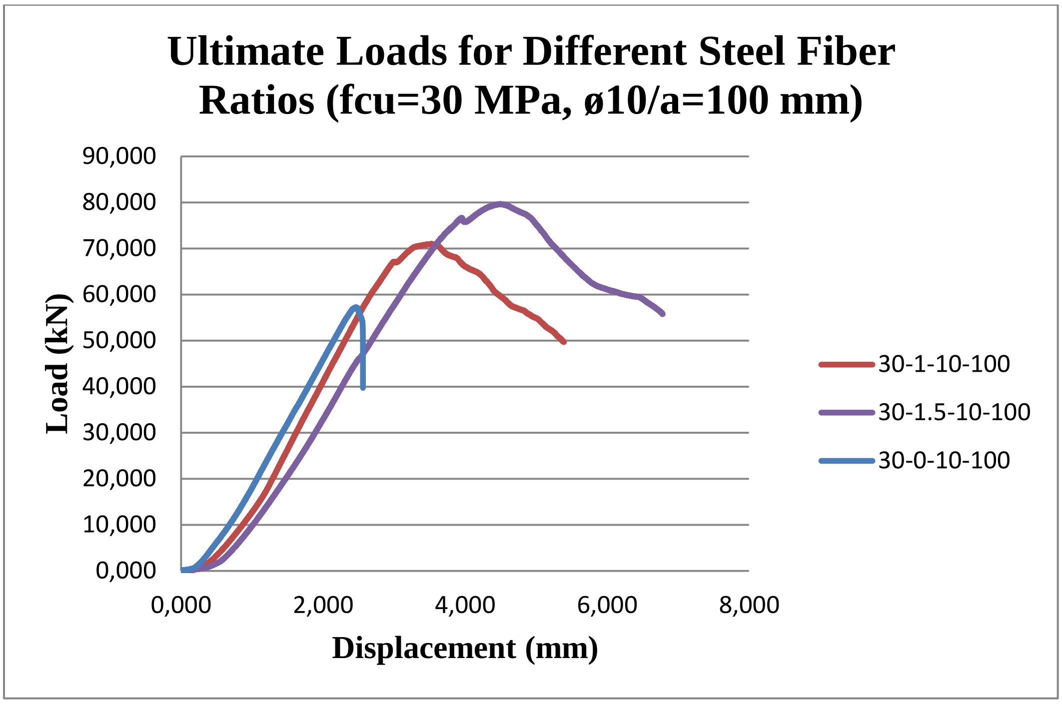

Figure 3.12 Ultimate Loads under Different Steel Fiber Amounts (f_{cu}=30MPa, ϕ10, a=100 mm)

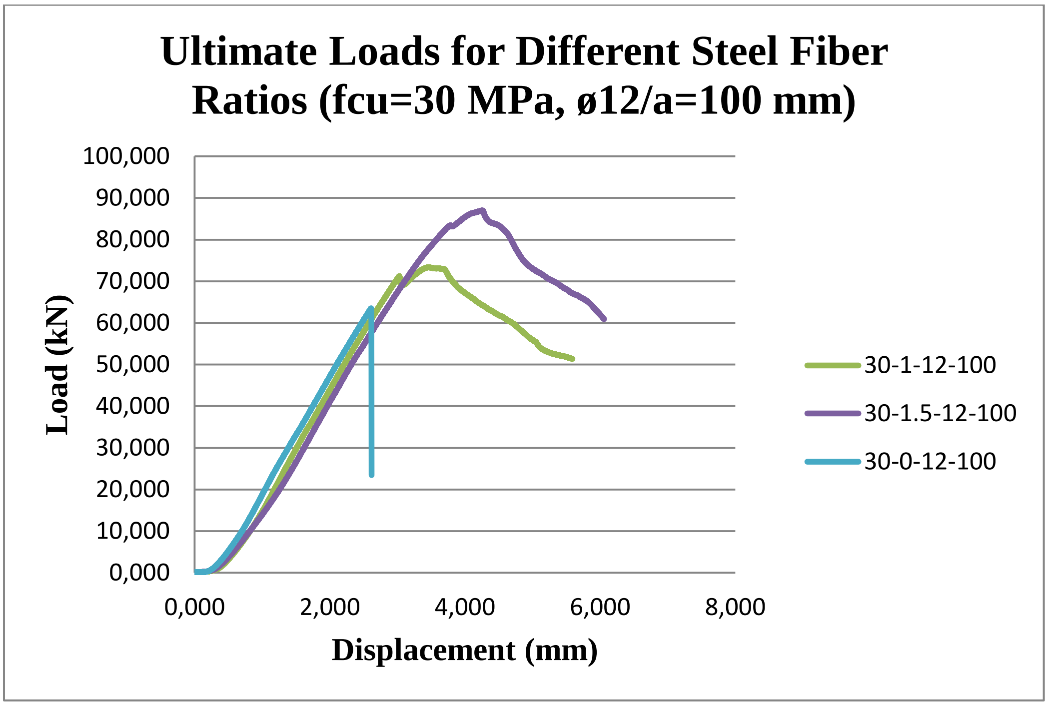

Figure 3.13 Ultimate Loads under Different Steel Fiber Amounts (f_{cu}=30MPa, ϕ12, a=100 mm)

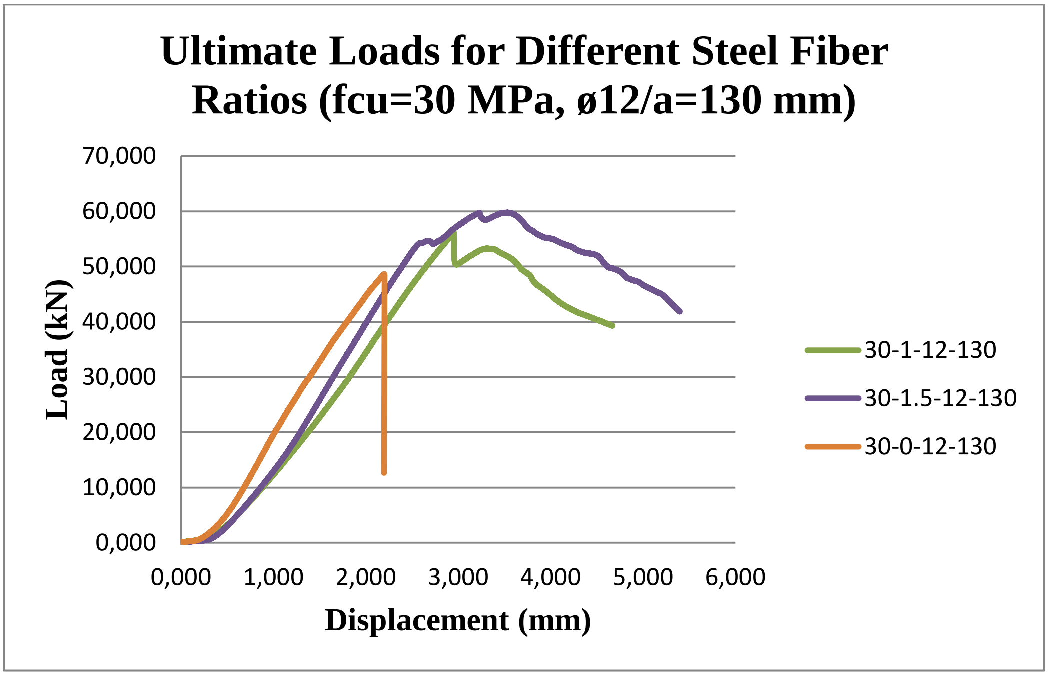

Figure 3.14 Ultimate Loads under Different Steel Fiber Amounts (f_{cu}=30MPa, ϕ12, a=130 mm)

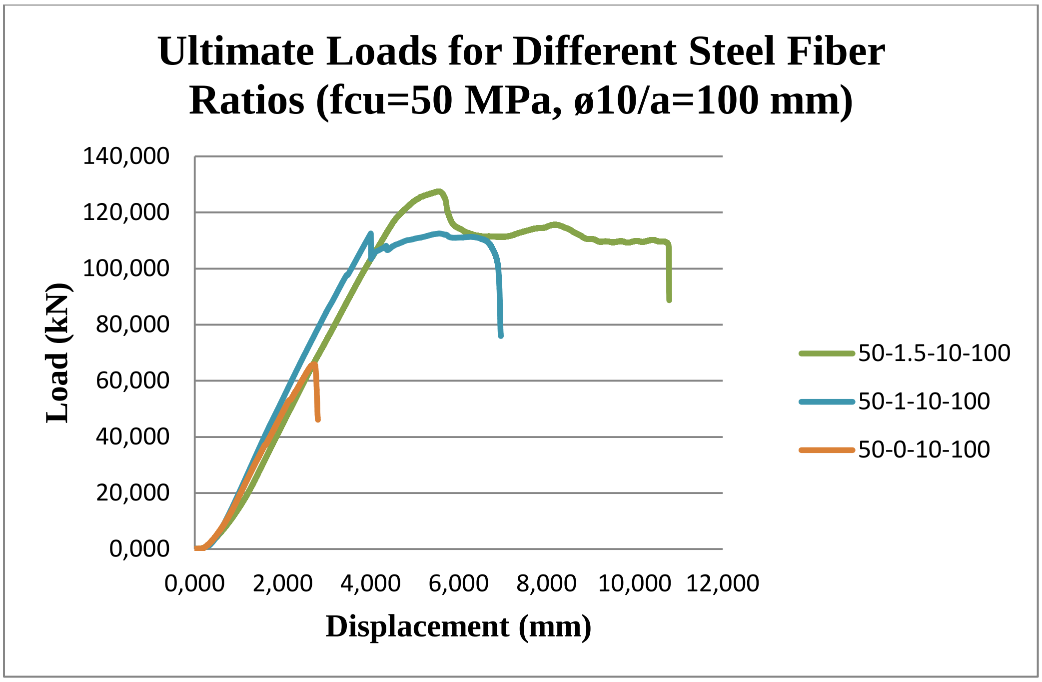

Figure 3.15 Ultimate Loads under Different Steel Fiber Amounts
(f_{cu}=50MPa, ϕ10, a=100 mm)

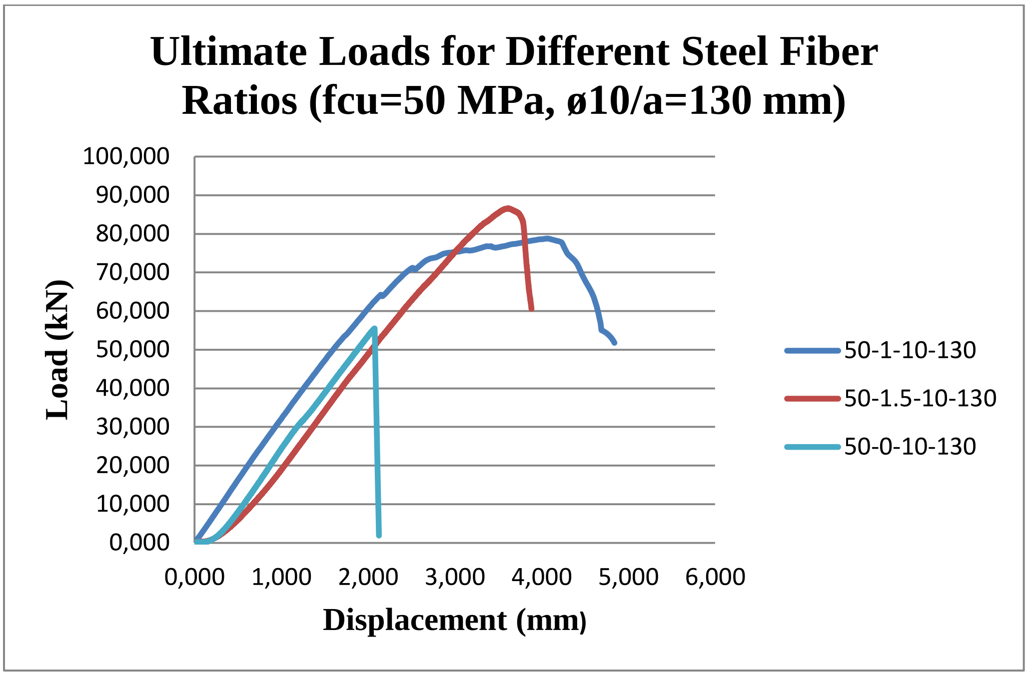

Figure 3.16 Ultimate Loads under Different Steel Fiber Amounts
(f_{cu}=50MPa, ϕ10, a=130 mm)

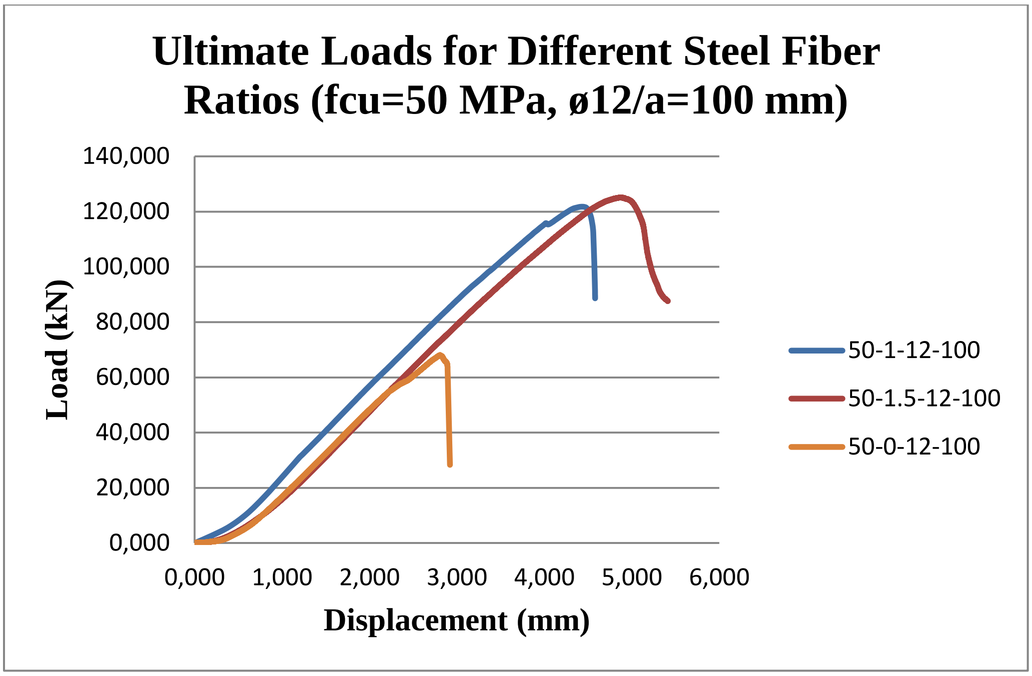

Figure 3.17 Ultimate Loads under Different Steel Fiber Amounts (f_{cu}=50MPa, ϕ12, a=100 mm)

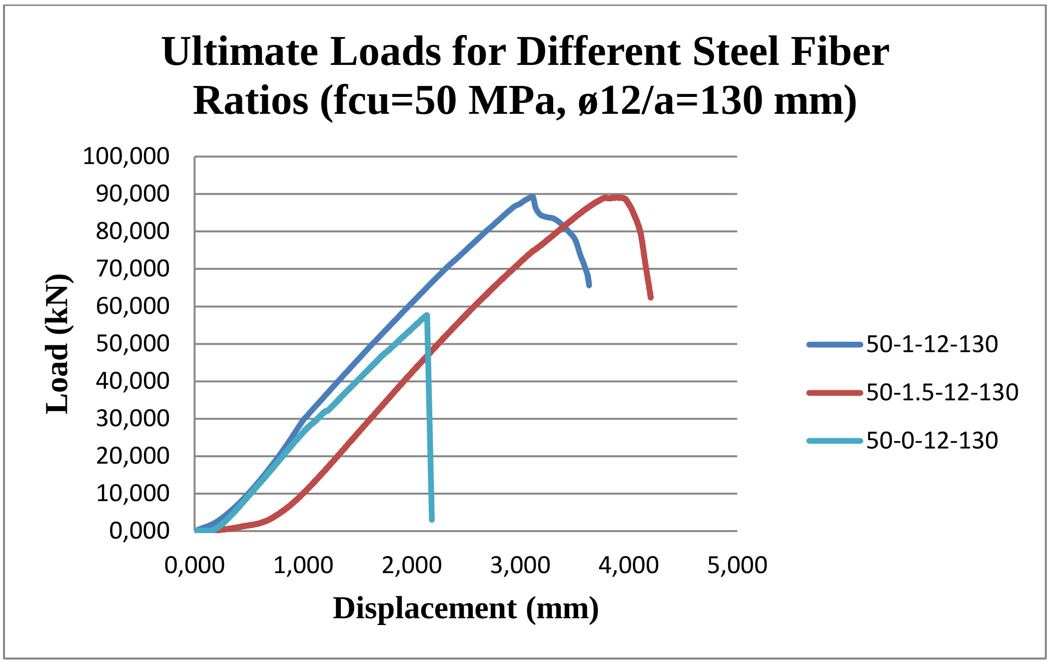

Figure 3.18 Ultimate Loads under Different Steel Fiber Amounts (f_{cu}=50MPa, ϕ12, a=130 mm)

3.5.2.3 Effect of steel reinforcement ratio (ρ %)

Steel reinforcement ratio is not as much effective as compressive strength and steel fiber percentage on load carrying capacity of SFRC corbels (Figs. 3.19-3.22). However, steel reinforcement ratio is very significant parameter about ductility and failure trend of steel fiber reinforced concrete corbels.

In higher compressive strengths (f_{cu}=50 MPa), no ductility can be achieved in high reinforcement ratios. For instance, if Fig. 3.19 is examined in detail, when 12 mm bars are used as main reinforcement; concrete failure exists before yielding of the reinforcement. Therefore, failure is sudden, but not brittle because of steel fibers. On the other hand, in lower reinforcement ratios (for example, when 10 mm steel bars are used), a ductile behavior can be observed.

Ductility effect becomes more apparent in the case of corbels produced from lower compressive strength concrete. This situation can be explained by crushing of concrete. In high compressive strength concrete corbels, the fibers lose their fiber bridging effect up to concrete crushing occurs. However, in low compressive strength corbels, since crack width is much smaller, the fibers can exhibit the bridging effect and therefore, ductile behavior is achieved or sudden failure is prevented (Figs. 3.21 and 3.22).

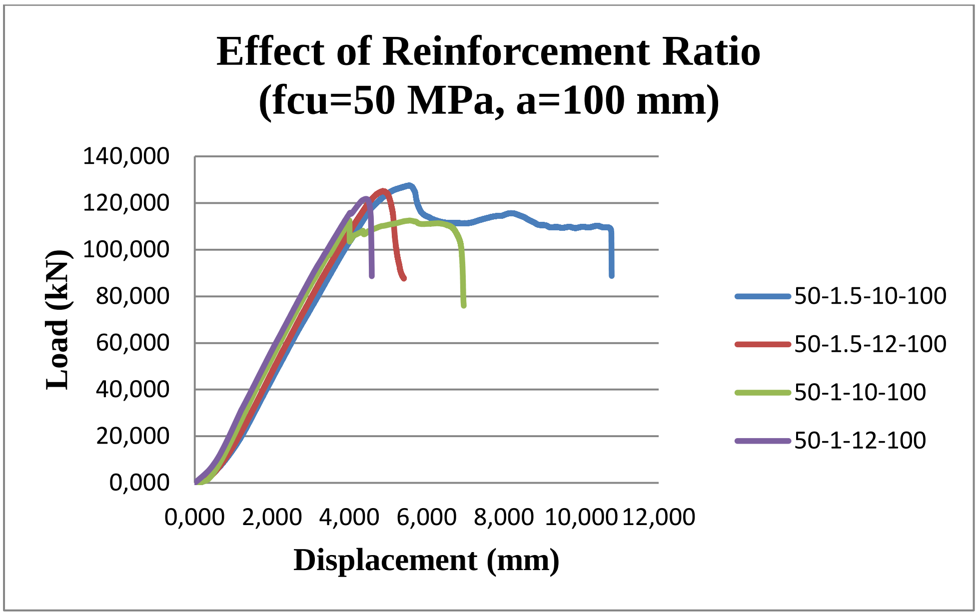

Figure 3.19 Effect of Reinforcement Ratio for f_{cu}=50 MPa and a=100 mm

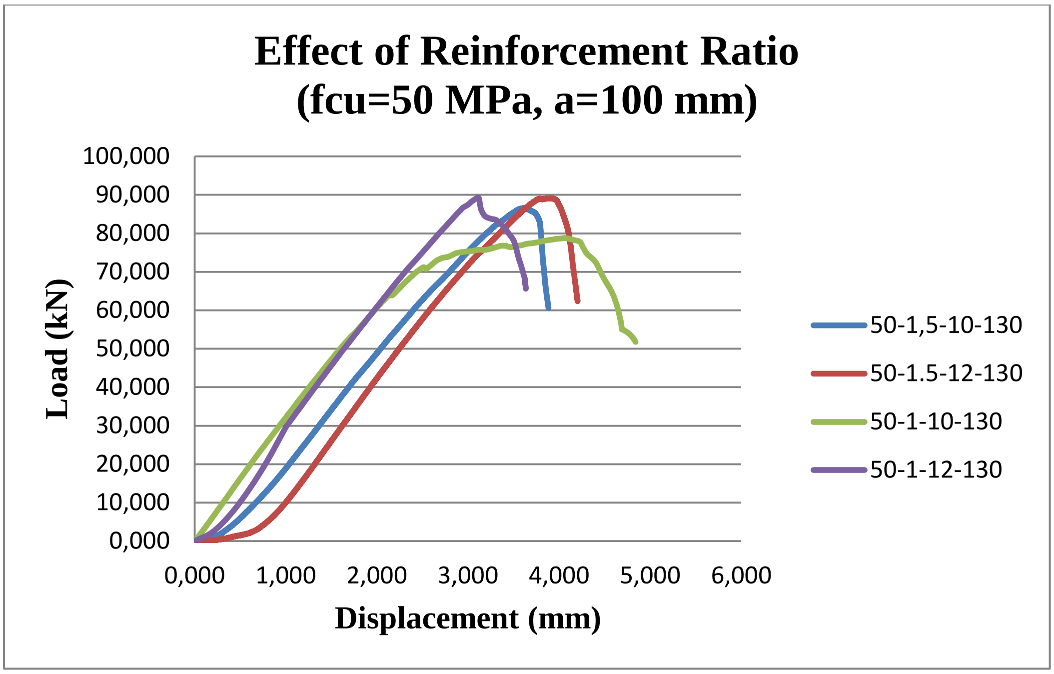

Figure 3.20 Effect of Reinforcement Ratio for f_{cu}=50 MPa and a=130 mm

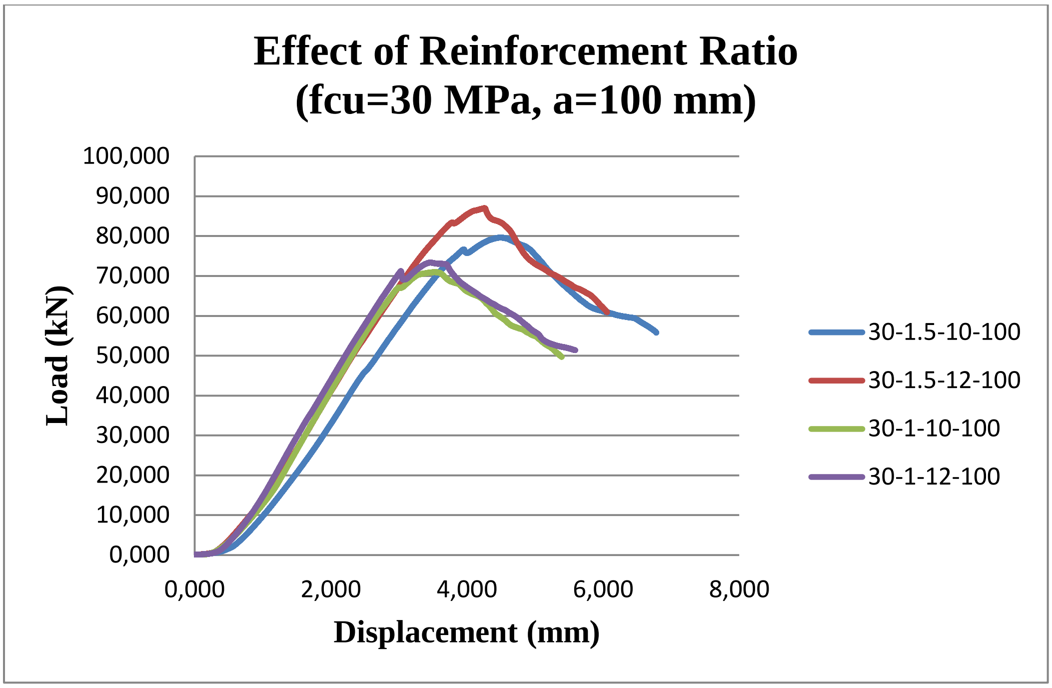

Figure 3.21 Effect of Reinforcement Ratio for f_{cu}=30 MPa and a=100 mm

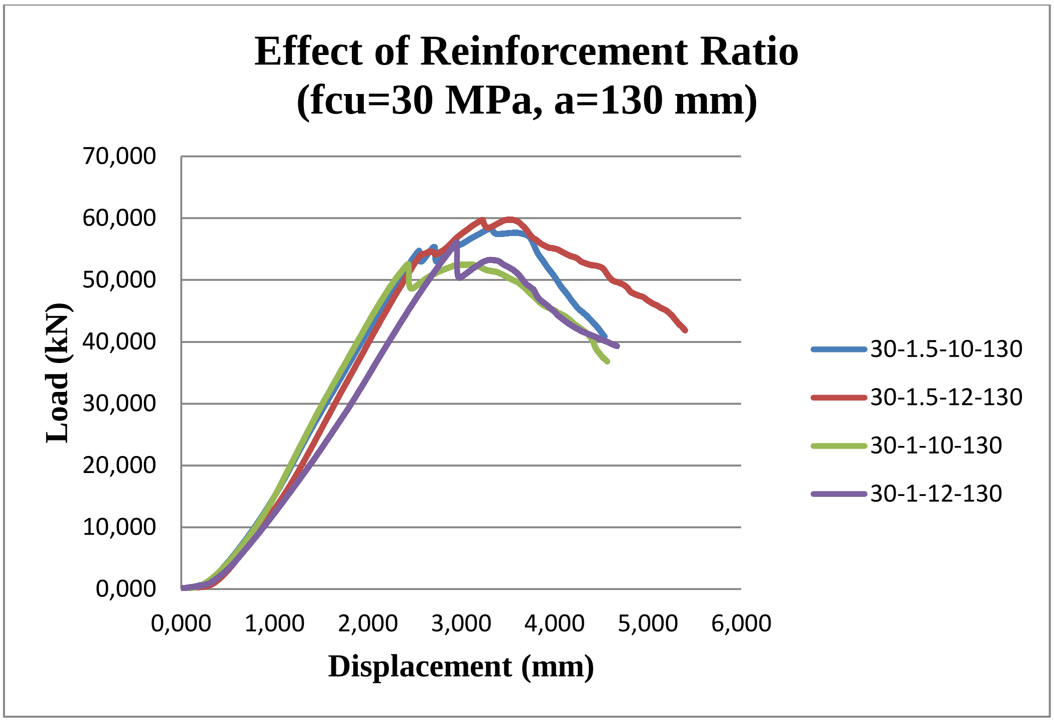

Figure 3.22 Effect of Reinforcement Ratio for f_{cu}=30 MPa and a=130 mm

3.5.2.4 Effect of shear span

As expected, load carrying capacities of both reinforced concrete and steel fiber reinforced concrete corbels decrease as the shear span is increased (Figs. 3.23-3.26). However, this rule is valid for effective depth values which are close to each other. Even if the shear span is same, the load carrying capacity can show different trends depending on effective depth values since the tension and compression zone is changed by the alteration of effective depth. This topic was discussed by Fattuhi (1994a). Therefore, a designer has to be careful during the determination of shear span and has to consider the effective depth of the corbel.

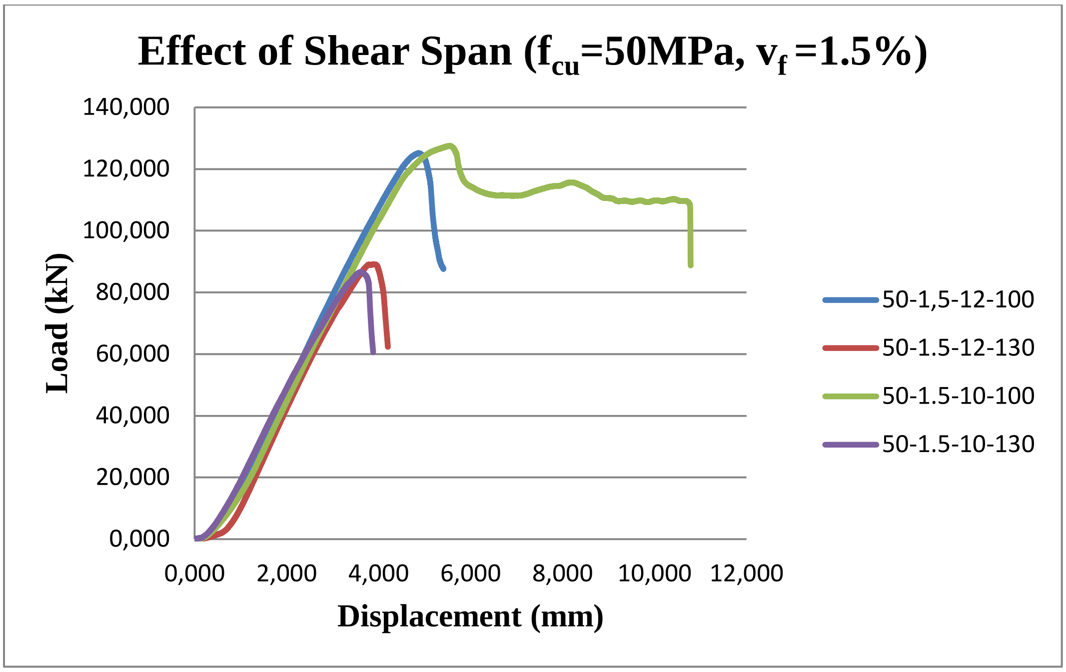

Figure 3.23 Effect of Shear Span on Load Carrying Capacity of Corbels (f_{cu}=50 MPa and v_f=1.5%)

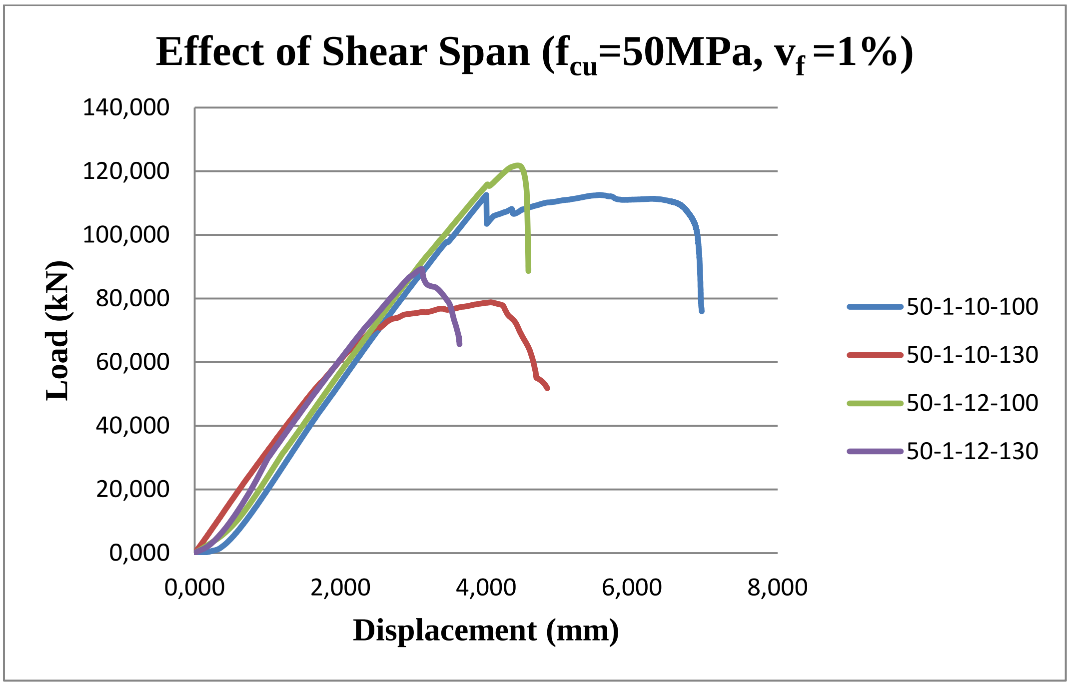

Figure 3.24 Effect of Shear Span on Load Carrying Capacity of Corbels (f_{cu}=50 MPa and v_f=1%)

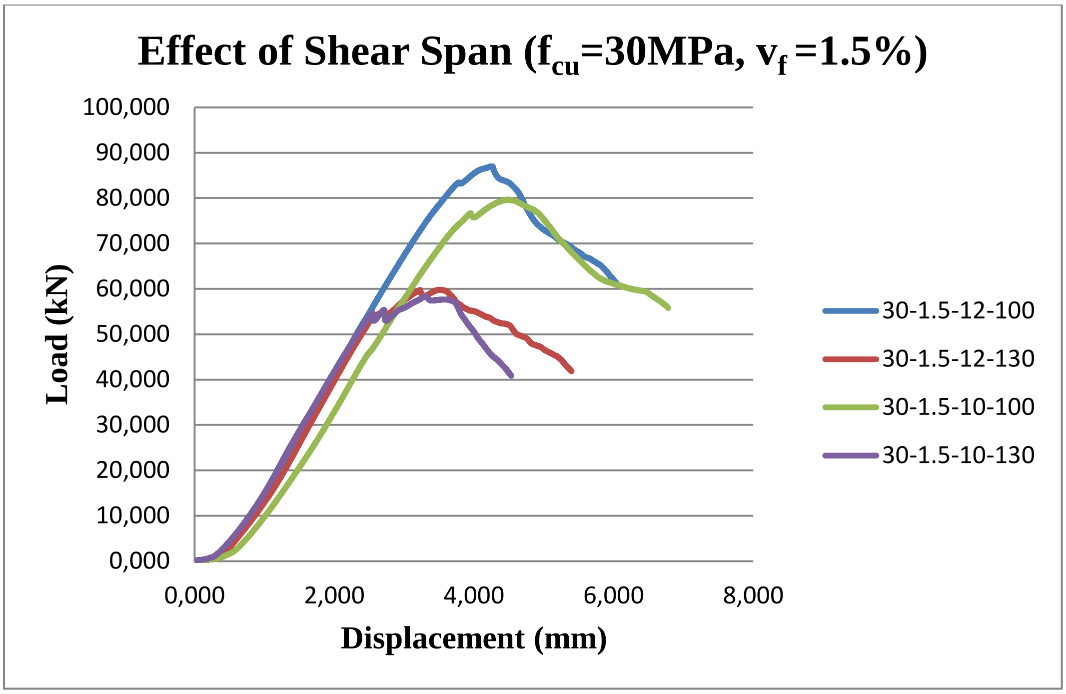

Figure 3.25 Effect of Shear Span on Load Carrying Capacity of Corbels (f_{cu}=30 MPa and v_f =1.5%)

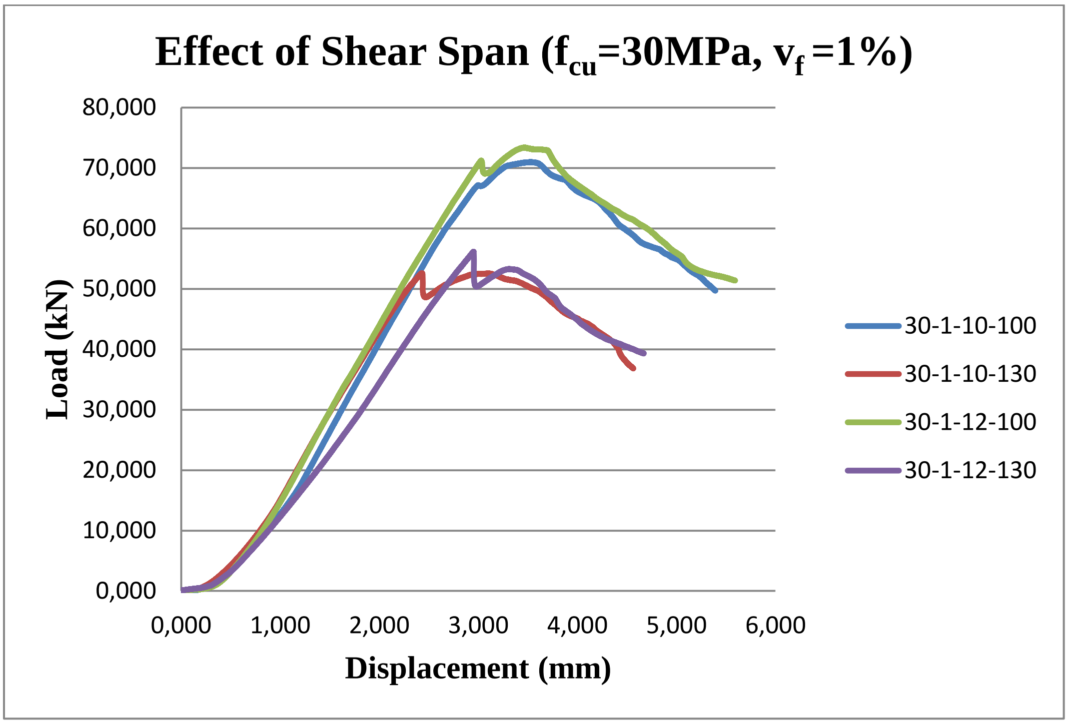

Figure 3.26 Effect of Shear Span on Load Carrying Capacity of Corbels (f_{cu}=30 MPa and v_f =1%)

CHAPTER 4

FINITE ELEMENT MODELING OF STEEL FIBER REINFORCED CONCRETE (SFRC) CORBELS

4.1 Introduction

In this section, finite element analyses of steel fiber reinforced concrete (SFRC) corbels were carried out by a special software, namely as "ATENA". ATENA is an effective and reliable tool for nonlinear modeling of reinforced concrete structures.

Firstly, theoretical background implemented by ATENA is specified in this chapter. Then, finite element (FE) modeling of SFRC corbels is introduced. Results of the analysis were compared with experimental results which had been carried out before. A good fit is observed between experimental results and FE results.

4.2 Theoretical Basis

4.2.1 Formulation for Material Model

The material model formulation is originated from the strain decomposition into elastic ε_{ij}^{e}, plastic ε_{ij}^{p} and fracturing ε_{ij}^{f} strain components (De Borst, 1986).

$$\varepsilon_{ij} = \varepsilon_{ij}^{e} + \varepsilon_{ij}^{p} + \varepsilon_{ij}^{f} \tag{4.1}$$

Therefore, formula for the new stress state can be expressed as;

$$\sigma_{ij}^{n} = \sigma_{ij}^{n-1} + E_{ijkl}(\Delta\varepsilon_{kl} - \Delta\varepsilon_{kl}^{p} - \Delta\varepsilon_{kl}^{f}) \tag{4.2}$$

The increments of plastic strain and fracturing strain are evaluated based on the used material models.

4.2.2 Fracture Model for Concrete

Rankine failure criterion is used to model tensile behavior and cracking of concrete. The criterion can be stated as the following expression;

$$\sigma_{ii}^{'t} - f_{ti}^{'} \leq 0 \tag{4.3}$$

Strains and stresses are evaluated according to material directions. There are two choices to determine material directions: Rotated Crack Model and Fixed Crack Model. In rotated crack model material directions are defined by principal directions according to current stress state. However, material directions are the principal directions at the onset of cracking in fixed crack model. Therefore $\sigma_{ii}^{'t}$ and $f_{ti}^{'}$ are the trial stress and the tensile strength in material direction *i*, respectively. The trial stress state is evaluated by the elastic predictor;

$$\sigma_{ij}^{'t} = \sigma_{ij}^{'n-1} + E_{ijkl} + \Delta\varepsilon_{kl}^{'} \tag{4.4}$$

Whenever the trial stress does not satisfy the expression stated in eq. (4.3), this means that fracture starts and fracturing strain can be calculated providing that the final stress state must provide the following condition;

$$\sigma_{ii}^{'n} - f_{ti}^{'} = \sigma_{ii}^{'t} - E_{iikl}\Delta\varepsilon_{kl}^{'f} - f_{ti}^{'} = 0 \tag{4.5}$$

The behavior is assumed to be linear and elastic up to ultimate tensile strength. The behavior after ultimate tensile strength is represented by exponential softening rule (Fig. 4.1).

The crack opening (w_t) is the sum of the total fracturing strain and the current increment of fracturing strain ε^f multiplied by the characteristic length (L_t) which is calculated as a size of the element projected into the crack direction (Cervenka et al., 2013).

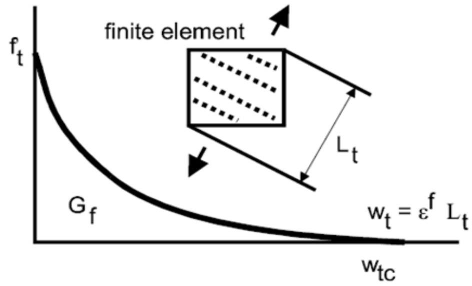

Figure 4.1 Tensile Exponential Model Used in ATENA (Cervenka et al., 2013)

4.2.3 Material Model for Concrete Crushing

Menetrey, William (Menetrey and William, 1995) failure surface is used for material model of concrete crushing;

$$F_{3P}^{p} = [\sqrt{1.5}\frac{\rho}{f_c^{'}}]^2 + m[\frac{\rho}{\sqrt{6} + f_c^{'}}r(\theta,e) + \frac{\xi}{\sqrt{3}f_c^{'}}] - c = 0 \tag{4.6}$$

where;

$$m = 3\frac{f_c^{'2} - f_t^{'2}}{f_c^{'} f_t^{'}}\frac{e}{e+1} \tag{4.7}$$

$$r(\theta,e) = \frac{4(1-e^2)\cos^2\theta + (2e-1)^2}{2(1-e^2)\cos\theta + (2e-1)[4(1-e^2)\cos^2\theta + 5e^2 - 4e]^{1/2}} \tag{4.8}$$

In the above expressions ξ, ρ, θ are Heigh-Vestergaard coordinates, $f_c^{'}$ is compressive strength and $f_t^{'}$ is tensile strength. Parameter *e* represents the roundness of the failure surface and its value between 0.5 and 1.

The failure surface can move according to value of strain hardening/softening parameter. Parameter *c* controls the hardening/softening for Menetrey-William surface and its value between 0 and 1. The value of *c* is computed by the following formula;

$$c = (\frac{f_c^{'}(\varepsilon_{eq}^{p})}{f_c^{'}})^2 \tag{4.9}$$

$f_c^{'}(\varepsilon_{eq}^{p})$ points out the hardening/softening law. This law is resulted from the uniaxial compressive test and is shown in Fig. 4.2. (Van Mier, 1986)

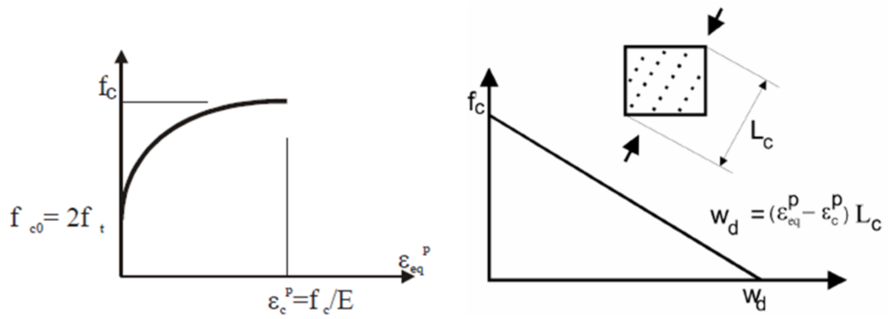

Figure 4.2 Compressive Hardening/Softening Rule Implemented in ATENA (Van Mier, 1986)

According to Fig. 4.2, the softening curve is linear and the elliptical ascending curve can be represented by the following expression;

$$\sigma = f_{c0} + (f_c - f_{c0})\sqrt{1 - \left(\frac{\varepsilon_c - \varepsilon_{eq}^p}{\varepsilon_c}\right)^2} \qquad (4.10)$$

The law on the ascending branch is based on strains ε_c^p; while the descending branch is based on displacements to introduce mesh objectivity into the finite element solution. About the descending curve, the equivalent plastic strain ε_{eq}^p is transformed into displacements w_d according to the length parameter L_c (Fig. 4.2). This parameter corresponds to the projection of element size into the direction of minimum principal stresses (Cervenka et al., 2013).

4.2.4 Strain Hardening Cementitious Composite Material Model Modification

In ATENA-GiD module a special material module is used for fiber reinforced concrete. It is named as “CC3DNONLINCEMENTITIOUS2SHCC” and it is an efficient material model for steel fiber reinforced concrete. The model has the same features stated in section 3.2.1, 3.2.2 and 3.2.3, except tensile softening trend and shear retention factor. The tensile softening trend and shear retention factor are changed according to the model proposed by Kabele (2002). Representative volume element (RVE), which includes both distributed multiple cracks (hardening) and localized cracks (softening), is introduced by this model (Fig. 4.3).

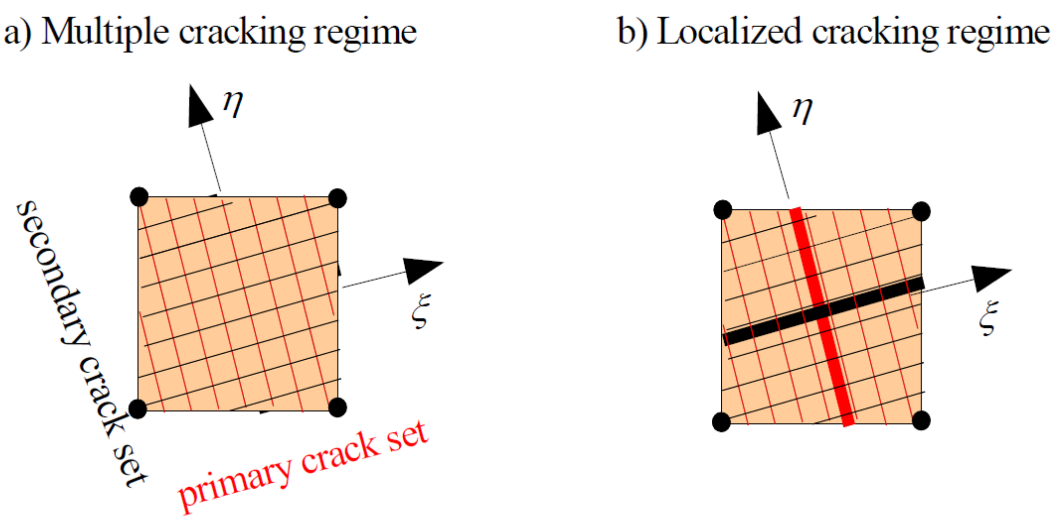

Figure 4.3 Representative Volume Element with Cracks (Cervenka et al., 2013)

Basic assumptions for RVE can be listed as follows (Cervenka et al., 2013):

a) Multiple Cracking Regime (Hardening)

- Parallel planar multiple cracks form when maximum principal stress reaches to first cracking strength ($\sigma_{\max} = \sigma_{fc}$).
- Crack planes are normal to the maximum normal stress ($\sigma_{\max}$).
- Secondary cracks are normal to primary cracks providing that normal stress in the related direction exceeds first cracking strength.
- Cracks can slide, if principal stress direction variation exists.
- Fiber bridging effect tries to prevent crack opening and sliding.
- According to cracking strains, crack opening and sliding displacements are averaged over the representative volume element.

b) Localized Cracking Regime (Softening)

- Formation of localized crack within a set of multiple cracks occurs if the related normal cracking strain exceeds the cracking strain capacity which is a material constant.

- Opening and sliding displacements of the localized cracks (Δ_i^{ξ}, Δ_i^{η}) are handled by the crack band model (they are converted into cracking strains by dividing them by the corresponding band with w_c^{ξ} or w_c^{η}).

The total strain of representative volume element is calculated as a summation of strain of material between cracks, cracking strains because of multiple cracks, and cracking strains resulted from localized cracks;

$$\varepsilon_{ij} = \varepsilon_{ij}^{s} + \varepsilon_{ij}^{mc,\xi} + \varepsilon_{ij}^{mc,\eta} + \varepsilon_{ij}^{lc,\xi} + \varepsilon_{ij}^{lc,\eta} \tag{4.11}$$

In this formulation, lower indices (*i*, *j*) refer to components of tensor or vector, upper indices (*mc*, *lc*) refer to multiple or localized cracks. ξ and η are associated primary and secondary crack directions, respectively.

Crack opening of the material model is shown in Fig. 4.4. It must be emphasized that for multiple cracks, it is assumed that they do not close unless exposed to crack-normal compression (plasticity-like unloading) while a localized crack is assumed to close so that normal stress decreases linearly to reach zero at zero crack opening displacement (COD) (Cervenka et al., 2013).

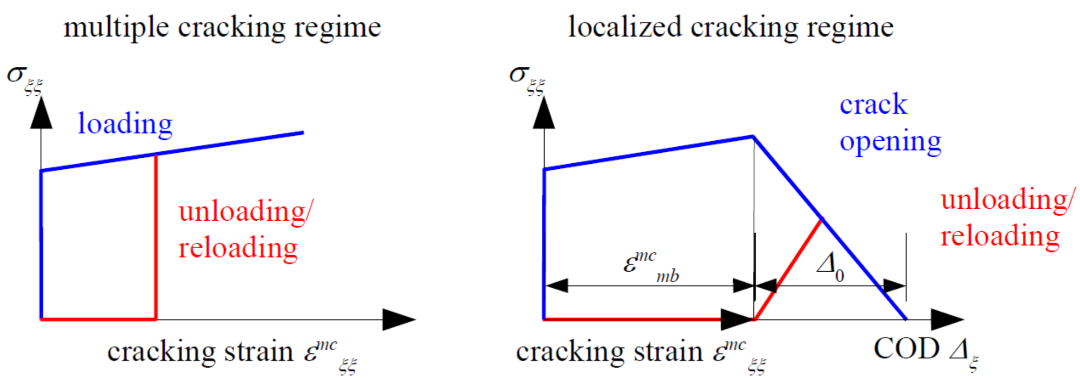

Figure 4.4 Stress vs. Cracking Strain Relations in Crack-Normal Direction (Cervenka et al., 2013)

The model for crack sliding phenomena is implemented by means of a variable shear retention factor β. The shear retention factor is defined as a ratio of the material post cracking shear stiffness G^c to its elastic shear stiffness *G*,

$$\varphi = \frac{G^c}{G} \tag{4.12}$$

Let us determine stiffness G^c, while considering the most general 2-D case of an element, which contains two perpendicular sets of multiple cracks and two perpendicular localized cracks. If the problem is defined in plane $\xi - \eta$, then the total engineering shear strain has only one non-zero component, which is obtained as:

$$\gamma_{\xi\eta} = 2\varepsilon^{s}_{\xi\eta} + 2\varepsilon^{mc,\xi}_{\xi\eta} + 2\varepsilon^{mc,\eta}_{\xi\eta} + 2\varepsilon^{lc,\xi}_{\varepsilon\eta} + 2\varepsilon^{lc,\eta}_{\xi\eta} \tag{4.13}$$

which can be rewritten with use of the shear bridging model (Kabele, 2002) as:

$$\gamma_{\xi\eta} = [\frac{1}{G} + \frac{1}{M(\varepsilon^{mc,\xi}_{\xi\xi})} + \frac{1}{M(\varepsilon^{mc,\eta}_{\eta\eta})} + \frac{1}{w^{\xi}_{c} N(\Delta^{\xi}_{\xi})} + \frac{1}{w^{\eta}_{c} N(\Delta^{\eta}_{\eta})}]\sigma_{\xi\eta} = \frac{1}{G^c}\sigma_{\xi\eta} \tag{4.14}$$

Functions *M* and *N* are defined by;

$$M(\varepsilon) = \frac{V_f k G_f}{2\varepsilon} \tag{4.15}$$

$$N(\Delta) = (\frac{1}{2} - \frac{\Delta}{2\Delta_0}) \frac{V_f k G_f}{\Delta[1 + \frac{4kG_f}{3E_f}(\frac{\Delta}{d_f})^2]}, \quad \text{for } \Delta \le \Delta_0 \tag{4.16}$$

Here V_f is the fiber volume fraction, G_f is the fiber shear modulus, E_f is the fiber Young's modulus, d_f is the fiber diameter, and k is the fiber cross-section shape correction factor. The quantity Δ_ξ and Δ_η indicates the crack opening in direction ξ and η, respectively. The parameter Δ_0 represents the limiting value of the crack opening displacement, when no tensile stress can be transferred across the crack, i.e. the point when the stress-displacement diagram in Fig. 4.4 drops to zero. These parameters are to be supplied by the user with the exception of the parameter Δ_0 , which is automatically extracted from the provided stress-strain law for tension. The shear retention factor is then expressed as (Cervenka et al., 2013);

$$\varphi = \frac{1}{1 + G[\frac{1}{M(\varepsilon_{\xi\xi}^{mc,\xi})} + \frac{1}{M(\varepsilon_{\eta\eta}^{mc,\eta})} + \frac{1}{w_c^{\xi} N(\Delta_{\xi}^{\xi})} + \frac{1}{w_c^{\eta} N(\Delta_{\eta}^{\eta})}]} \tag{4.17}$$

Note that for an element containing only multiple cracks (before localization) $\Delta_{\xi}^{\xi} = \Delta_{\eta}^{\eta} = 0$ and $1/N$ terms approach zero. For an uncracked element, $\varepsilon_{\xi\xi}^{mc,\xi} = \varepsilon_{\eta\eta}^{mc,\eta} = \Delta_{\xi}^{\xi} = \Delta_{\eta}^{\eta} = 0$ and $1/M$ and $1/N$ approach zero, giving φ =1.

4.3 Finite Element Modeling of SFRC Corbels

In this thesis, 84 steel fiber reinforced concrete corbels which had been experimented by Fattuhi and Hughes (1989-1994) were modeled by ATENA. Required material parameters for FE modeling were taken from related articles of Fattuhi and Hughes (1989-1994) whose experimental data are listed in Table A.1. Experimental set-up of Fattuhi and Hughes is shown in Fig. 4.5.

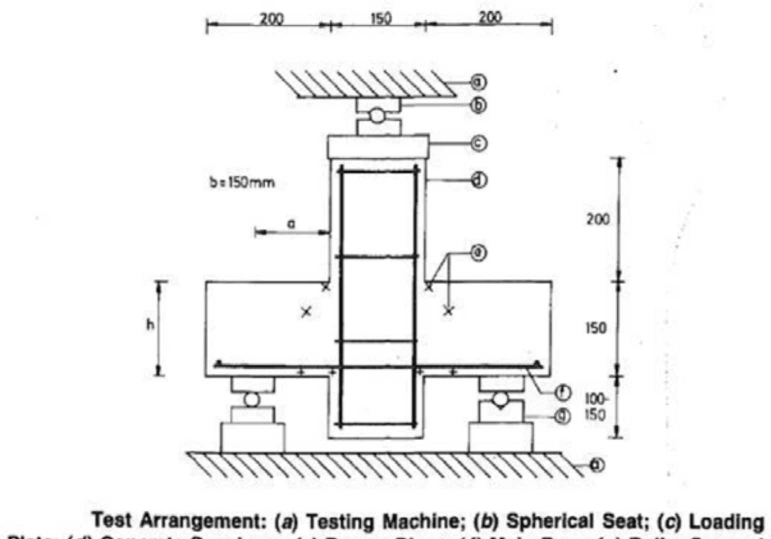

Figure 4.5 Test Configuration of Corbels Experimented by Hughes and Fattuhi (1989-1994)

Elastic perfectly plastic (bilinear) model was used for reinforcement modeling. Steel plates were modeled by the use of three dimensional elastic isotropic material model to prevent premature failure of the corbels. Effective concrete material model provided by the software (ATENA), called as “3D Nonlinear Cementitious 2” was used to model the concrete material behavior. Basic assumptions of the model are stated in Section 3.2. To reflect the effect of fibers, a small modified version of “3D Nonlinear Cementitious 2”, called as “CC3DNonlinCementitious2SHCC” was used by ATENA-GiD. All parameters stated to both models are same, except properties of fibers (volume fraction, diameter etc.) can be specified to latter one. Perfect connection between the reinforcement and concrete material was assumed for analyses. Smeared crack approach and fixed crack model were selected for nonlinear finite element analyses of the corbels. Finite element model and reinforcement configuration of a typical corbel are shown in Fig. 4.6a and 4.6b, respectively.

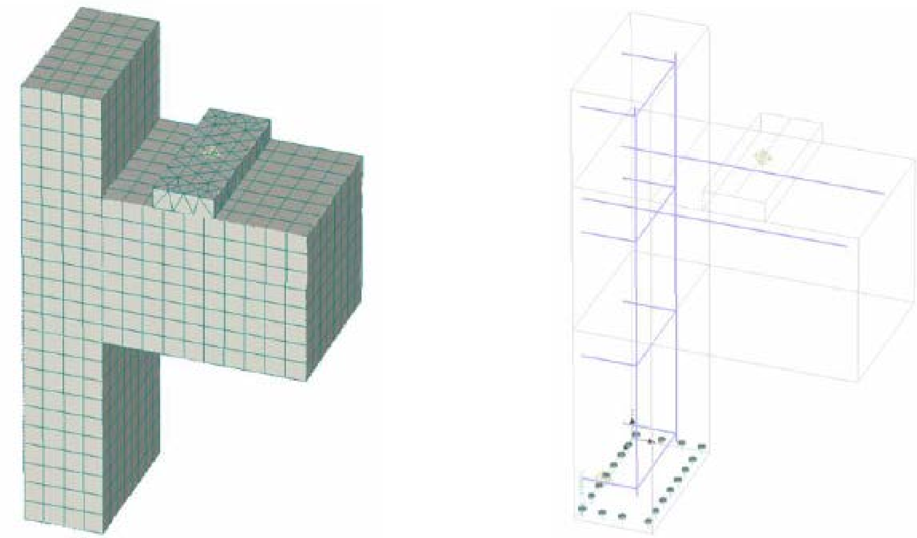

a) Mesh Configuration b) Reinforcement Configuration

Figure 4.6 Finite Element Model of a Typical SFRC Corbel

Half of the system was modeled to save time and disc space. Therefore, symmetry surface of the corbel was restrained to prevent translation and rotation along this surface. The plate on the corbel was restrained in vertical direction and also restrained in the direction along the corbel width to prevent the rigid body motion along this direction. Loading scheme of FE solution was achieved as upside down configurations. That is, initial displacement (0.1 mm) is given to the bottom surface of the column in upward direction and it was increased step by step as 0.1mm. Displacement values were recorded from bottom surface of column part and support reactions were obtained from the middle of the steel plate on the corbel (Fig. 4.6).

Perfect connection was assumed between steel plate and the corbel on the contact surface. On the contact surface of the plate and corbel, master element and slave element was selected by the software automatically to achieve mesh consistency. The software selects the element which has rougher meshes as master element and regulates the element type of corbel and plate accordingly. Therefore, mesh compatibility was achieved by the mesh generator of the software. Newton-Raphson method was used as solution algorithm.

Various sizes (0.012, 0.015, 0.02, 0.025 and 0.03m) were tried for meshing process. Mesh size versus load carrying capacity graph of T3 corbel is shown in Fig. 4.7. According to graph, there is no big difference between results of considered mesh sizes. Indeed, 4-6 elements per thickness are sufficient for bending problems. However, 8 elements per thickness, that is 0.02 m was selected as mesh size to achieve all failure modes including bending and to obtain both good accuracy and crack propagation by the consideration of time saving.

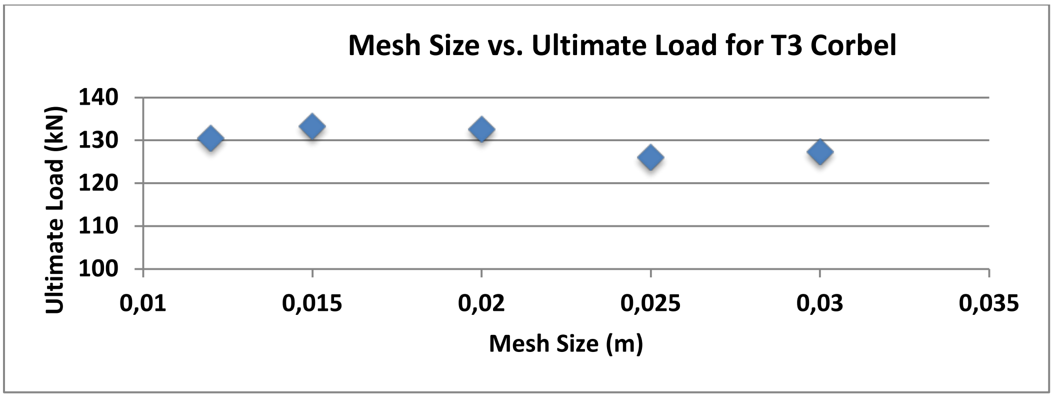

Figure 4.7 Mesh size vs. Ultimate Load for T3 Corbel

4.4 Results of Finite Element Analyses

According to FE results listed in Table A.1, ultimate load capacities of SFRC corbels calculated by nonlinear finite element analysis (V_{NLFEA}) were observed to very close to experimental results (V_{exp}). Mean, standard deviation, coefficient of variation and coefficient of correlation of V_{NLFEA}/V_{exp} were calculated as 1.036, 0.048, 0.047 and 0.974 respectively. These results prove the accuracy of nonlinear finite element analyses of considered corbels (Fig. 4.8).

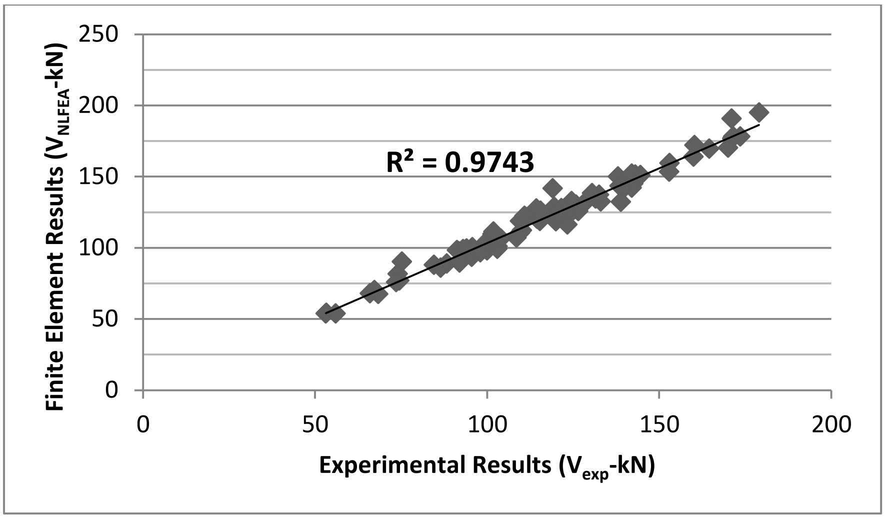

Figure 4.8 Comparisons between Finite Element and Experimental Results about Load Carrying Capacities

Additionally, crack patterns of FE models at ultimate load were compared with experimental results carried out by Fattuhi and Hughes (1989 and 1990) which were observed to be very similar to each other. In Figs. 4.9-4.14, comparison of crack patterns between FE analyses and experimental results are shown.

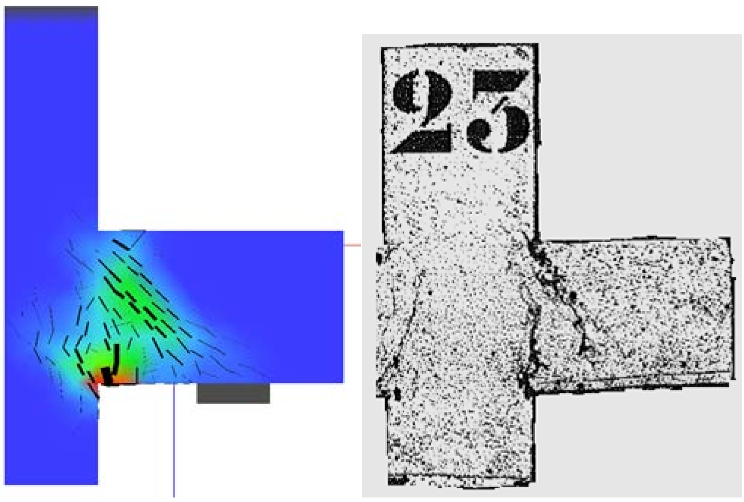

Figure 4.9 Comparison of Crack Pattern for Corbel Number 23

Not only crack patterns, but also failure modes of corresponding corbels were observed to be almost the same for experimental and finite element results (For example, the failure mode is of flexural type for corbel 23 and of shear type for corbel 35). Maximum crack widths and crack patterns occur in same regions for both results.

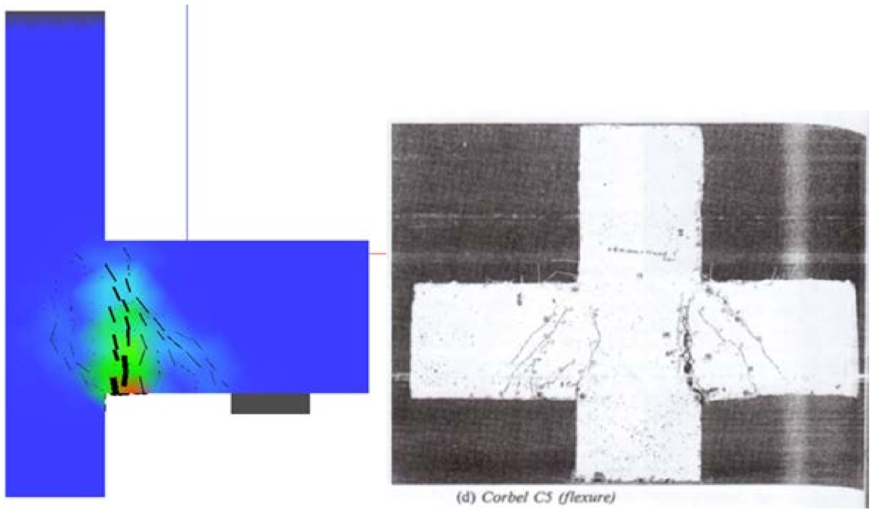

Figure 4.10 Comparison of Crack Pattern for Corbel Number C5

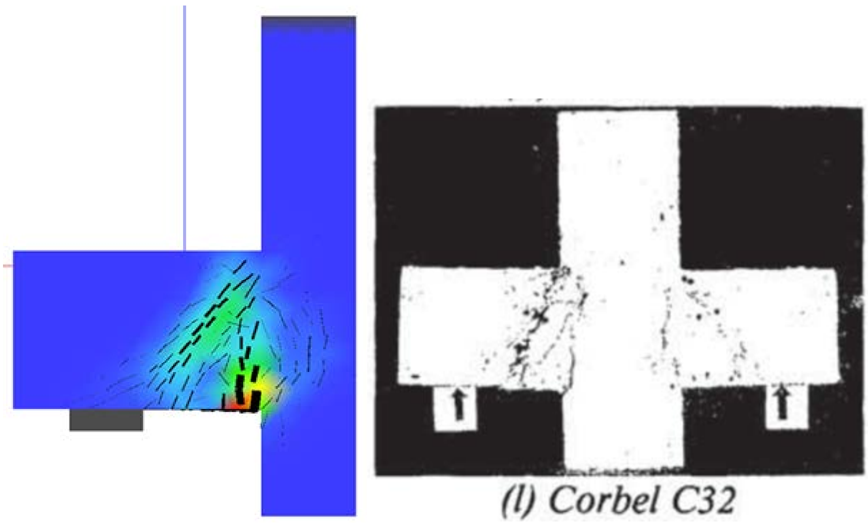

Figure 4.11 Comparison of Crack Pattern for Corbel Number C32

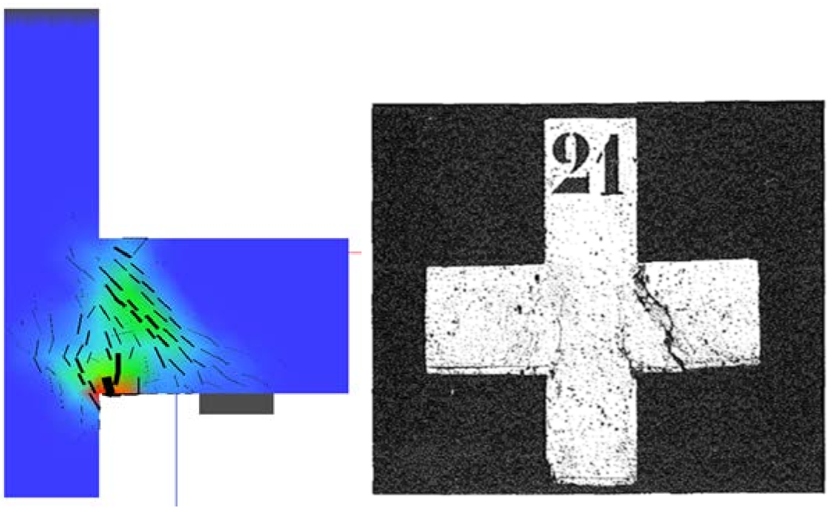

Figure 4.12 Comparison of Crack Pattern for Corbel Number 21

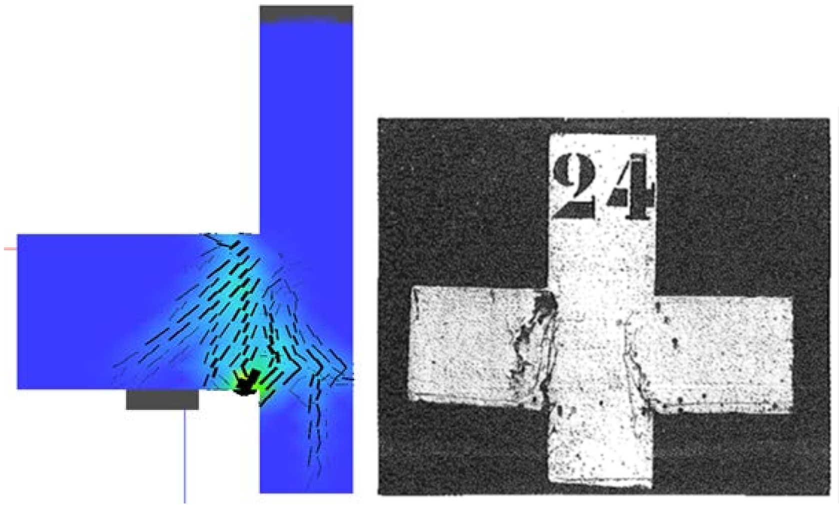

Figure 4.13 Comparison of Crack Pattern for Corbel Number 24

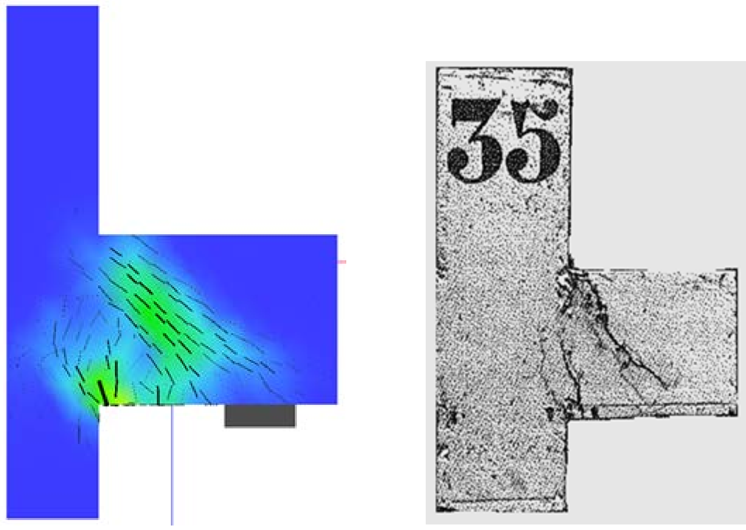

Figure 4.14 Comparison of Crack Pattern for Corbel Number 35

Finite element modeling of experimental studies which had been carried out for the thesis studies were also handled and it was observed that a good fit exist between results of finite element analyses and experimental results about load carrying capacities (Table A.1) and crack patterns (Figs. 4.15-4.20).

Maximum principal stress distribution of some corbels after first crack formation is shown in Figs. 4.21-4.24. Since steel fibers retard the first crack formation, maximum principal stresses are propagated more widely in corbels containing larger amounts of steel fibers. This situation can be observed between Corbel 23 (v_f =2%) and Corbel C5 (v_f =0.7%).

Figure 4.15 Comparison of Crack Pattern for Corbel Name 30-1-12-130

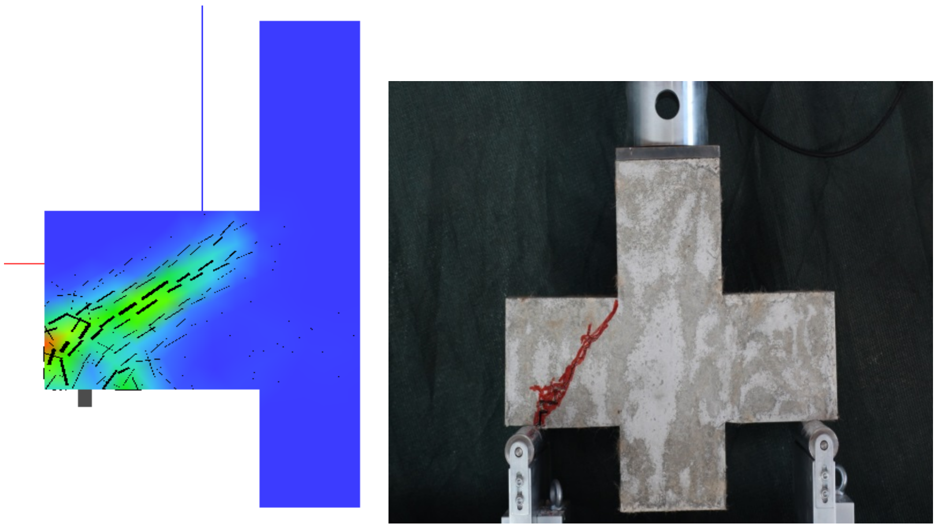

Figure 4.16 Comparison of Crack Pattern for Corbel Name 30-1.5-10-130

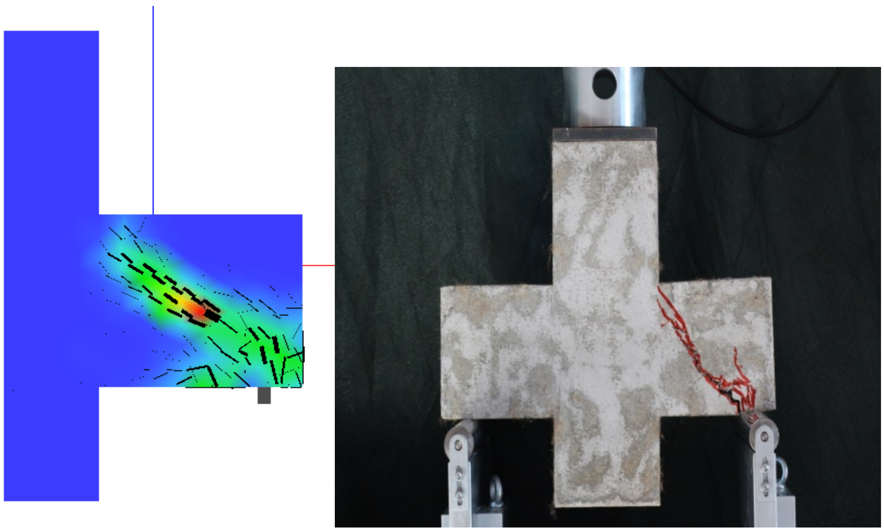

Figure 4.17 Comparison of Crack Pattern for Corbel Name 30-1.5-12-130

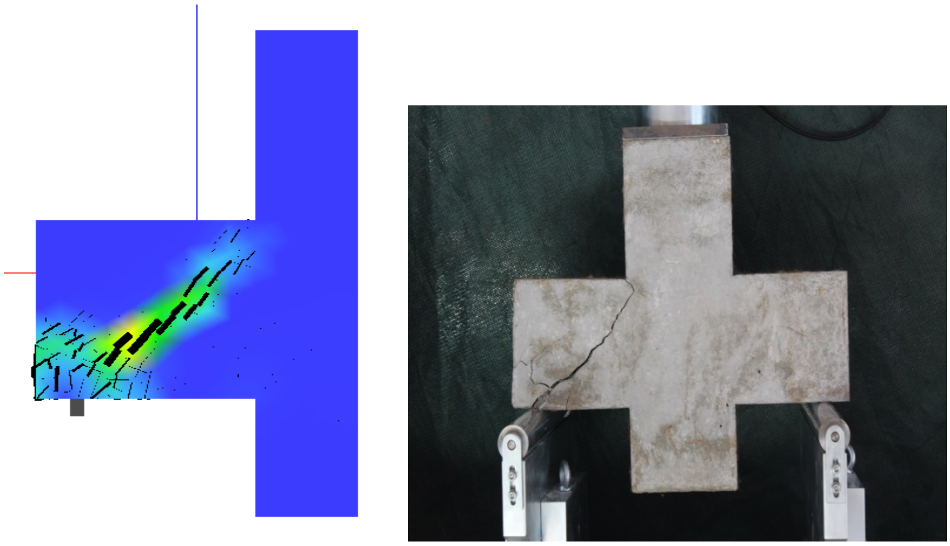

Figure 4.18 Comparison of Crack Pattern for Corbel Name 50-0-12-130

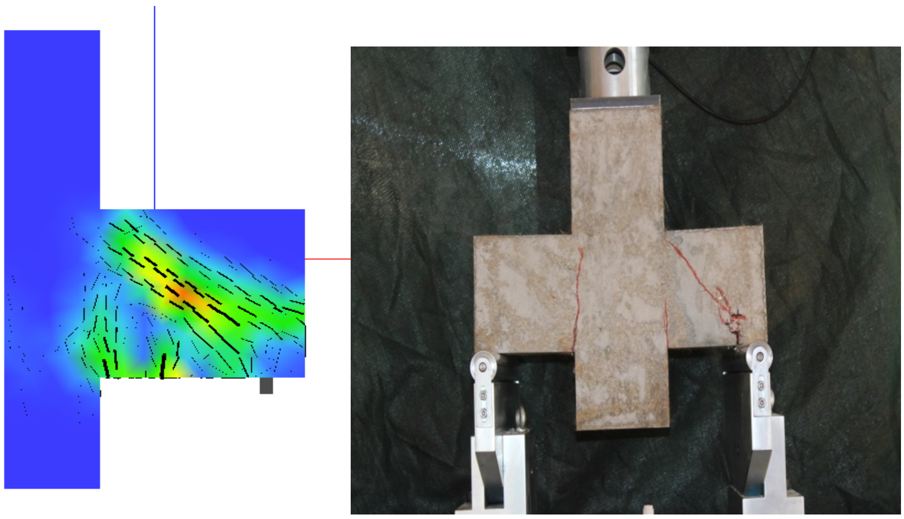

Figure 4.19 Comparison of Crack Pattern for Corbel Name 50-1-10-130

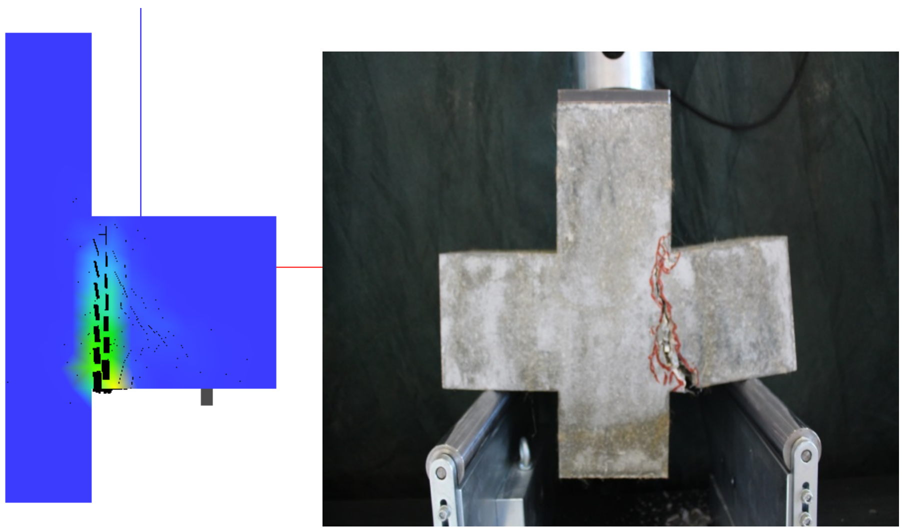

Figure 4.20 Comparison of Crack Pattern for Corbel Name 50-1.5-10-100

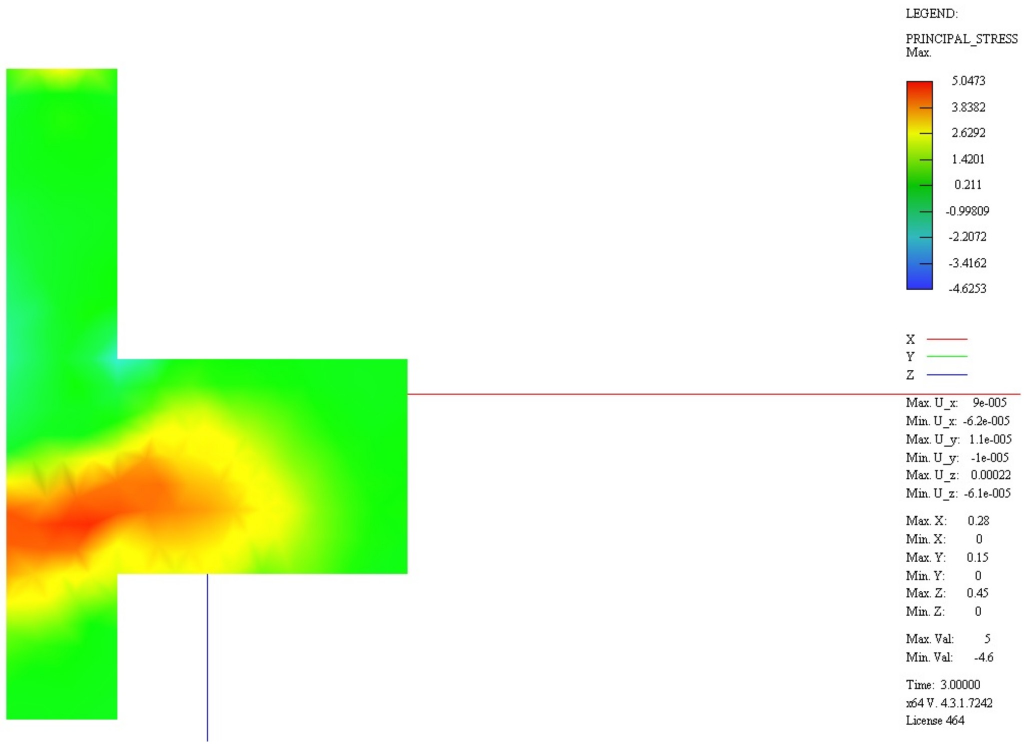

Figure 4.21 Maximum Principal Stress Distribution after First Cracking for Corbel 23

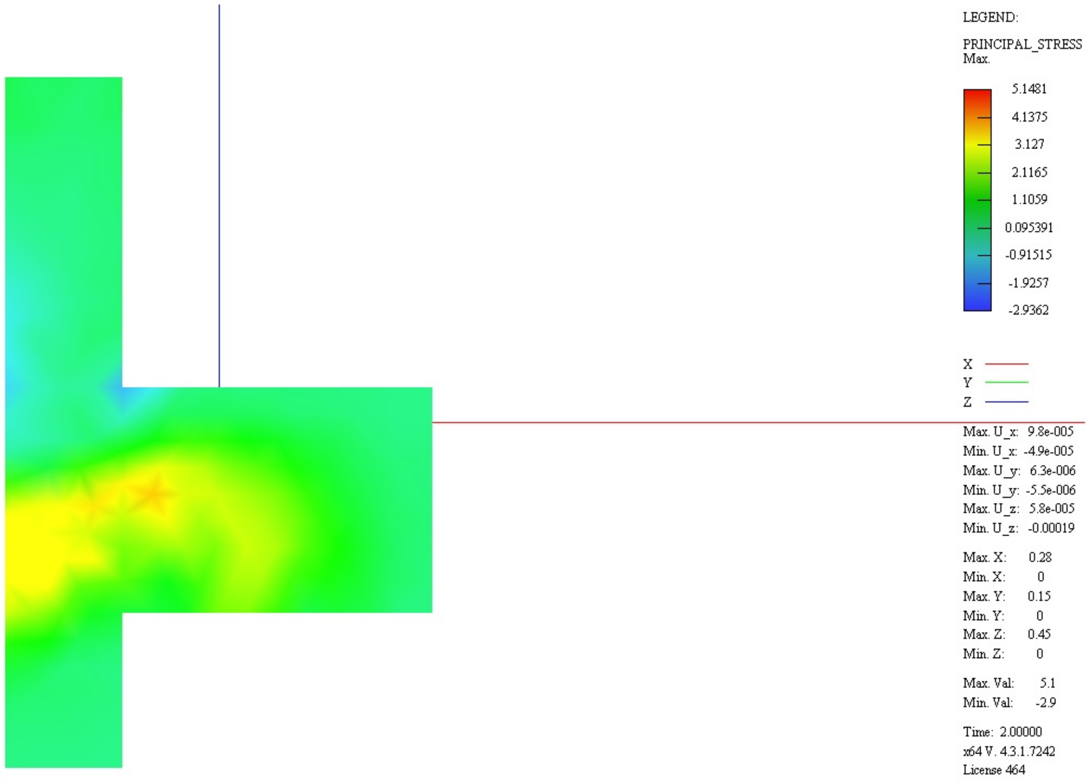

Figure 4.22 Maximum Principal Stress Distribution after First Cracking for Corbel C5

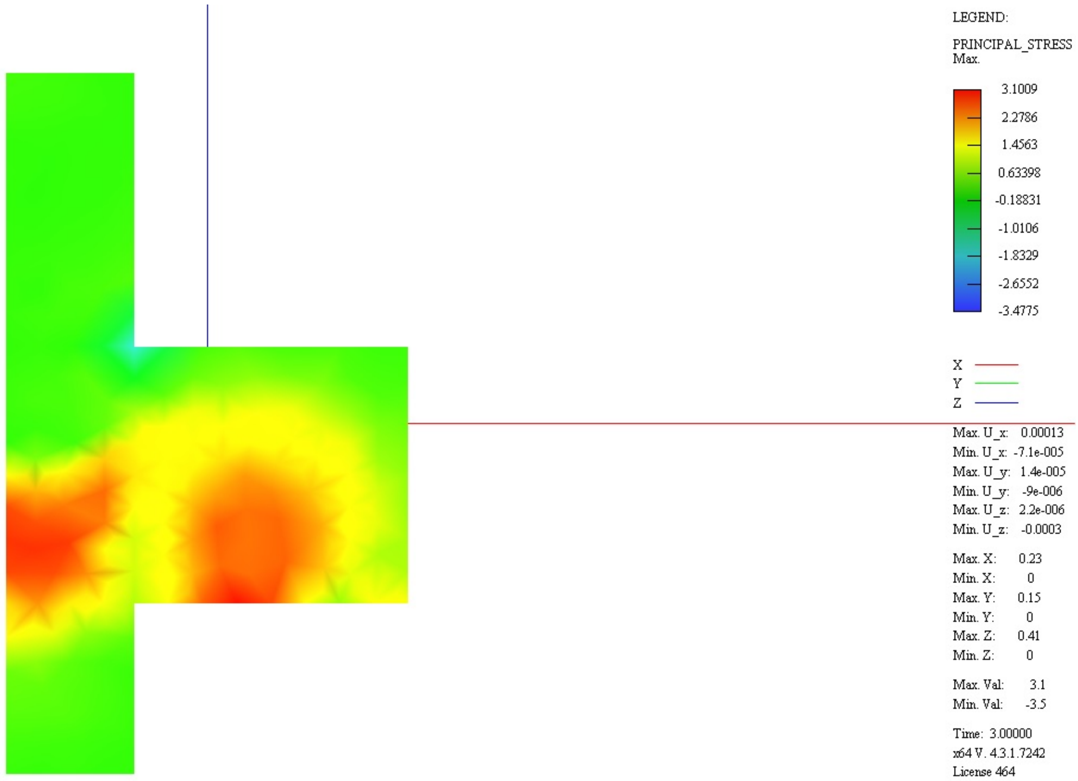

Figure 4.23 Maximum Principal Stress Distribution after First Cracking for Corbel 30-1.5-12-130

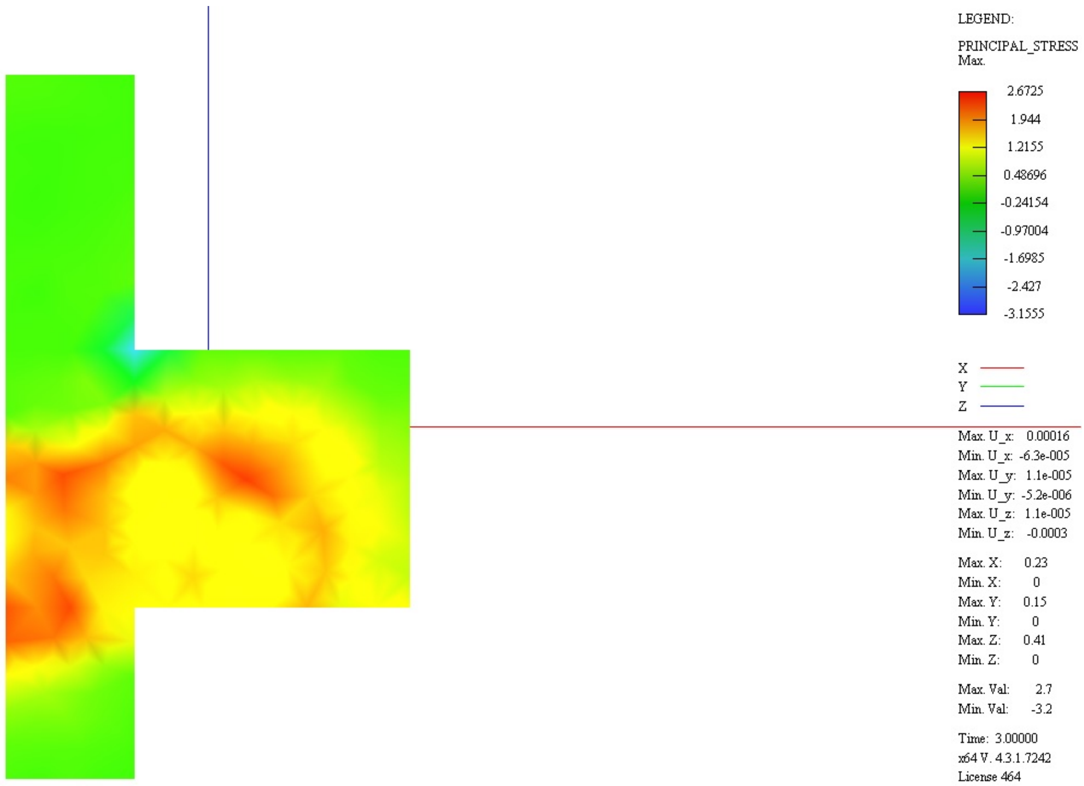

Figure 4.24 Maximum Principal Stress Distribution after First Cracking for Corbel 50-0-12-130

4.5 Crack Pattern and Failure Mode Analysis of Steel Fiber Reinforced Concrete (SFRC) Corbels

4.5.1 Introduction

Predicting crack pattern and failure type of a structural element during design process provides significant advantages about serviceability and maintenance of it. For instance, when strengthening a structural element, only specified regions can be strengthened by the true prediction of crack propagation and failure determination. Inexpensive rehabilitation can be achieved with such a process and life of a structure can be extended effectively. Required measures can be taken into account before failure of a structural element by an influential crack analysis.

Use of steel fibers instead of horizontal stirrups in reinforced concrete corbels is a new and modern application for the construction sector. Estimation of mechanical responses of SFRC corbels has been considered a complex phenomenon because of difficulties in modeling the mechanical properties of steel fiber reinforced concrete numerically and lots of changeable parameters i.e, steel fiber volume ratio, reinforcement ratio and tensile strength. However, by the development of computer and software technology, this topic can be handled effectively. Therefore, crack patterns and failure modes of SFRC corbels can be predicted truly beforehand by a complete and detailed finite element modeling process.

4.5.2 Parametric Study for Crack Patterns

Nineteen SFRC corbels which had been experimented by Fattuhi and Hughes (1989-1994) were considered for parametric study. Their mechanical and geometrical properties are listed in Table A.1. As a result of finite element analyses, reinforcement ratios, steel fiber volume ratios (indirectly tensile strengths) and shear span to effective depth ratios (*a/d*) are observed as the most important parameters which influence the ultimate load carrying capacity of SFRC corbels. Therefore, these parameters were selected for parametric study. For main reinforcement 2-ϕ8 mm, 2-ϕ10 mm, 2-ϕ12 mm and 3-ϕ12 mm reinforcement bars were used, which corresponds to 0.516%, 0.806%, 1.16% and 1.74% as reinforcement ratio (A_s / bd), respectively. Shear span values were selected as 89 mm, 110 mm and 125 mm which corresponds to 0.685, 0.846 and 0.962 as *a*/*d* ratio, respectively. Considered steel fiber volume ratio values are 0.7%, 1.4% and 2.1%. Since fiber volume ratio influences the tensile strength significantly, tensile strength values were also altered correspondingly. Tensile strength values were selected from samples which had been measured by Fattuhi and Hughes (1989) (C4, T5 and T12 corbels etc.) according to related compressive strength values. Tensile strength values are 4.79, 6.19 and 9.28 MPa which corresponds to 0.7%, 1.4% and 2.1% steel fiber volume ratio, respectively for cubic compressive strength values around 55 MPa (between 55 and 65 MPa). However, lower tensile strength values were used for the same steel fiber volume ratios (0.7%, 1.4% and 2.1%) corresponding to compressive strength values between 25 and 35 MPa to achieve the reliability of results. Usual values used in the precast structure sector were considered about compressive strength values of corbels (between 25-65 MPa). Besides, since steel fiber does not influence the compressive strength considerably and its effect on compressive strength of concrete is negligible, compressive strength values were not changed with respect to steel fiber volume ratio.

4.5.3 Parametric Study Results

As a result of lots of finite element analyses of SFRC corbels which were implemented by the alteration of the parameters stated in part 3.5.2, important results were obtained about crack pattern of SFRC corbels. The outputs can be listed as follows:

- For high tensile strength corbels (f_{ct} is above or nearly 6 MPa), if reinforcement ratio drops to 0.516% or smaller values, only flexural cracks occur in corresponding corbels (Fig. 4.25). The failure is not brittle, but in sudden manner.

- In low and normal tensile strength SFRC corbels (f_{ct} is below 6 MPa) whose reinforcement ratio reduces to 0.516% or smaller values (e.g. 2 - ϕ8 mm) and a/d ratio is 0.846 or higher value, both flexural and shear cracks are observed, but flexural cracks are predominant (Fig. 4.26). Therefore, if this rule and the rule stated above are considered, it can be said that the SFRC corbel fails certainly in flexural manner for almost all *a/d* ratio and possible steel fiber percentages as the reinforcement ratio drops to 0.516% or lower values (Fig. 4.27).

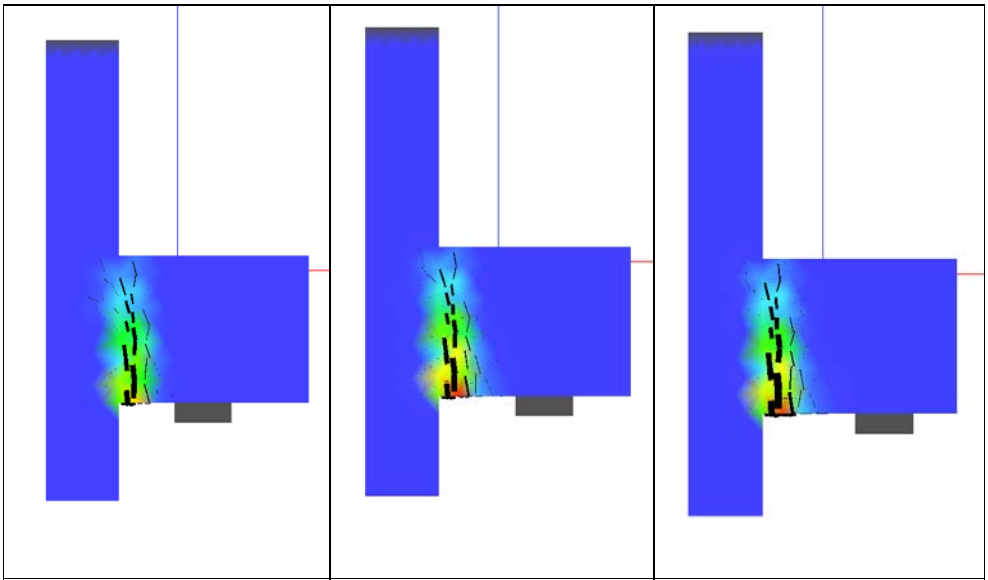

a) Corbel C29 (*a/d* = 0.685) | b) Corbel C29 (*a/d* = 0.846) | c) Corbel C29 (*a/d* = 0.962)

Figure 4.25 Crack Pattern of Corbel C29 under Same Reinforcement Ratio (0.516%) with Different Span Ratios (f_{ct} is above 6 MPa)

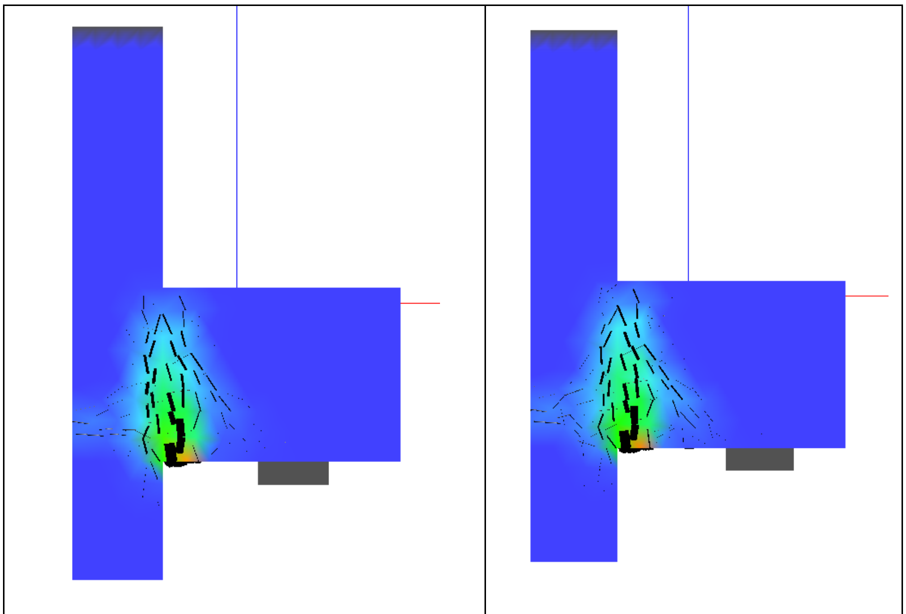

a) Corbel C5 (*a/d* = 0.846) | b) Corbel C5 (*a/d* = 0.962)

Figure 4.26 Crack Pattern of Corbel C5 under Same Reinforcement Ratio (0.516%) and with Different Span Ratios (f_{ct} is below 6 MPa)

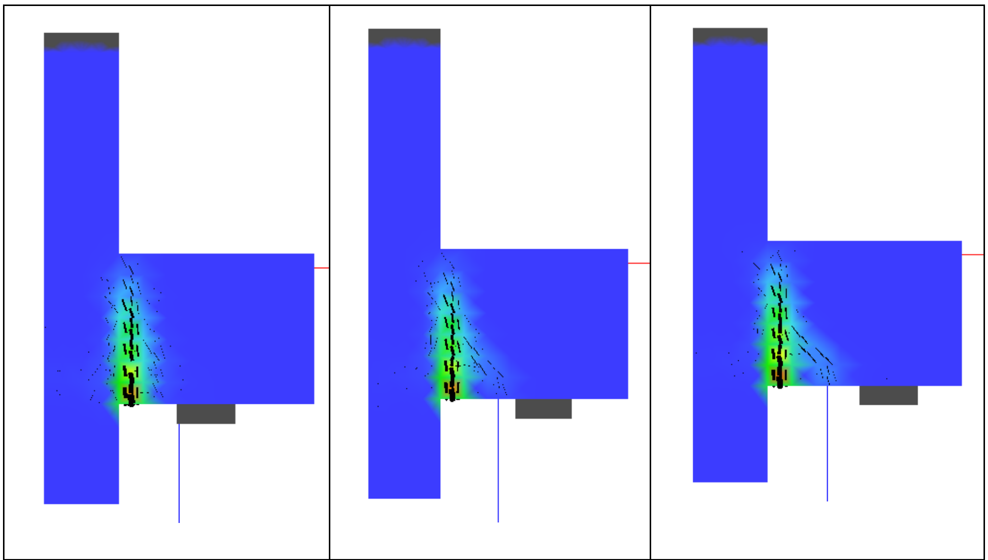

a) Corbel 24 (a/d=0.685) | b) Corbel 24 (a/d=0.846) | c) Corbel 24 (a/d=0.962)

Figure 4.27 Crack Pattern of Corbel 24 under Same Reinforcement Ratio (0.516%) and Fiber Percentage (0.7%)

- In low and normal tensile strength corbels, for reinforcement ratios above 0.516% (e.g. 2 - ϕ10 mm) and steel fiber volume ratios up to 1.4% both flexural and diagonal cracks form for almost all applicable a/d ratios (Fig. 4.28). However, as the reinforcement ratio is increased to 1.16% and higher values, flexural cracks start to lose its prepotency, especially in large *a/d* ratios (Fig. 4.29).

- Increase of steel fiber ratio not only influence the tensile strength of concrete and load carrying capacity of corbels, but also affect the crack width of SFRC corbels. Even if, the failure type and crack patterns are same, crack widths measured at failure becomes smaller, as steel fiber amount is increased.

- The shear span is not effective as much as reinforcement ratio about crack pattern of SFRC corbels. However, they influence the crack width at failure and ultimate load carrying capacity of SFRC corbels.

- For a/d ratio smaller than 0.96, increase of steel fiber volume decreases the diagonal cracks significantly. Flexural cracks become more predominant.

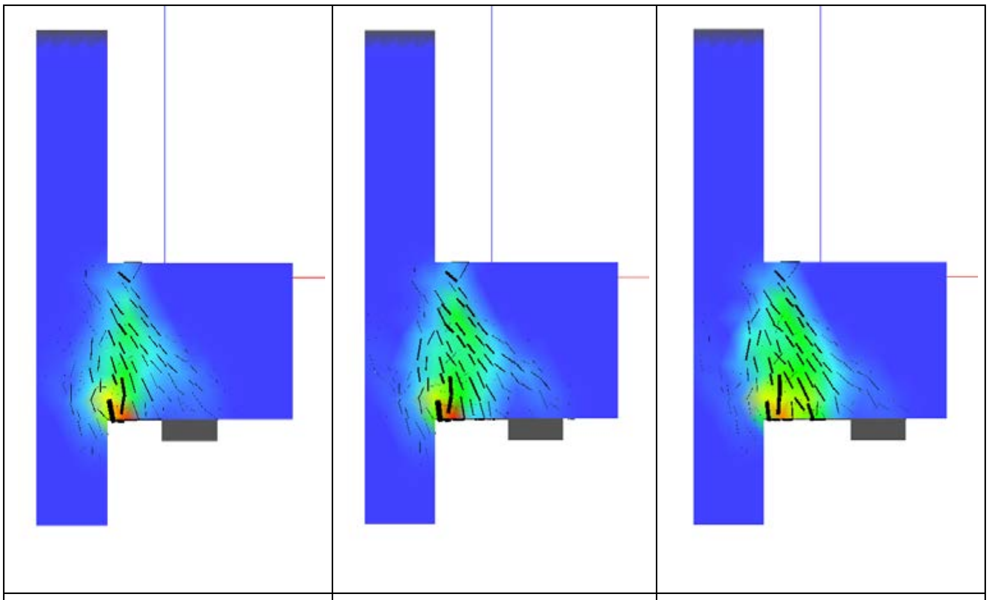

a) Corbel C27 (*a/d* = 0.685)	b) Corbel C27 (*a/d* = 0.846)	c) Corbel C27 (*a/d* = 0.962)

Figure 4.28 Crack Pattern of Corbel C27 under Same Reinforcement Ratio (0.806%) and Same Fiber Percentage (0.7 %) with Different Span Ratios

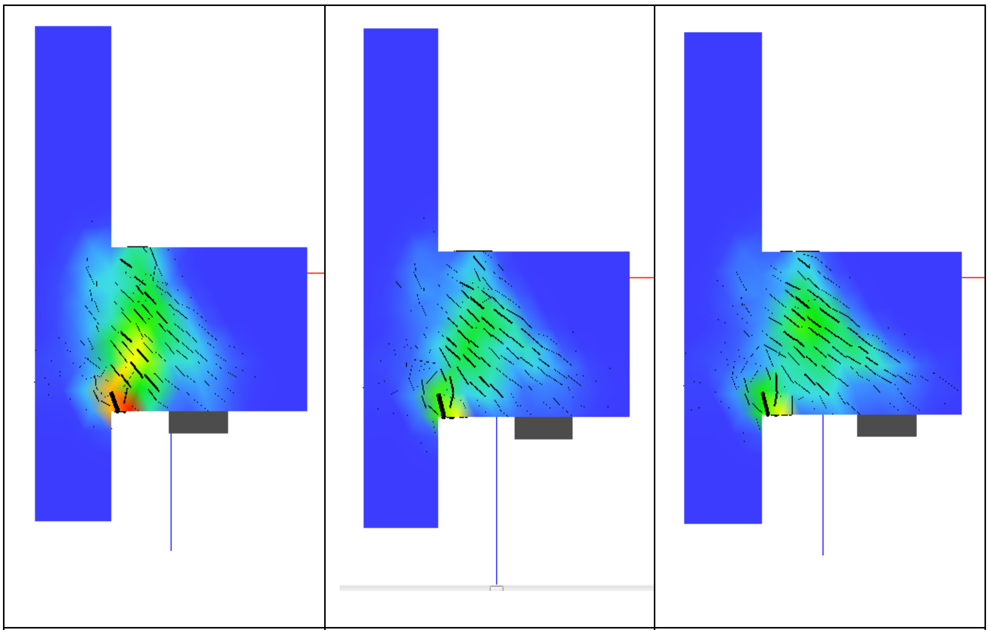

a) Corbel 35 (*a/d* = 0.685)	b) Corbel 35 (*a/d* = 0.846)	c) Corbel 35 (*a/d* = 0.962)

Figure 4.29 Crack Pattern of Corbel 35 under Same Reinforcement Ratio (1.579%) and Same Fiber Percentage (0.7%) with Different Span Ratios

- If tensile strength of concrete is very high (higher than 9 MPa), flexural cracks are predominant, even if *a/d* ratio is higher and reinforcement ratio is above 0.516%. However, both diagonal shear and flexural cracks can form by the alteration of steel fiber and reinforcement ratio. For instance, decreasing the steel fiber percentage (that is, decreasing the tensile strength for the same concrete) and increasing the reinforcement ratio above 0.516% leads to both flexural and shear cracks in the corbel as stated in the third rule of this section (Fig. 4.30).

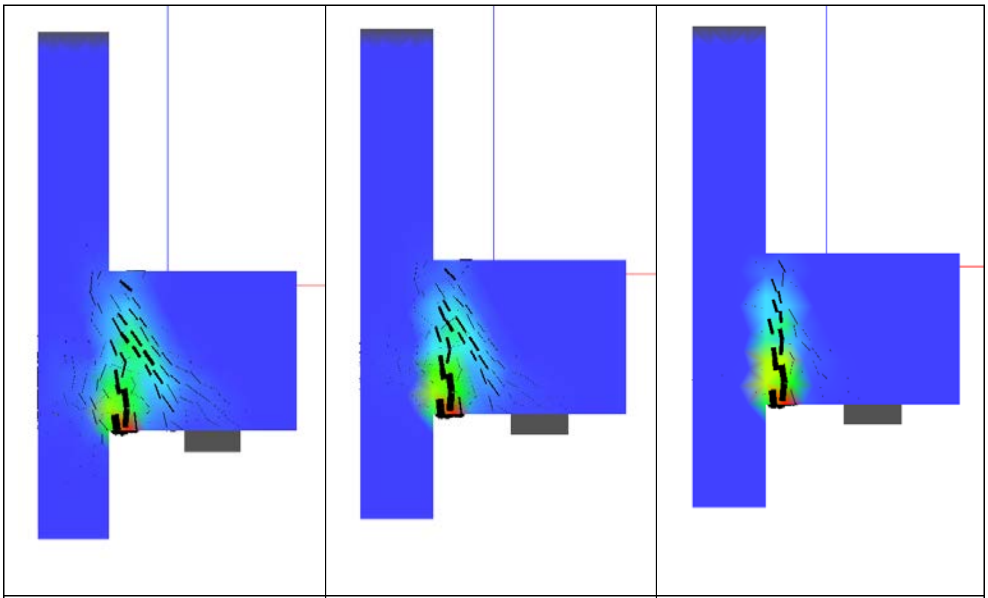

a) Corbel T5 (v_f =0.7%)	b) Corbel T5 (v_f =1.4%)	c) Corbel T5 (v_f =2.1%)

Figure 4.30 Crack Pattern of Corbel T5 under Same Reinforcement Ratio (1.16%) and Same *a/d* Ratio (0.846) with Different Amount of Steel Fibers

- For a/d ratios larger than or equal to 0.96, effect of increase of steel fiber content depends on the reinforcement ratio and resulting tensile strength. If reinforcement ratio is higher than or equal to 1.16% (e.g. 2 - ϕ12), diagonal cracks do not disappear even if volume fraction of the fiber increases. However, diagonal cracks are converted to flexural cracks when reinforcement ratio decreases below 1.16% and resulted tensile strength is higher than or equal to 6 MPa for lower compressive strength concrete corbels (Fig. 4.31).

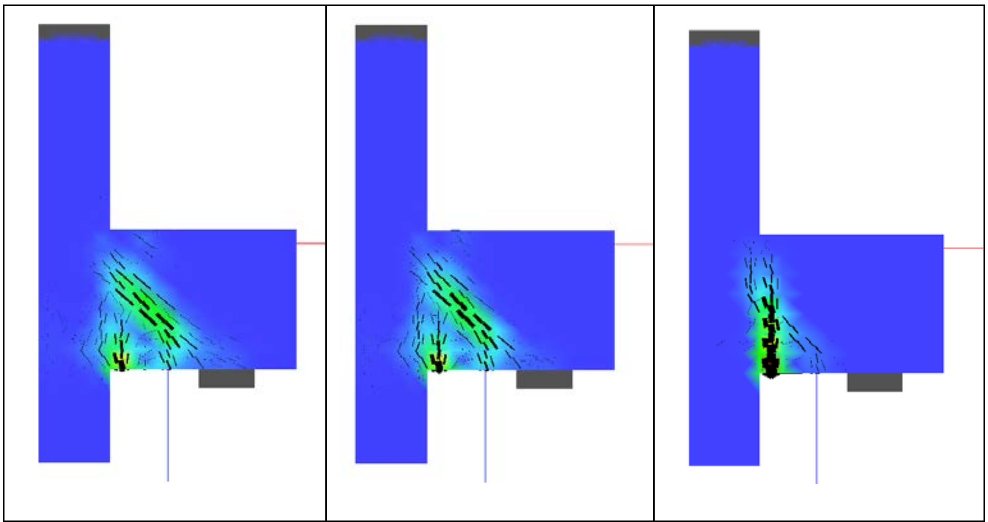

a) Corbel 24 (v_f =0.7%) Rein. Ratio = 1.16%	b) Corbel 24 (v_f =1.4%) Rein. Ratio = 1.16%	c) Corbel 24 (v_f =2.1%) Rein. Ratio = 0.806%

Figure 4.31 Crack Pattern of Corbel 24 under Same *a/d* Ratio (0.962)

4.6 Failure and Crack Formation Prediction for SFRC Corbels

According to the parametric studies implemented for crack patterns, experimental studies gathered from the literature and carried out in this thesis, inferences were made about failure mode and crack pattern of SFRC corbels. These inferences are corresponding to S420 class steel reinforcement, because it is the most frequently selected reinforcement class in the reinforced concrete and precast construction sector. The predicted failure modes are expressed in Figs. 4.32 and 4.33 as flowcharts. For given values of compressive strength, steel fiber amount (indirectly tensile strength), reinforcement ratio and *a*/*d* ratio, the failure mode and crack pattern of a SFRC corbel can be predicted easily by using these flowcharts. Shear span of typical corbels was selected between 6 and 14 cm during design and construction process. Therefore, proposed failure modes are valid between these shear span values. Moreover, applicable effective depth values were considered according to geometry of corbel (nearly 2 or 3 cm) for main reinforcement.

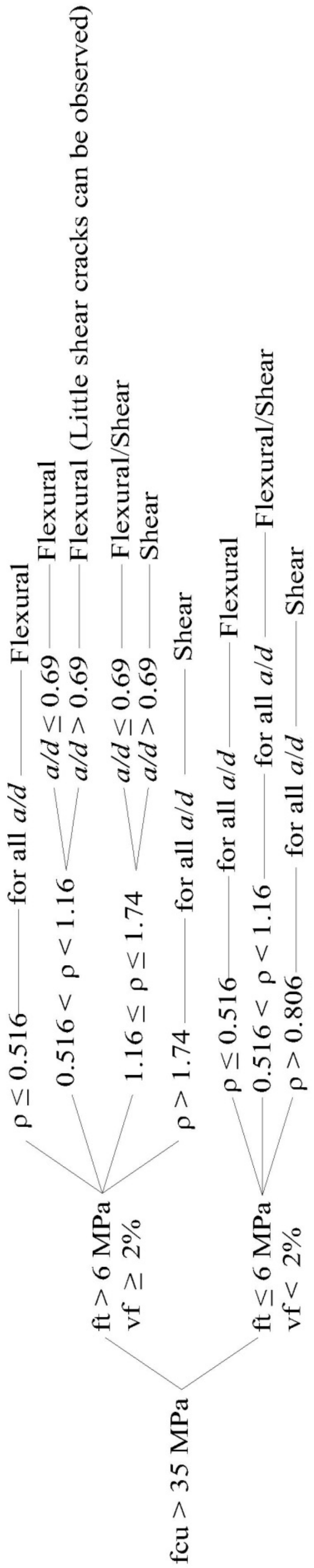

Figure 4.32 Prediction of Failure Mode of SFRC Corbels for f_{cu} > 35 MPa

Figure 4.33 Prediction of Failure Mode of SFRC Corbels for $f_{cu} \leq 35$ MPa

CHAPTER 5

PROBABILISTIC AND RELIABILITY ANALYSES OF STEEL FIBER REINFORCED CONCRETE (SFRC) CORBELS

5.1 Introduction

Stochastic and reliability analysis of steel fiber reinforced concrete (SFRC) corbels are mentioned in this chapter. Stochastic analysis of SFRC corbels were carried out by a special software, called as SARA. SARA works compatible with ATENA. SARA prepares the samples according to uncertainties in related inputs and sends it to ATENA for finite element analysis. Then, it gathers the results from ATENA and evaluates the results statistically. Reliability analysis of SFRC corbels was also implemented according to outputs of stochastic analysis. Finally, resistance factor, bias factor and coefficient of variation values were proposed based on reliability analysis results.

5.2 Reliability Analysis Concept

In general, logic of structural design is dimensioning the structural elements in a manner that it satisfies different criteria of safety, serviceability and durability under the applied loads. It can also be stated as the structure has to be designed such that its resistance is higher than the effect caused by the loads (Vorechovsky, 2004). Basic idea used for reliability analysis can be summarized in Fig. 5.1 by considering two variables. One is based on the load *S* on the structure and the other is based on resistance *R* of the structure. Both *S* and *R* are random in nature; their randomness is represented by the corresponding probability density functions $f_S(s)$ and $f_R(r)$, respectively. Qualitative measure of probability of failure can be determined by the area of overlap (shaded area in Fig 5.1) between the two curves (Novak et al., 2002).

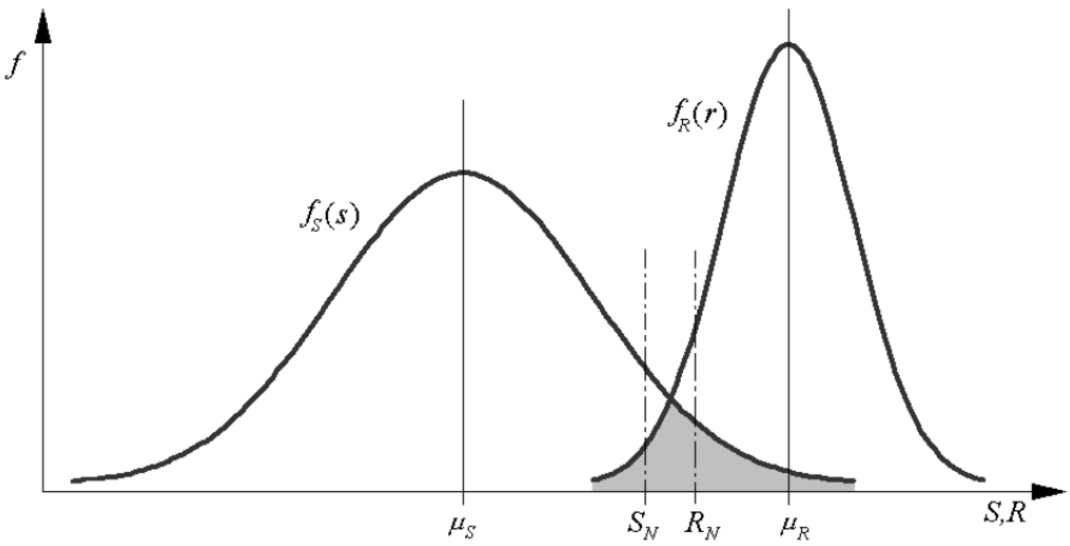

Figure 5.1 Determination of Probability of Failure (Novak et al., 2002)

This overlap area depends on three factors;

- **The relative positions of the two curves:** Distance between two curves is inverse proportional to the reliability (probability of failure) of the system. If distance between curves increases, the probability of failure decreases. Means of load and resistance (μ_s and μ_R) are factors to determine the positions of the curves.

- **The dispersion of the two curves:** Standard deviations (σ_S and σ_R) characterize the dispersion of the two variables. The probability of failure is small when the two curves are narrow.

- **The shape of the two curves:** Probability distribution functions ($f_S(s)$ and $f_R(r)$) determine the shape of curves of variables.

5.2.1 Limit State Function

Limit state function is a basic concept in structural reliability theory. Failure condition is determined by the function of considered random variables;

$$F = f(\mathbf{X}) = \mathrm{f}(X_1, X_2, X_3, \ldots\ldots, X_n) \tag{5.1}$$

In this formulation, $f(X)$ can be considered as computational model and demonstrates the functional relationship between inputs of vector **X**. Vector **X** is generally consisted of geometrical and material uncertainties.

Provided that F represents the safety region, $g(.)$ is called limit state function (L). The most famous equation of limit state function is obtained using the comparison of a real load (S) and resistance load (R);

$$L = R - S \tag{5.2}$$

The failure event is determined according to condition of L function. Whenever L takes negative value ($L < 0$), failure of the system occurs. While, if L > 0 condition is provided, the system is in survival region. Besides, determinacy of the structural collapse condition, limit state function also determines the line of equation to determine an important parameter defining the safety of a system called as, “Reliability Index”.

5.2.2 Reliability Index

Reliability index is frequently used safety parameter used in structural reliability concept. Second moment statistics (means and variance) are used to determine reliability index. Reliability index is defined as the distance from the mean of the limit state function to the limit state function itself;

$$\beta = \frac{\mu_F}{s_F} \tag{5.3}$$

where, μ_F and s_F are the mean and standard deviation values of the limit state function F, respectively. Indeed, reliability index is reciprocal value of coefficient of variation (COV) value of safety margin in this formulation.

It can be considered from Eq. (5.3) that reliability index is the minimum distance of function $f(X)$ to the origin in the analytical space. Hasofer and Lind (1974), propose a generalized equation for reliability index by this idea.

According to Hasofer and Lind (1974), the reliability index is the shortest distance from the origin of reduced variables to the line $f(Z_R, Z_S) = 0$

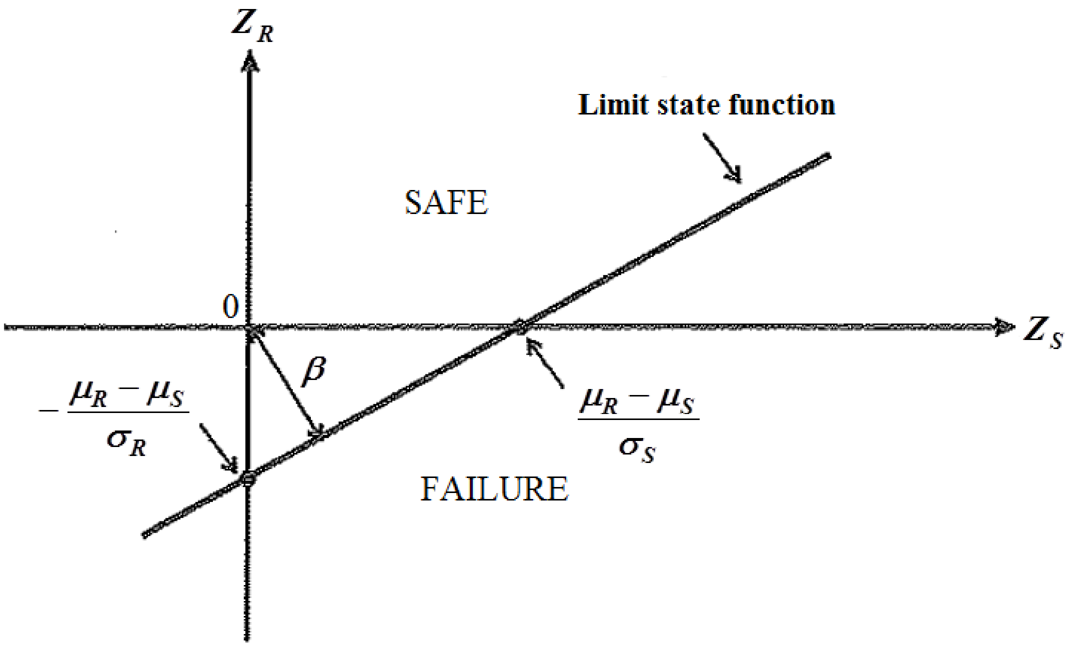

Figure 5.2 Relibility Index Expressed as the Shortest Distance in the Space of Reduced Variables (Nowak and Collins, 2000)

According to Fig 5.2, reliability index can be formulated by using the geometry;

$$\beta = \frac{\mu_R - \mu_S}{\sqrt{s_R^2 + s_S^2}} \tag{5.4}$$

In this formulation, μ_R and μ_S represent mean values, s_R and s_S represent standard deviation values of resistance load and external load, respectively.

For different limit state functions (other than $L = R$-S), determination of reliability index can be generalized as (Nowak and Collins, 2000);

- Set of reduced variables $\{Z_1, Z_2, Z_3, \ldots\ldots, Z_n\}$ are prepared by Eq. 5.5

$$Z_i = \frac{X_i - \mu_{X_i}}{s_{X_i}} \tag{5.5}$$

- Arrange the limit state function by the replacement of considered variables by the corresponding reduced variables $\{Z_1, Z_2, Z_3, \ldots\ldots, Z_n\}$.

- The reliability index is the shortest distance from the origin in the n-dimensional space of reduced variables to the curve defined by $g(Z_1, Z_2, Z_3,\ldots\ldots,Z_n) = 0$.

5.3 Stochastic Finite Element Method (SFEM)

Stochastic or probabilistic finite element method is a tool which uses finite element method to account for uncertainties in the geometry and/or material properties of a structure, as well as the external loads. Considered uncertainties are generally spatially distributed over the system region. Yamazaki et al. (1988), Vanmarcke et al. (1986), Kleiber and Hien (1992) showed several works on stochastic finite element method in their studies.

Even a small uncertainty in geometrical or material properties can adversely affect the safety of a structure. Moreover, sensitivity to these uncertainties can be more critical in case of highly nonlinear problems of nonlinear fracture mechanics problems. Therefore, stochastic analysis of concrete structures has become popular recently (Novak et al., 2002).

5.3.1 Modeling of Uncertainties

Uncertainties are modeled as random variables characterized by their probability distribution functions (PDF). Random values of selected uncertain parameters are generated according to probability distribution function of related parameters and specified statistical parameters (mean value, coefficient of variation, standard deviation) by robust sampling methods (Monte Carlo simulation, Latin Hypercube sampling). Set of input parameters for computational model are prepared as a result of modeling of uncertainties.

Several distribution functions exist in the literature (Normal, Lognormal, Weibull, Gumbel, Gausian etc.) to model uncertainties. However, theoretical knowledge is given in the following subsections for only PDF’s used in the thesis studies.

5.3.1.1 Normal distribution function

Normal distribution is the most commonly used probability distribution because it was found identical to the most natural phenomena. It was found that normal distribution is the best probability curve to show concrete strength in laboratory tests, which were performed on concrete in most countries of the world (El-Reedy, 2013).

The equation, mean and standard deviation of the function:

General equation: $f(x) = (\frac{1}{s2\pi^{0.5}})e^{-\frac{0.5(x-\mu)^2}{s^2}}$ (5.6)

Mean: $\mu = \frac{\sum x_i}{n}$ (5.7)

Standard Deviation: $s = [(\frac{1}{n})\sum x^2 - \mu^2]^{0.5}$ (5.8)

where, s is the standard deviation, μ is the mean of the distribution, x_i is value of each individual in population, n is number of samples in population.

5.3.1.2 Lognormal distribution function

This distribution is used when a phenomenon does not take a negative value. The equation, mean and standard deviation for lognormal distribution function is;

General equation: $f(x) = (\frac{1}{2\pi\eta})x^{-1}e^{-(inx-\frac{s^2}{2\eta^2})}$ (5.9)

Mean: $\ln \overline{x_G} = \frac{\sum(\log x)}{n} = \mu_G$ (5.10)

Standard deviation: $\ln s = [(\frac{1}{n})\sum(\ln x)^2 - (\ln \mu_G)^2]^{0.5}$ (5.11)

5.3.1.3 Weibull distribution function

Weibull (minimum) distribution is mostly used for fracture energy in probabilistic analysis of reinforced concrete structures.

The equation, mean and standard deviation for weibull minimum distribution function is (Nowak and Collins, 2000);

General equation: $f(x) = 1 - e^{-(\frac{x-\varepsilon}{u-\varepsilon})^k}$ for $x \geq \varepsilon$ (5.12)

Mean: $\mu = \varepsilon + (u+\varepsilon)\Gamma(1+\frac{1}{k})$ (5.13)

Standard deviation: $s = (u-\varepsilon)[\Gamma(1+\frac{2}{k}) - \Gamma^2(1+\frac{1}{k})]^{0.5}$ (5.14)

where u, ε and k are constant parameters, Γ is the gamma function and it is defined as;

$\Gamma(k) = (k-1)(k-2)................(2)(1) = (k-1)!$ (5.15)

5.3.2 Monte Carlo Simulation Technique

Latin Hypercube Sampling (LHS) method is used for preparing set of random input parameters. LHS is an advanced type of Monte Carlo simulation technique. Lots of simulations were generated in this technique. A pseudo-random value between 0 and 1 is generated for each random variable in each simulation. Then the generation of a variable X_i is achieved by the use of inverse transformation of cumulative probability distribution function (CPDF) of corresponding random variable (Novak et al., 2002). The sampling process is shown in Fig. 5.3. The general equation of Monte Carlo simulation method can be defined as stated in Eq. 5.16;

$x_{i,j} = \Phi_{X_i}^{-1}(u_{i,j})$ (5.16)

Where $\Phi_{X_i}(.)$ is the cumulative distribution function of X_i. Selected random variables for a structural system can have different CPDF's.

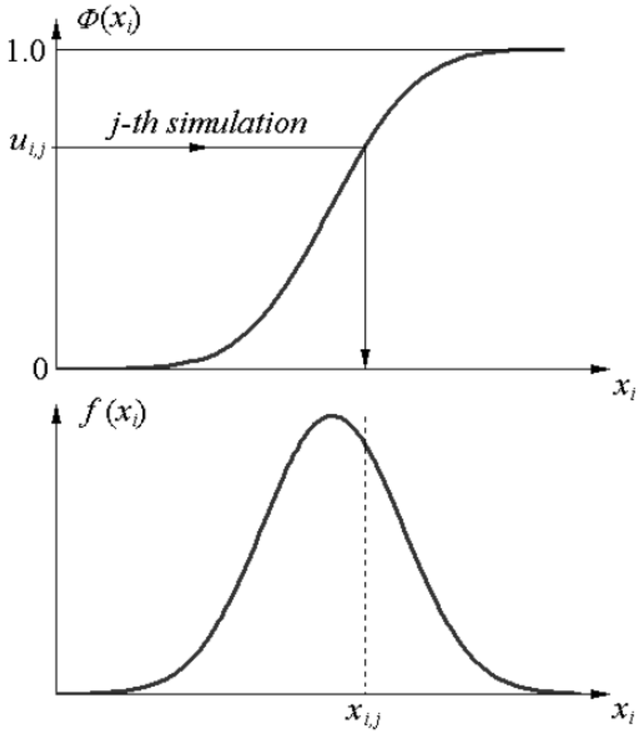

Figure 5.3 Generation of Random Values in Monte Carlo Simulation Technique (Novak et al., 2002)

5.3.3 Latin Hypercube Sampling (LHS) Method

Latin Hypercube Sampling (LHS) is a special type of Monte Carlo simulation technique which uses the stratification of the probability distribution function of input random variables. Efficiency of LHS for the determination of first two or three statistical moments of a structural response was proved by Novak and Teply (1991), Novak et al. (1998). LHS method requires a relatively small number of simulations as compared to crude Monte Carlo sampling method.

Latin Hypercube Sampling technique consists of two steps:

- Samples for each variable are strategically chosen to represent the variables CPDF
- Samples are ordered to match required statistical correlations among variables.

For first step of the technique, the probability distribution functions for all random variables are divided into *N* equivalent intervals (*N* is a number of repetitive calculations); the centroids of intervals are then used in simulation process. This means that the range of the probability distribution function $\Phi(X_i)$ of each random variable X_j is divided into N intervals of equal probability $1/N$ (Fig. 5.4). The samples are chosen directly from the CPDF with the following formulation (Novak et al., 2002):

$$x_{i,k} = \Phi_i^{-1}\left(\frac{k-0.5}{N}\right) \tag{5.17}$$

where, $x_{i,k}$ is the k-th sample of the i-th variable X_i, Φ_i^{-1} is the inverse of cumulative probability distribution function for variable X_i.

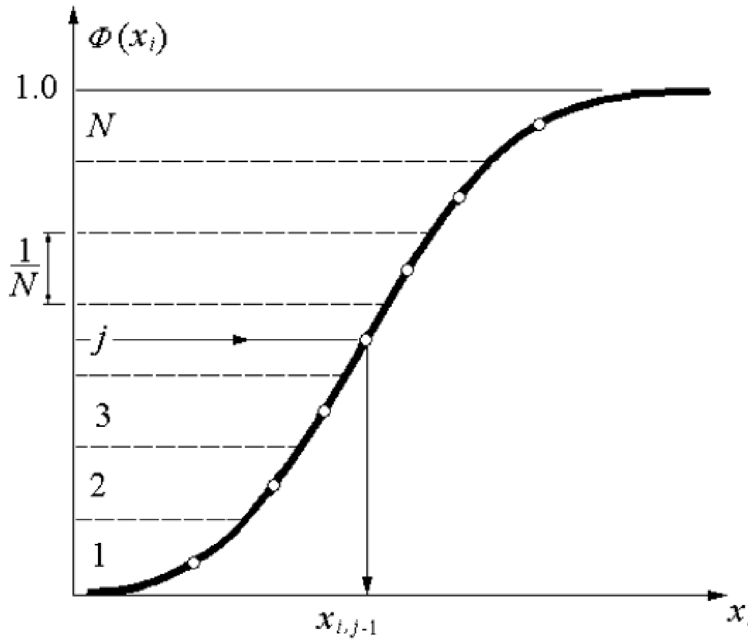

Figure 5.4 Sampling Process with LHS Technique (Novak et al., 2002)

The representative parameters of variables are selected randomly based on random permutations of integers 1, 2, 3, …..,j, ….., N. Every interval of each variable must be used only once during the simulation. Based on this precondition a table of random permutations can be used conveniently, each row of such a table belongs to the specific simulation and the column corresponds to one of the input random variables. Example of such a table is shown in Table 5.1 for a number of simulation, N = 10 and number of random variable, n = 5.

Table 5.1 Example of Random Permutation Table for LHS Method

N	***n***				
	1	**2**	**3**	**4**	**5**
1	5	4	6	3	7
2	4	8	10	5	3
3	3	7	7	2	6
4	8	3	1	8	10
5	10	1	5	4	9
6	2	2	8	1	5
7	7	5	2	6	4
8	9	10	4	9	2
9	1	6	3	7	8
10	6	9	9	10	1

An up-to-date technique was used to impose statistical correlation between basic random variables. The technique is based on the stochastic method of optimization called simulated annealing has been proposed by Vorechovsky and Novak (2003). The imposition of the prescribed correlation matrix into the sampling scheme can be understood as an optimization problem: The difference between the prescribed **K** and the generated **S** correlation matrices should be as small as possible. A suitable measure of quality of the overall statistical properties can be introduced, e.g. a norm which utilizes the deviations of all correlation coefficients:

$$E_{overall} = \sqrt{\sum_{i=1}^{N_V-1} \sum_{j=i+1}^{N_V} (S_{i,j} - K_{i,j})^2} \tag{5.18}$$

The norm E stated in Eq. 5.18 has to be minimized from the point of view of the definition of the optimization problem using simulated annealing optimization approach, N_v random variables realizations are related to the ordering in the sampling scheme.

5.4 Stochastic Analysis Implemented for SFRC Corbels

5.4.1 Inputs for Stochastic Analysis

As a result of nonlinear finite element analyses, it is concluded that the most important factors which influence the ultimate load carrying capacity of steel fiber reinforced concrete corbels are mechanical properties of steel fiber reinforced concrete. Therefore, uncertain parameters considered for stochastic analysis can be listed as follows;

- Tensile strength of steel fiber reinforced concrete (SFRC)
- Compressive strength of SFRC
- Modulus of elasticity of SFRC
- Fracture energy of SFRC

Mean value, coefficient of variation (*COV*) and probability distribution functions of related material characteristics are necessary to define the degree of uncertainty of corresponding material characteristics. These statistical and probabilistic parameters are listed in Table 5.2 (Mordini 2006). Related values specified by Fattuhi and Hughes for their experimental works were taken as mean values.

Besides uncertainty of SFRC properties, the correlation coefficients between each parameter are also important. For example, there is strong relationship between modulus of elasticity and compressive strength and this interdependence should be considered in stochastic analyses. Hence, material sets were prepared by taking into accounts both probabilistic parameters and relations between considered properties for repetitive calculations. In this manner, material sets which are contradictory to actual material behavior are avoided.

The correlation coefficients between considered material properties are specified in Table 5.3 by correlation coefficient matrix (Strauss et al., 2006).

Table 5.2 Probabilistic Parameters of Considered Uncertain Variables (Mordini, 2006)

Material Property	Probability Distribution Function (PDF)	Coefficient of Variation (COV)
f_c (Compressive Strength)	Normal	0.1
f_{ct} (Tensile Strength)	Lognormal (2 parameters)	0.12
E_c (Modulus of Elasticity)	Lognormal (2 parameters)	0.08
G_f (Fracture Energy)	Weibull min. (2 parameters)	0.25

Table 5.3 Imposed Correlation Coefficient Matrix between Considered Variables

	E_c	f_{ct}	f_c	G_f
E_c	1	0.7	0.9	0.5
f_{ct}		1	0.8	0.9
f_c			1	0.6
G_f				1

5.5 Stochastic Analysis Results

In this study, a special module, called as "SARA" is used for stochastic analysis of steel fiber reinforced concrete corbels. The stochastic analysis module (SARA) runs the FE program (ATENA) and sends the stochastic simulation results to the statistical module (FREET). 84 SFRC corbels which had been studied by Fattuhi and Hughes (1989-1994) were considered for stochastic analysis. Stochastic analyses were carried out according to the procedure stated by Bergmeister et al. (2009) and Novak et al. (2014). For each corbel, 30 material set inputs were prepared by taking into account the uncertainties in related material characteristics (by the use of Latin Hypercube Sampling Method). These 30 samples of each corbel were analyzed separately. Consequently, 2520 analyses were carried out in total and ultimate load carrying capacity resulted from each analysis was determined and recorded.

Results of stochastic analysis (minimum, maximum and mean load carrying capacities, standard deviations) are listed in Table A.2. Also the most suitable probability distribution function (PDF's) for each SFRC corbel according to dispersion of ultimate loads is listed in the same table. According to resulting suitable PDF results and the frequency of occurrence of PDF's among 84 SFRC corbels, it is extracted that the most suitable probability distribution function is "Lognormal 3. Parameter" type of distribution (Fig. 5.5). Also "Beta" and "Rayleigh Negative" type of distributions can be considered to represent the uncertainty in the ultimate load carrying capacity of steel fiber reinforced concrete corbels.

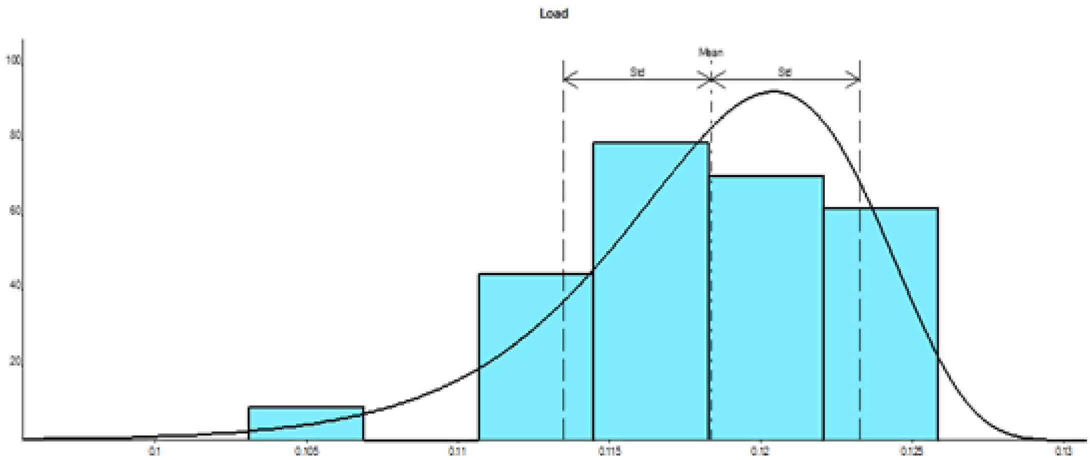

Figure 5.5 Probability Distribution of Load Carrying Capacity of Corbel Number 45 (Lognormal 3 parameter distribution)

Results of stochastic analysis indicate that the highest uncertainty was observed in corbel number 61 (Table A.2). Therefore, statistical outputs of this corbel (standard deviation (s) is 7.36 kN and *COV* is 0.074) can be used in design process and reliability calculations, as it is the most risky case.

As a result of sensitivity analysis, it was concluded that fracture energy and tensile strength of SFRC are the most sensitive parameters to uncertainty in load carrying capacity of SFRC corbels. Sensitivity results of corbel T4 for the load carrying capacity is displayed in Figs. 5.6 and 5.7 for tensile strength and fracture energy of the concrete. Similar outputs were obtained for almost all considered corbels. This is an expected situation, since orientation of steel fibers cannot be controlled during concreting process and so uncertainty in tensile properties of SFRC can be higher due to uncertainty in the orientation of steel fibers.

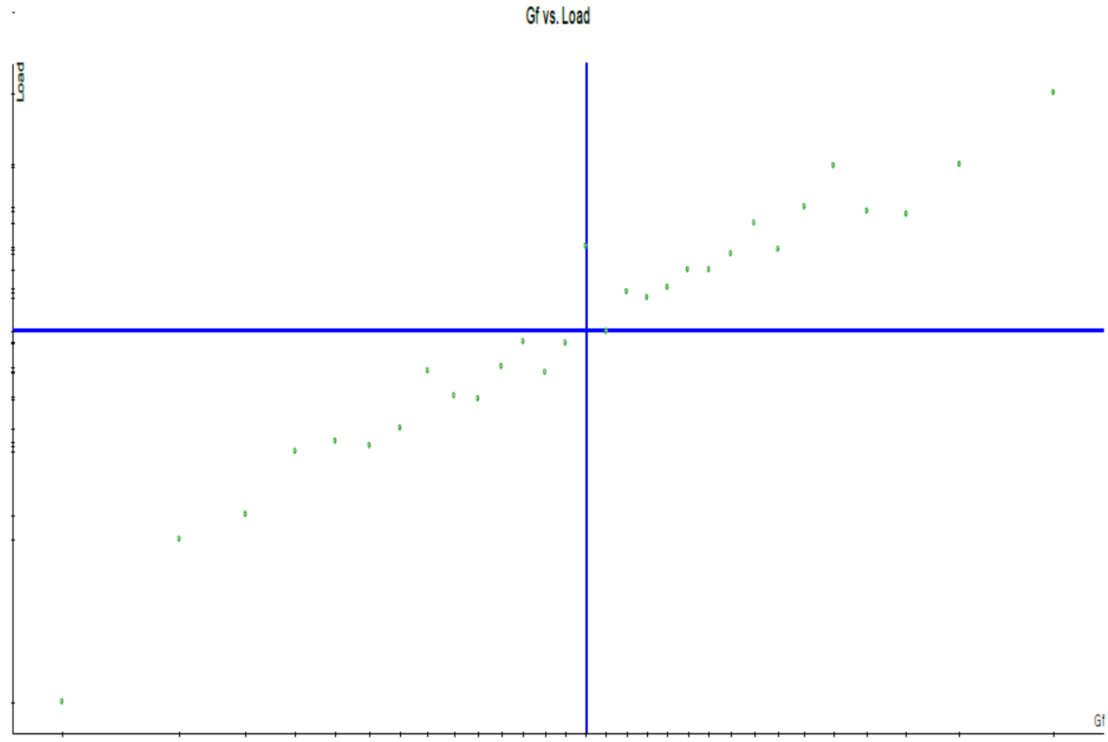

Figure 5.6 Sensitivity Analysis Results for Fracture Energy of T4 Corbel

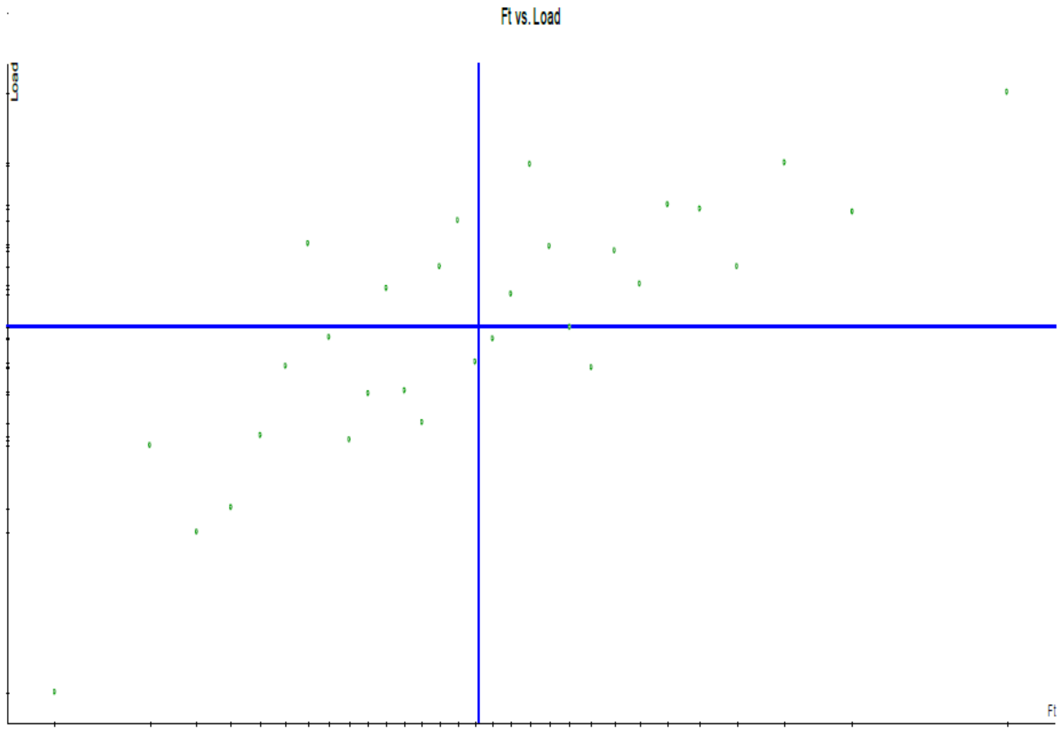

Figure 5.7 Sensitivity Analysis Results for Tensile Strength of T4 Corbel

5.6 Load and Resistance Factor Design Approach (LRFD)

Current design codes specify design and detailing requirements that are aimed to achieve a minimum acceptable safety level. Formulas and procedures are used to express the code provisions. In the allowable stress design (ASD) approach, the allowable strength is obtained by the division of strength of a material by a safety factor. In load and resistance factor design (LRFD) or limit state design (LSD), load components are multiplied by load factors and resistance is multiplied by a resistance factor (Nowak and Collins, 2000). Although load factor is greater than 1, resistance factor is smaller than 1. The basic form of the LRFD equation is:

$$\phi R \geq \sum \gamma_i Q_i \tag{5.19}$$

Where γ_i is a load factor applied to load component Q_i and ϕ is a resistance factor applied to the resistance (measure of load carrying capacity) R. The meaning of Eq. 5.19 is that the resistance of the structural member (modified by the factor ϕ) must be larger than the total effect of all the loads acting on the member. Code committees containing practicing engineers, researchers and scientists develop the design equations. Given this type of design equation, it is the designer's responsibility to make sure that for given load and resistance factors (specified in the code), the design loads and resistance satisfy the inequality expressed in Eq. 5.19 (Nowak and Collins, 2000).

5.7 Determination of Statistical Parameters of SFRC Corbel by Reliability Analysis

Since there is no design code on steel fiber reinforced concrete corbels, there is a lack of information about determination of their statistical parameters (bias factors, coefficient of variation, etc.). Moreover, absence of resistance factor (strength reduction factor) for SFRC corbels leads to difficulties about determination of design load carrying capacities (design resistance) to achieve required safety levels during design process. To overcome these shortcomings specified above, a method was proposed to determine bias factor (λ) and resistance factor (ϕ) for SFRC corbel. The procedure is given as follows (also stated as a flowchart in Fig. 5.8):

- Select a conservative target reliability index compatible with several design codes.

- Calculate the nominal dead load and nominal live load by the use of Eq. 5.4 according to the ratio of dead load to sum of dead load and live load (*D/(D+L)*) is equal to 0.5. Since corbels can be considered as a kind of beam and common load ratios in beams are between 0.3 and 0.7 (Szerszen and Nowak, 2003), 0.5 was considered to achieve a general approach.

- Calculate the nominal resistance of the corbel by the use of design formula which is commonly used in the literature considering several selected resistance factors. Design formula which is stated in ASCE 7-98 (1998) standard was considered for this study;

$$1.2D + 1.6L \leq \phi R \tag{5.20}$$

In this formula, D and L represent nominal dead load and nominal live load, respectively. R is nominal resistance and ϕ is strength reduction factor.

- Extract the mean resistance and coefficient of variation values of the corbels from results of stochastic finite element analyses of them.

- Calculate the bias factor of resistance by dividing mean resistance to calculated nominal resistance for each corbel.

- Calculate the bias factor of resistance by dividing mean resistance to calculated nominal resistance for each corbel.

- Propose the most appropriate and conservative bias factor and resistance factor by comparison of calculated bias factors from the procedure and bias factors from literature.

Probability of failure was taken into account to select the target reliability index. The relation between probability of failure and reliability index is:

$$p_f = \Phi(-\beta) \tag{5.21}$$

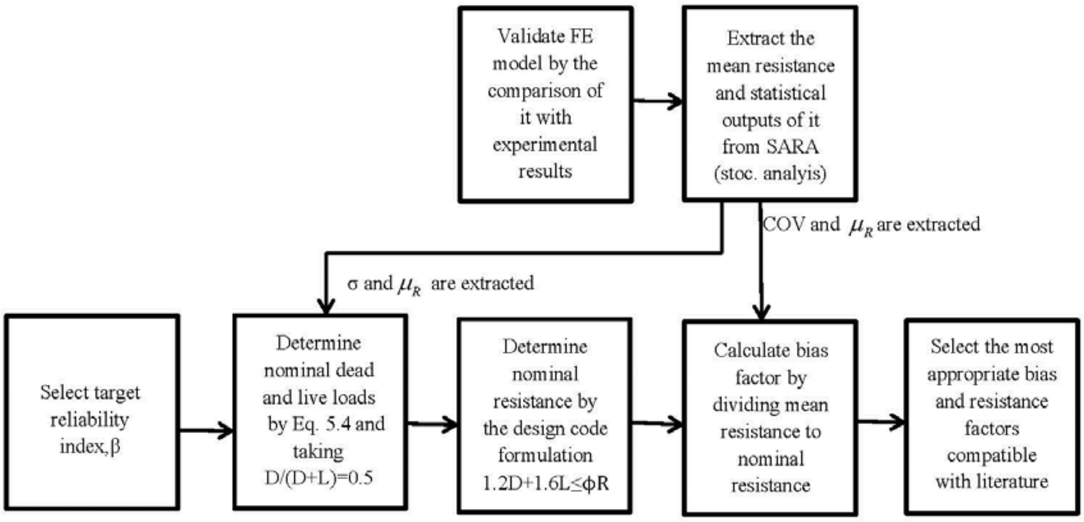

Figure 5.8 Flowchart of the Procedure Implemented in the Study

In eq. 5.21, p_f and β represents probability of failure and reliability index, respectively. Φ is the cumulative distribution function for the standard normal distribution. Calculated values of Eq. 5.21 are listed in the corresponding table (Table A.5) in "Appendix A". Corresponding probability of failure values can be obtained from the table up to reliability index value of 8.9.

Target reliability index was selected as 4.7 (equal to 1.3×10^{-6} about probability of failure value) for the procedure. If the reliability indices used in most of the design codes (Eurocode, ACI, ASCE design codes, etc.) are handled, this value can be considered a conservative and a reliable value. Moreover, most of these design codes (TS 500, ACI, Eurocodes, etc.) either use or permit the selection of 4.7 as reliability index value. Statistical values for dead load and live load were selected according to common values used in the literature. Since corbels are generally used in precast structures, bias factor and coefficient of variation values of dead load was taken as 1.03 and 0.08, respectively, while 1.00 and 0.18 were used as bias factor and coefficient of variation value, respectively for live load (Ellingwood et al. 1980).

Nominal resistances of corbels were calculated according to Eq. 5.20 considering the possible values for resistance factors (ϕ= 0.9, 0.85, 0.8, 0.75). Calculated nominal resistance values are listed in "Appendix A (Table A.4)".

5.7.1 Numerical Implementation

Calculated bias factors obtained as a result of the proposed procedure above are listed in Table A.3 according to the considered resistance factors. The numerical implementation of the proposed method is illustrated for corbel number 46 given as follows;

Statistical parameters of corbel 46 extracted from stochastic nonlinear finite element analysis are: μ_R = 76.57kN, s = 5.2kN and COV = 0.068.

Rearranging Eq. (5.4) by taking into account the coefficient of variation (*COV*) and bias factor equation;

$$COV = \frac{\sigma}{\mu} \tag{5.22}$$

$$\lambda = \frac{MEAN}{NOMINAL} \tag{5.23}$$

$$\beta = \frac{\mu_R - (\lambda_D * D + \lambda_L * L)}{\sqrt{s_R^2 + (\lambda_D * D * COV_D + \lambda_L * L * COV_L)^2}} \tag{5.24}$$

where *D* and *L* are nominal values of dead load and live load, respectively. Since *D*/(*D*+*L*) = 0.5 is assumed, if *D*+*L* is considered equal to *T* (Total Load), *D* and *L* are both equal to 0.5*T*. Therefore, Eq. (5.24) can be rewritten by substituting the related values;

$$4.7 = \frac{76.57 - (1.03 * 0.5T + 1 * 0.5T)}{\sqrt{5.2^2 + (1.03 * 0.5T * 0.08 + 1 * 0.5T * 0.18)^2}} \tag{5.25}$$

From Eq. (5.25), *T* was found as 40.86 kN, *D* and *L* are both equal to 20.43 kN. Substituting these calculated load values into Eq. (5.20), nominal resistance can be obtained according to selected resistance factors (for example ϕ = 0.85);

$$R = \frac{1.2 * 20.43 + 1.6 * 20.43}{0.85} \tag{5.26}$$

R is calculated as 67.3 kN according to Eq. (5.26), from now on bias factor can be calculated as;

$$\lambda = \frac{76.57}{67.3} = 1.14 \tag{5.27}$$

5.7.2 Determination of Nominal Load Carrying Capacities of SFRC Corbels

It was emphasized in section 5.7 of this chapter that the bias factor is determined by the comparison of bias factor calculated in this study and bias factors resulted from previous literature works. Truss model and flexural model which were proposed by Fattuhi (1994a) to determine the ultimate load carrying capacity of SFRC corbels were taken as reference to achieve the comparison. Load carrying capacities of all of the corbels analyzed in this study were calculated according to proposed models by Fattuhi. Capacities of corbels which failed in flexural mode were calculated according to flexural model, while capacities of corbels whose failure mode was any mode, except flexural mode were calculated according to truss model. Calculated resistance values (V_{MODEL}) and bias factors (V_{exp}/V_{MODEL}) are listed in Table A.4.

5.7.2.1 Flexural Model

Fattuhi (1994a) proposed the following model for load carrying capacity of SFRC corbels that fail in flexural mode (Fig. 5.9);

$$V_{MODEL} = \frac{f_y A_s}{a}\left(d - \frac{a_1}{2}\right) + \frac{k_0 f_{ct} b}{2a}\left(h - \frac{a_1}{\beta_1}\right)\left(h + \frac{a_1}{\beta_1} - a_1\right) \tag{5.28}$$

where,

$$k_0 = \frac{9.519}{(f_c)^{0.957}} \quad \text{and} \quad a_1 = \frac{f_y A_s + k_0 f_{ct} h b}{0.85 f_c b + k_0 f_{ct}\left(\frac{b}{\beta_1}\right)} \tag{5.29}$$

In Eqs. 5.28 and 5.29 a, d and h are shear span, effective depth and total depth of the corbel, respectively, f_y and A_s represent yield strength and cross sectional area of the main reinforcement, f_c and f_{ct} are cylindrical compressive strength and splitting tensile strength of steel fiber reinforced concrete, respectively. β_1 is selected according to cylindrical compressive strength of the concrete specified in ACI Building Code requirements (1999).

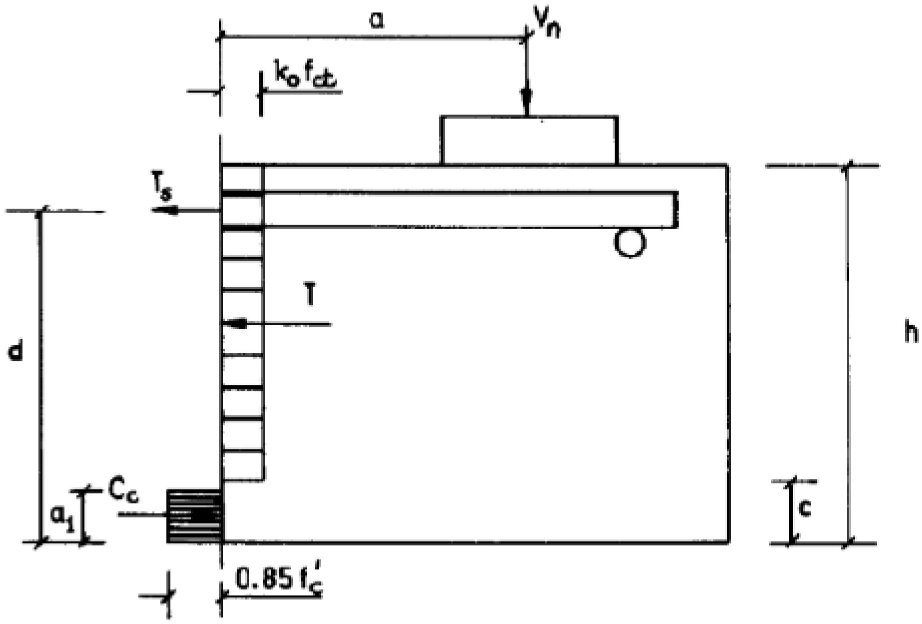

Figure 5.9 Flexural Model for Corbel Proposed by Fattuhi (1994a)

5.7.2.2 Truss Model

According to truss model (Fig. 5.10) proposed by Fattuhi (1994a) for SFRC corbels whose failure mode is different from flexural mode, ultimate load carrying capacity is calculated by the following equation;

$$V_{MODEL} = \frac{f_y A_s (d - (\frac{l \sin\beta}{2})) + 0.5 k_0 f_{ct} bh(h - (l \sin\beta))}{a + 0.5(l \sin\beta)\cot\beta} \qquad (5.30)$$

$$l \sin\beta = \frac{f_y A_s + k_0 f_{ct} bh}{0.85 f_c b + k_0 f_{ct} b} \qquad (5.31)$$

and $\cot\beta$ is determined according to following quadratic equation;

$$
\begin{aligned}
&0.425 f_c b(l\sin\beta)^2 \cot^2\beta + 0.85 f_c ab(l\sin\beta)\cot\beta - f_y A_s\left(d - \frac{(l\sin\beta)}{2}\right) \\
&- 0.5 k_0 f_{ct} bh(h - (l\sin\beta)) = 0
\end{aligned} \tag{5.32}
$$

and k_0 is calculated in the same way as stated Eq. 5.29. Note that since corbels analyzed in this study do not contain stirrup reinforcements, the stirrup related terms are removed from Eqs. 5.30-5.32.

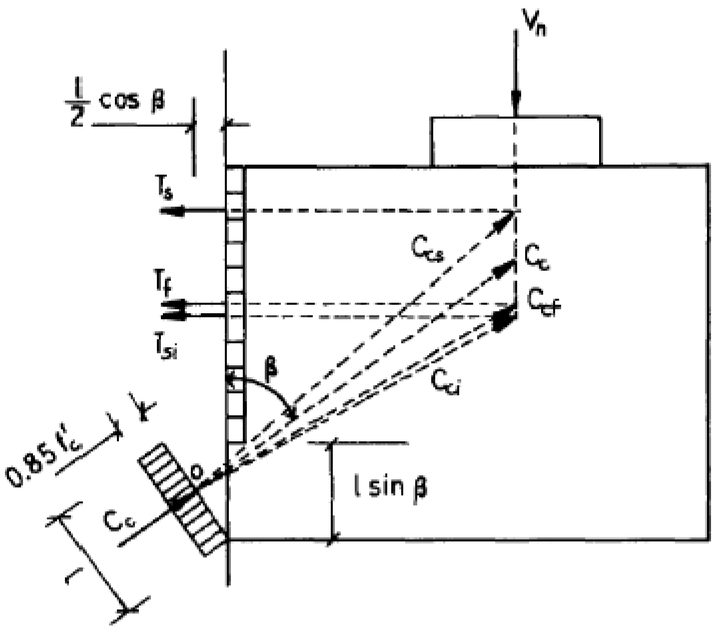

Figure 5.10 Truss Model for Corbel Proposed by Fattuhi (1994a)

5.7.3 Recommended Statistical Parameters and Resistance Factor for SFRC Corbels

According to bias factors calculated from flexural and truss models (Fattuhi, 1994a), mean value is 1.03 and highest value is 1.14 (Table A.4). If these values are compared with the bias factor resulted from reliability analysis (Table A.3), the most well matched point is corresponding to $\phi = 0.85$ (mean bias is 1.04 and the highest bias is 1.17). Besides, values lower than 0.9 are recommended for bias factors of SFRC structural elements given that fibrous concrete plays an important role in resisting mechanism (ACI Committee 544, 1999). Additionally highest uncertainty was observed in corbel number 61 (*COV*=0.074) as a result of stochastic finite element analysis.

In conclusion, recommended values are found to be as 0.85, 1.04 and 0.074 for resistance factor, bias factor and coefficient of variation value of SFRC corbels, respectively (Gulsan et al., 2015). If reliability indices are plotted versus *D*/(*D*+*L*) for the load combinations used in ACI 318-99, ASCE 7-98 and TS500 (Turkish Standard) (Figs. 5.11-5.13), it can be extracted that the proposed statistical parameters and resistance factor are suitable for the application of the related design codes.

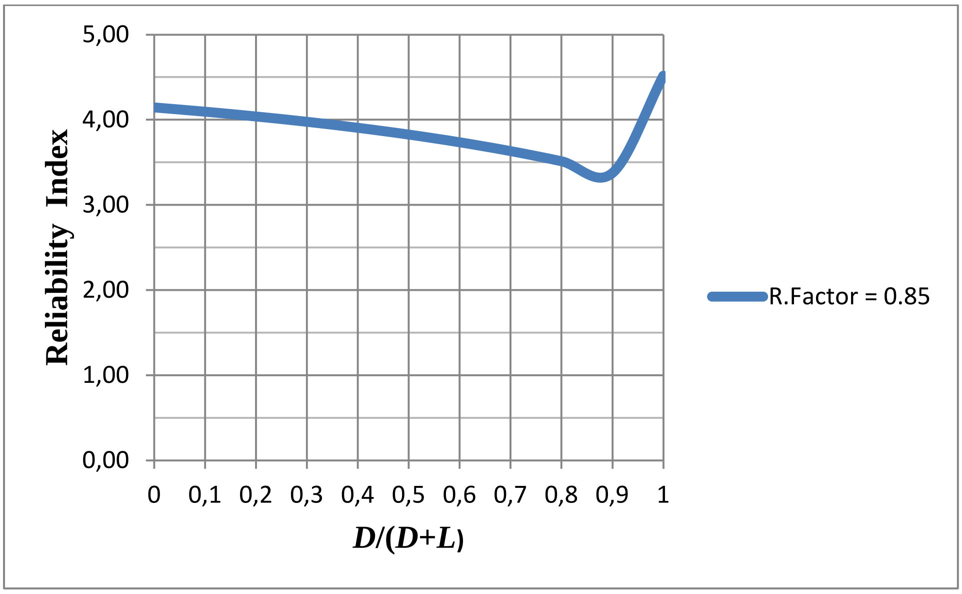

Figure 5.11 Reliability Index vs. Load Ratio according to ASCE 7-98 (1.2*D*+1.6*L* or 1.4*D*)

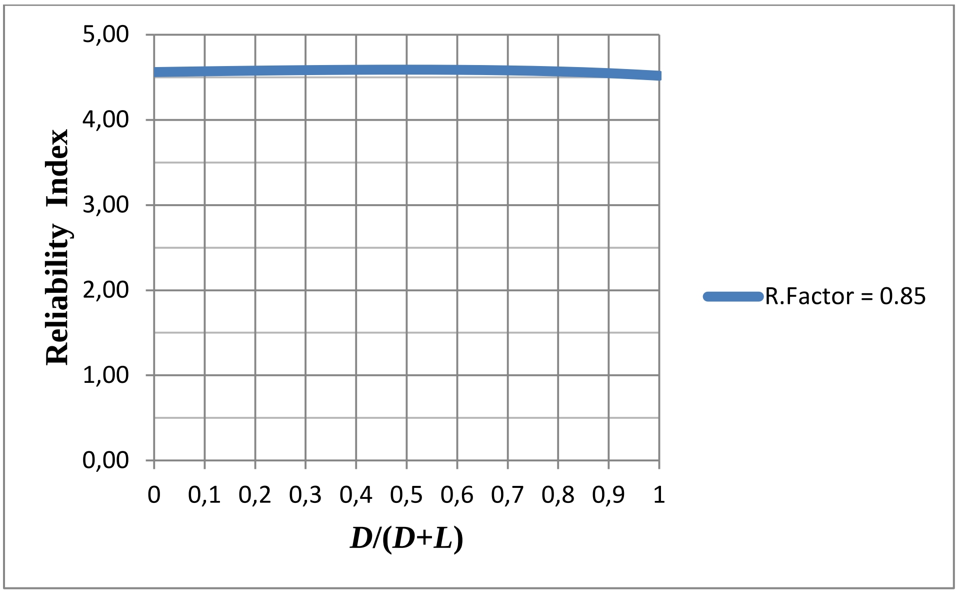

Figure 5.12 Reliability Index vs. Load Ratio according to ACI 318-99 (1.4*D*+1.7*L*)

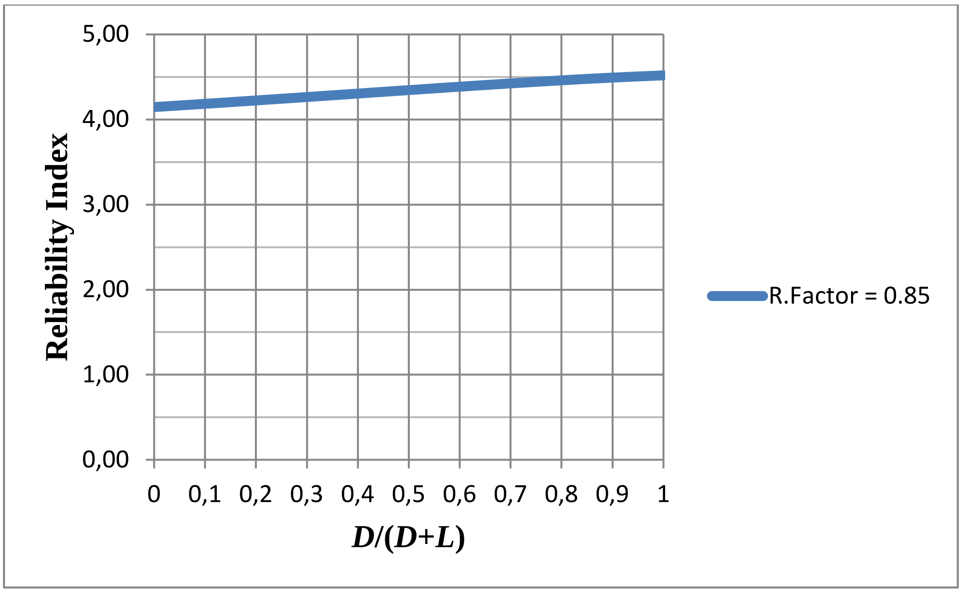

Figure 5.13 Reliability Index vs. Load Ratio according to TS 500 (1.4D+1.6L)

CHAPTER 6

NUMERICAL MODEL FOR LOAD CARRYING CAPACITY OF SFRC CORBELS

6.1 Introduction

Estimating the shear strength of a corbel beforehand provides important advantages during design process. Therefore, a new and simple formulation was proposed for load carrying capacity of steel fiber reinforced corbels. Necessary parametric studies were achieved for the model and generalization capability of the model was proved. The formulation was derived based on experimental results implemented by Fattuhi (1989-1994) using symbolic regression. The formulation represents good fit with experimental results. However, coefficients of the formulation were modified according to addition of new database to obtain more generalized and accurate equation.

6.2 Previous Proposed Formulations for SFRC Corbels

Fattuhi (1990b) proposed a practical empirical formulation based on experimental results which finds ultimate load of both RC and SFRC by considering some parameters which influence the mechanical behavior of corbels. The expression of the formula is;

$$V_u = k_1 bh(f_{ct})^{k_2} \left(\frac{a}{h}\right)^{k_3} \left(\frac{f_y}{f_{cu}}\right)^{k_4} \left(\frac{d}{h}\right)^{k_5} (\rho)^{k_6} \tag{6.1}$$

where, k_1 = 57.292, k_2 = 0.315, k_3 = -0.812, k_4 = -0.049, k_5 = 0.678 and k_6 = 0.626

Fattuhi (1994a) proposed two more models which are named as “Flexural Model” and “Truss Model” for the load carrying capacities of steel fiber reinforced concrete corbels. They are also mentioned in Chapter 5 of the thesis. Basic formulas for these models are;

Flexural Model;

$$V_{MODEL} = \frac{f_y A_s}{a}(d - \frac{a_1}{2}) + \frac{k_0 f_{ct} b}{2a}(h - \frac{a_1}{\beta_1})(h + \frac{a_1}{\beta_1} - a_1) \tag{6.2}$$

where;

$$k_0 = \frac{9.519}{(f_c)^{0.957}} \quad \text{and} \quad a_1 = \frac{f_y A_s + k_0 f_{ct} hb}{0.85 f_c b + k_0 f_{ct}(\frac{b}{\beta_1})} \tag{6.3}$$

Truss Model;

$$V_{MODEL} = \frac{f_y A_s (d - (\frac{l \sin\beta}{2})) + 0.5 k_0 f_{ct} bh(h - (l \sin\beta))}{a + 0.5(l \sin\beta)\cot\beta} \tag{6.4}$$

where,

$$l \sin\beta = \frac{f_y A_s + k_0 f_{ct} bh}{0.85 f_c b + k_0 f_{ct} b} \tag{6.5}$$

and $\cot\beta$ is determined from following quadratic equation;

$$\begin{aligned} &0.425 f_c b(l \sin\beta)^2 \cot^2\beta + 0.85 f_c ab(l \sin\beta)\cot\beta - f_y A_s (d - \frac{(l \sin\beta)}{2}) \\ &- 0.5 k_0 f_{ct} bh(h - (l \sin\beta)) = 0 \end{aligned} \tag{6.6}$$

k_0 is determined from Eq. 6.3.

6.3 Symbolic Regression

Symbolic Regression (SR) is a kind of regression analysis which uses genetic programming to find the simplest and the most accurate mathematical model for a system. It can be also said that symbolic regression is the method of extracting a symbolic equation, function or program that fits given numerical data (Banzhaf et al., 1998). In symbolic regression, no particular model is required to provide a starting point to the related algorithm. Instead, mathematical building blocks and necessary system parameters are defined and the best expression is searched. Since, there is no need a specific model to start for search, human errors and unknown gaps in the domain information does not influence the symbolic regression operations. Symbolic regression technique takes into account both error measures and complexity of produced models (Vladislavleva, et al., 2009).

Although there are many ways to perform symbolic regression, Holland's works (1975) showed that a genetic based algorithm search is the most sufficient one among them. Moreover, John Koza (1992) demonstrated the use of genetic programming for symbolic regression as one of several applications of genetic programming.

When differences of symbolic regression from other classical regression techniques are considered, conventional regression techniques try to optimize the parameters for an imposed model structure. However, symbolic regression extracts the model from the data and there is no need for any priori assumptions. This means that symbolic regression technique can be a valuable tool to extract the intrinsic relationship between the inputs of lots of experimental data. The other advantage of symbolic regression is that since diversity is required for the evolutionary algorithm to achieve detailed exploration of the search space, the possibility of finding out a good-fit model increases. This diversity leads to better insight to underlying process of the system and allows the user to understand the degree of importance of the parameters considered in the model. Therefore, better models can be produced in terms of accuracy and simplicity by taking into account the underlying process and requirements of the system.

Since symbolic regression method uses a much larger space to achieve search, powerful computers are necessary. Additionally, it can take much more time to find a suitable model and parameterization. But, this problem can be solved by proper selection of mathematical building blocks assigned to the algorithm and a detailed investigation on existing information of the system (experiment or finite element analysis results) that produces the data.

6.4 Proposed Numerical Model for Load Carrying Capacity of SFRC Corbels

For symbolic regression modeling process, an experimental database was used, taken from experimental studies carried out by Fattuhi and Hughes (1989-1994). 84 SFRC corbel test results were considered to propose the formula. Several input parameters which can influence the mechanical behavior of SFRC corbels were considered. As a consequence of the symbolic regression studies, the following formulation was proposed (Cevik and Gulsan, 2013):

$$V_{proposed-1} = 42.26bh(\frac{d}{a})^{0.8323}(f_{ct})^{0.3344}(0.01(\frac{A_s}{bh}))^{0.5903} \tag{6.7}$$

Where b and h are width and height of the corbel in mm, respectively, f_{ct} is the splitting tensile strength of fibrous concrete in MPa, d/a is the reciprocal of the shear span to depth ratio and A_s is sectional area of main reinforcement. The resulted ultimate load carrying capacity of SFRC corbel is in Newtons.

The results of the formulation are compared with the experimental results which were used for modeling process and a very good fit was observed given in Fig. 6.1. Correlation coefficient (R^2) of the proposed formulation is 0.9156, mean and coefficient of variation of $V_{\exp}/V_{proposed-1}$ is 0.992 and 0.0916, respectively. Load carrying capacities of considered corbels resulted from $V_{proposed\text{-}1}$ are listed in Appendix A (Table A.4).

To achieve a more general formulation for load carrying capacity of SFRC corbels, coefficients of the equation stated in Eq. 6.7 were modified by the addition of new database obtained from experimental results which had been carried out in this thesis. The same technique (symbolic regression) was used to handle modification process.

The new version of the formulation is specified in Eq. (6.8);

$$V_{proposed-2} = 38.54bh(\frac{d}{a})^{0.8321}(f_{ct})^{0.415}(0.01(\frac{A_s}{bh}))^{0.6} \quad (6.8)$$

Load carrying capacities of SFRC corbels obtained from $V_{proposed-2}$ equation are also listed in Appendix A (Table A.4). Higher correlation of coefficient (R^2=0.9233) were obtained as compared to $V_{proposed-1}$ (Fig. 6.2). Mean and coefficient of variation of ($V_{exp}/V_{proposed-2}$) are 1.002 and 0.087, respectively.

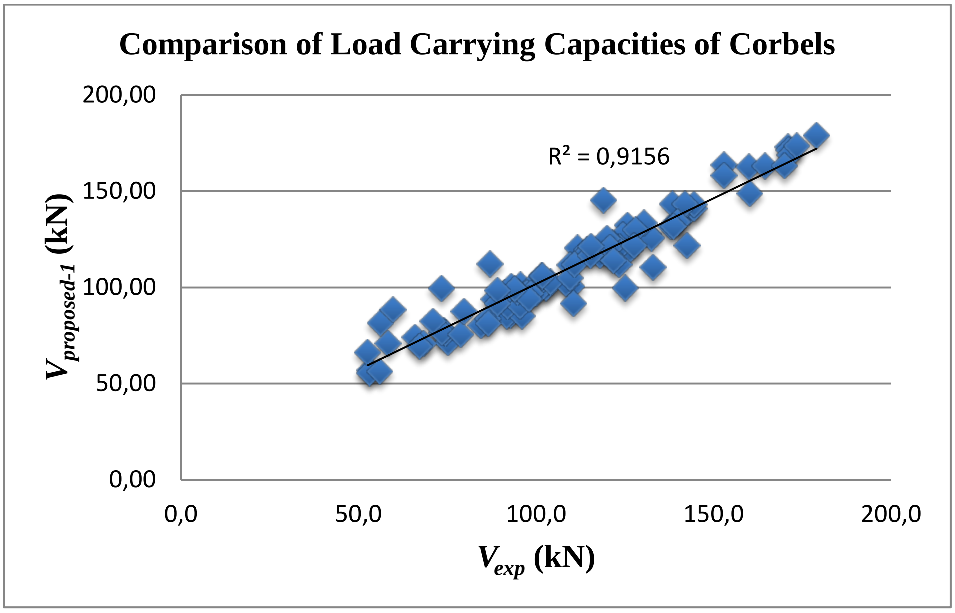

Figure 6.1 Comparisons of Load Carrying Capacities of Corbels for $V_{proposed-1}$ Equation

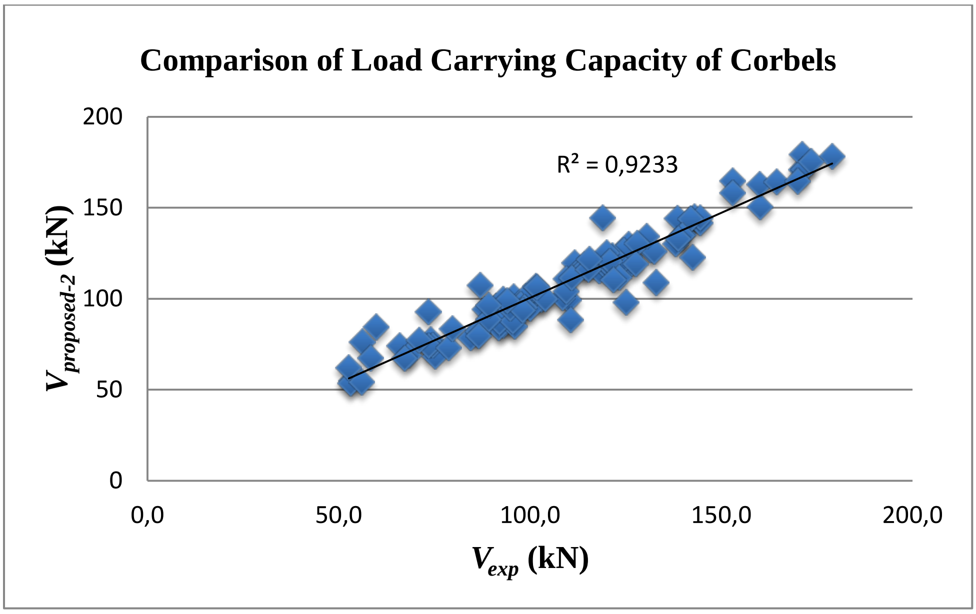

Figure 6.2 Comparisons of Load Carrying Capacities of Corbels for $V_{proposed-2}$ Equation

6.5 Parametric Study for the Proposed Formulation

A parametric study was implemented to prove the generalization capability of the proposed model ($V_{proposed\text{-}2}$).

The proposed formula has five main input parameters (b, h, f_{ct}, d/a and A_s/bh). Therefore, these parameters were considered for parametric studies.

3125 samples were generated for each parameter according to upper and lower limit values of them. Generated values were substituted into the proposed formulation to obtain related ultimate load capacity. Main effects plots, interactions plots and surface plots for ultimate load capacity of steel fiber reinforced concrete corbels were obtained to check the effectiveness of the formulation (Gulsan, 2013). Upper and lower limits for the generation of input values are listed in Table 6.1.

Table 6.1 Selected Intervals for Parametric Study of the Formulation

Input Parameter	Lower Limit	Upper Limit
b (mm)	150	250
h (mm)	150	250
d/a	0.9	2.00
f_{ct} (MPa)	2	9
A_s/bh	0.45	1.5

6.5.1 Main Effect Graphs

A main effect takes place when the mean response alters through different degrees of a parameter. The aim of this plot is to investigate the degree means for each parameter, to compare the degree means for numerous factors and to compare the proportional effectiveness of the influences across parameters.

The effectiveness of the main plot is apparent when several parameters exist to examine. Thereafter, the most efficient parameter on the response can be determined by comparing the changes in the degree means. A main effect exists, if the response is affected in different manner for different values of a parameter. For instance, one degree of a parameter can increase the mean when compared to the other degree. This situation causes a main effect.

Main effect graphs resulted from parametric studies are demonstrated in Fig. 6.3. According to the graphs shown in Fig. 6.3, all input parameters have significant effect on the ultimate load capacity of SFRC corbels and they are directly proportional to the response. However, these effects are valid for the limits of input parameters stated in Table 6.1. Indeed, the limits stated are compatible with the values utilized in the corbel production. Therefore, these effect graphs can be taken into account without any doubt. Not only main effect plot, but also two-dimensional and three dimensional interaction plots are important to prove the capability of the proposed model which is described in the following two sections.

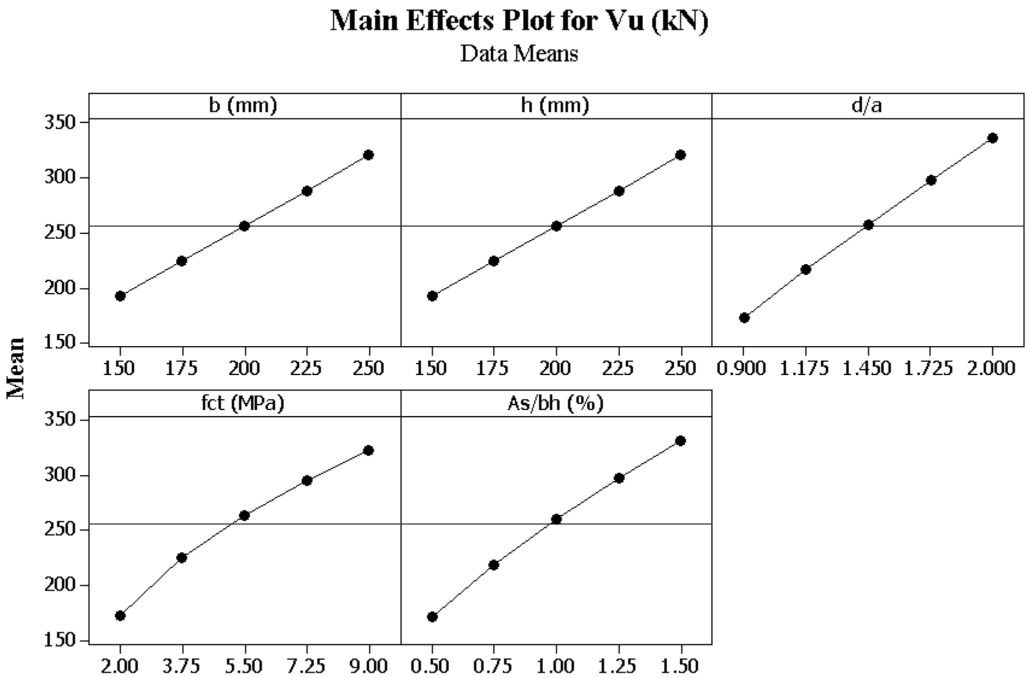

Figure 6.3 Main Effect Graphs Resulted From Parametric Studies

6.5.2 Interaction Graphs

Interaction plots exhibit interaction and relationship between two parameters according to the response variation. An interaction exists, if the variation in response for two degrees of a parameter is different from the variation in response for the same two degrees of a second parameter. That is, the effect of one factor is dependent on a second factor. The aim of interaction plot is to determine the necessity and importance of the two-way interactions of parameters to be included in the formulation, to prove the reliability and generalized applicability of the formulation and to compare the proportional effectiveness of the influences across parameters.

According to Fig. 6.4, it is proved that every parameter has an effect on the response. The interaction plot is compatible with the main plot. Therefore, the proposed formulation can be applied for obtaining the ultimate load capacity of steel fiber reinforced corbels.

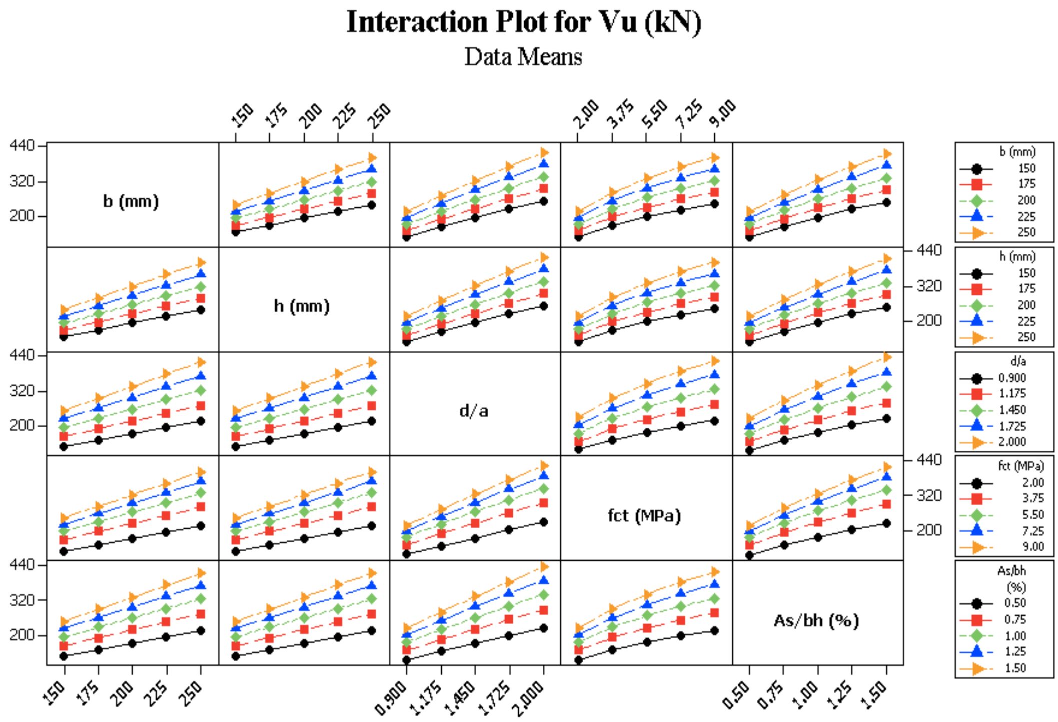

Figure 6.4 Two-Dimensional Interaction Diagrams Resulted from Parametric Studies

The two-way interaction graphs are compatible with the main effect plots and also it is important to note that all parameters considered in the proposed model has considerable influence on the load carrying capacity of corbels.

6.5.3 Three Dimensional Interaction Graphs

3D plot of input parameters for a response is useful to investigate the relationship between three parameters on a single graph and to visualize combinations of input parameters that develop suitable response values. In Figs. 6.5-6.14, all combinations of the parameters with the ultimate load capacity of SFRC corbels are sketched in three dimensional spaces.

When all of the 3D graphs are analyzed, it can be seen that there are no big differences in the peak values of input parameters and responses and there are no much higher peak values which violate trend of waves in the graphs. This situation demonstrates the applicability and suitability of the proposed formulation for determining the ultimate load capacity of SFRC corbels.

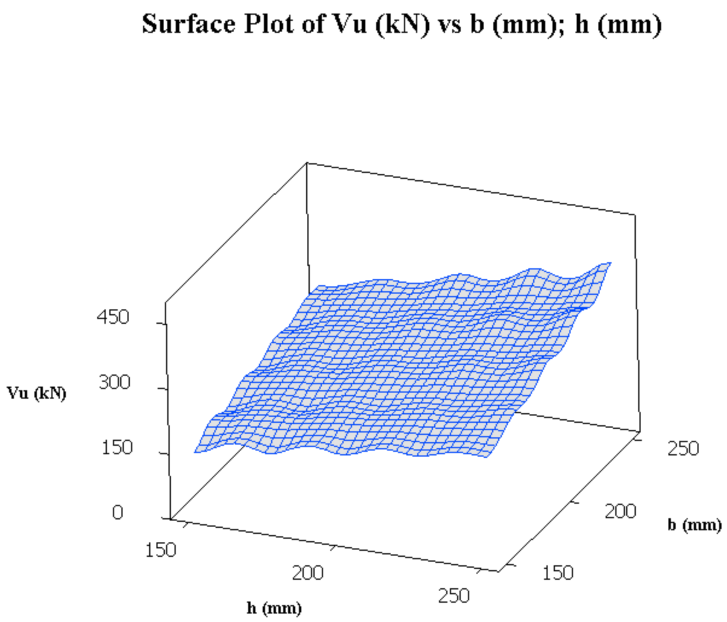

Figure 6.5 3D Interaction Diagram for Load, Height and Width

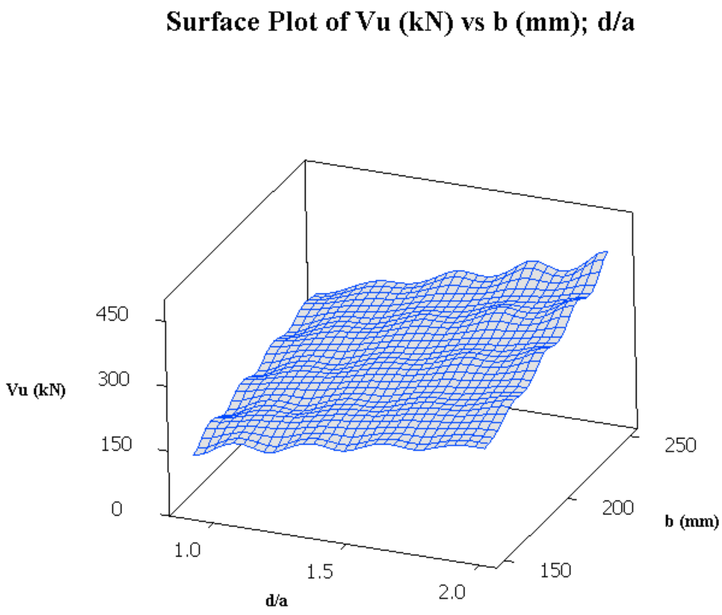

Figure 6.6 3D Interaction Diagram for Load, *d*/*a* and Width

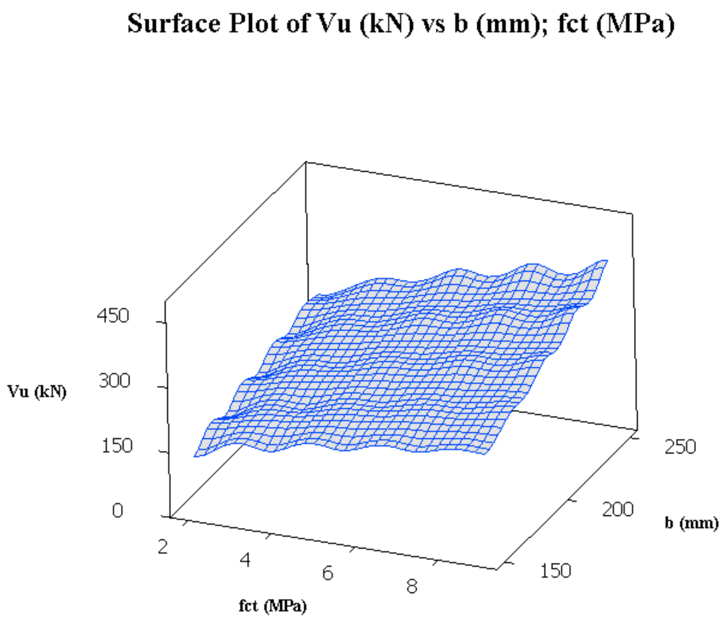

Figure 6.7 3D Interaction Diagram for Load, f_{ct} and Width

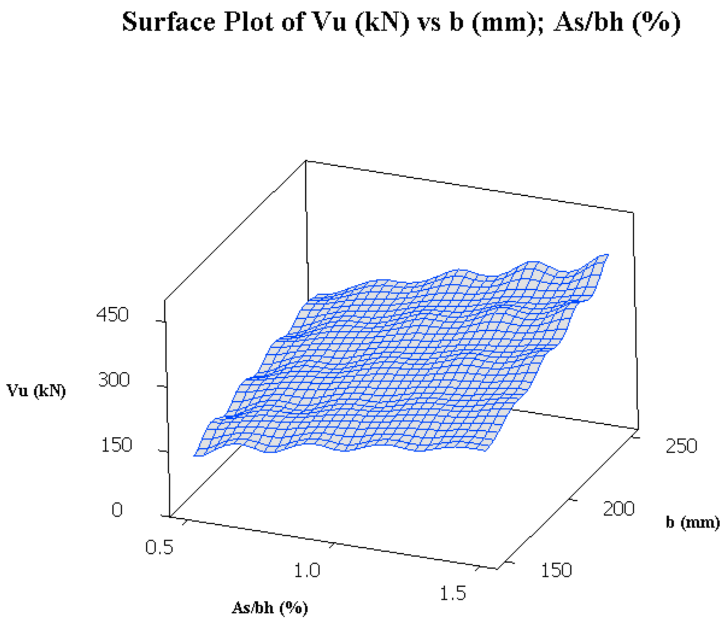

Figure 6.8 3D Interaction Diagram for Load, A_s/bh and Width

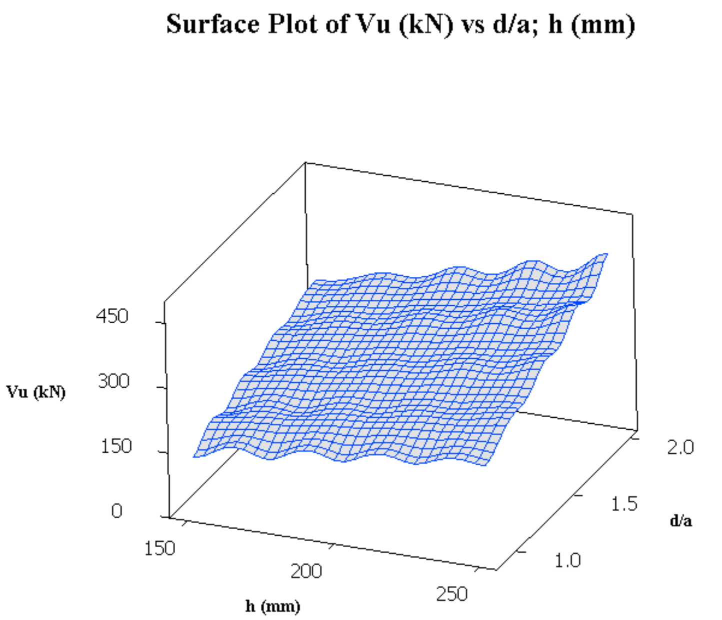

Figure 6.9 3D Interaction Diagram for Load, *d*/*a* and Height

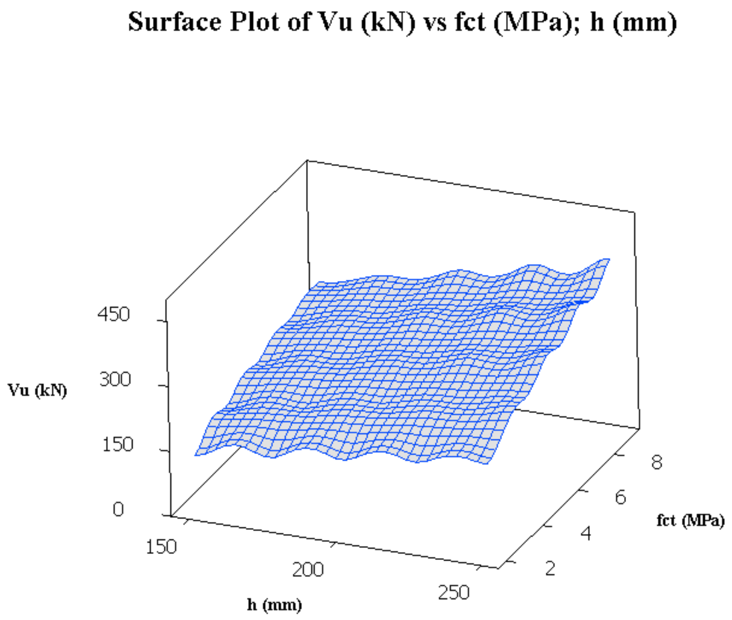

Figure 6.10 3D Interaction Diagram for Load, f_{ct} and Height

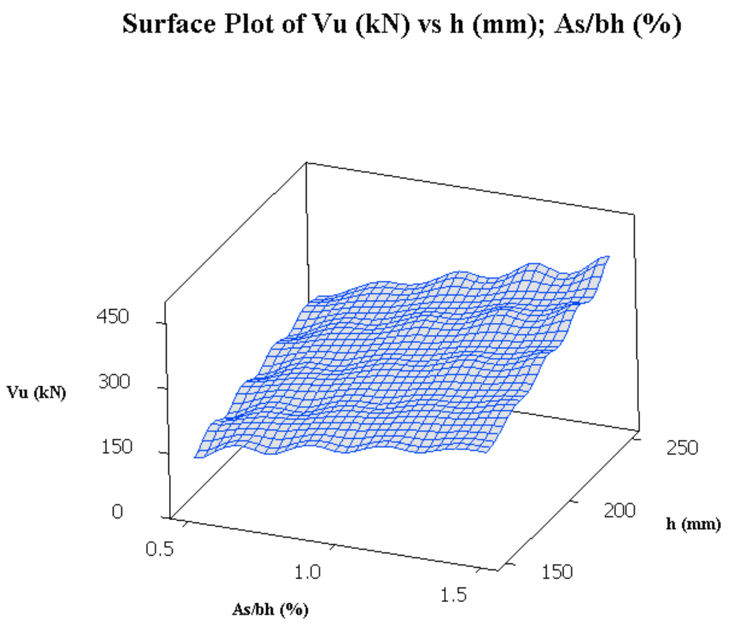

Figure 6.11 3D Interaction Diagram for Load, A_s/bh and Height

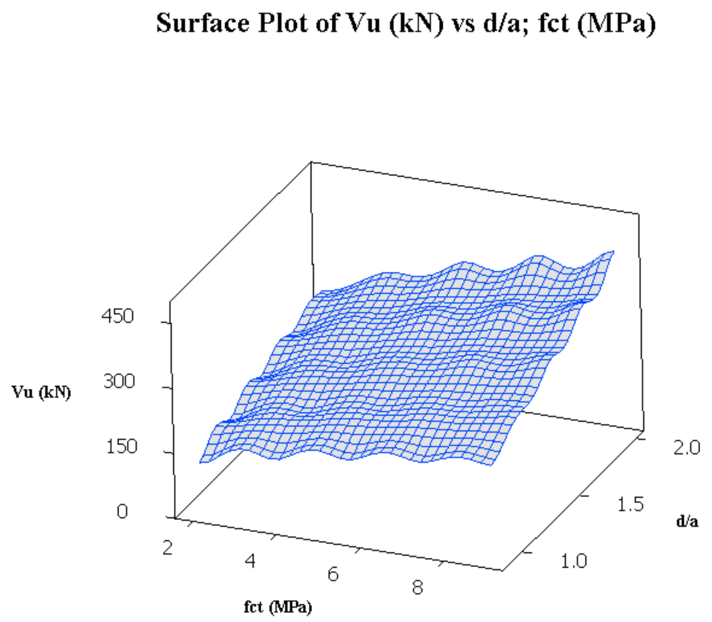

Figure 6.12 3D Interaction Diagram for Load, *d/a* and f_{ct}

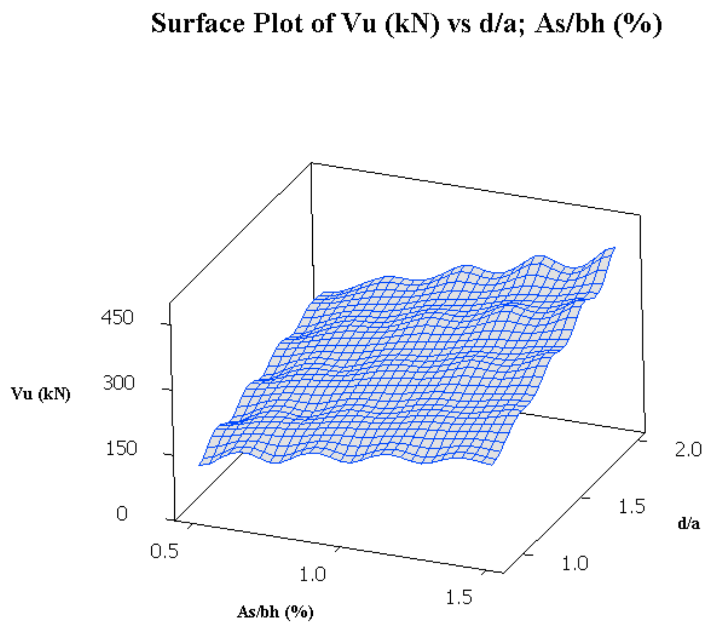

Figure 6.13 3D Interaction Diagram for Load, *d/a* and A_s/bh

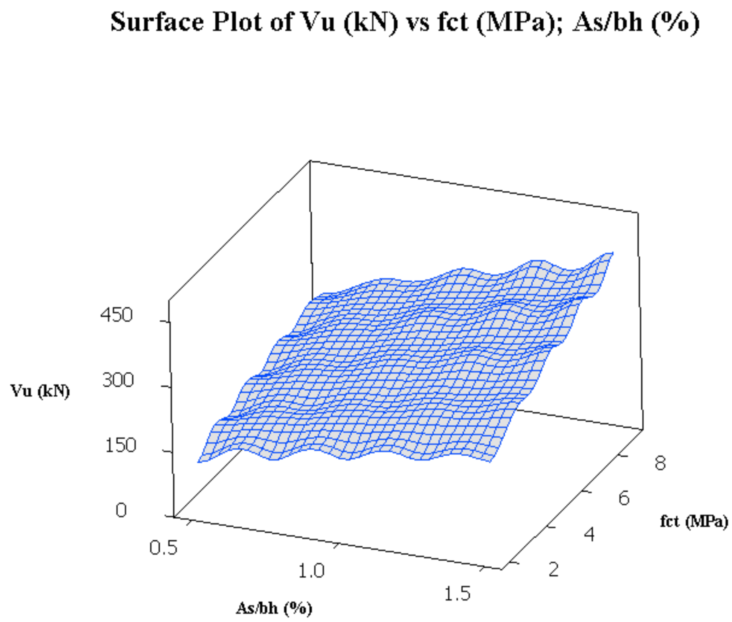

Figure 6.14 3D Interaction Diagram for Load, f_{ct} and A_s/bh

CHAPTER 7

CONCLUSION

7.1 Conclusion

Although Corbels are important structural elements and widely used frequently in construction industry little research has been carried so far as compared to other structural members. This thesis contributes the following topics regarding mechanical behavior of steel fiber reinforced concrete (SFRC) corbels:

- A comprehensive literature review on SFRC corbels is presented.
- An Experimental study has been carried out on SFRC corbels.
- Finite element (FE) analyses of SFRC corbels were compared with corresponding experimental results.
- Reliability and stochastic analysis of SFRC corbels were performed.
- A numerical formulation was proposed for load carrying capacity of SFRC corbels.

Corbels are significant structural elements used in precast construction and especially in industrial building sector. It transfers the load coming from the beam to the column or wall to which it is connected. Since it provides the beam-column connection, its strength, ductility and functionality are more critical as compared to other structural elements. Results of works and analyses carried out on SFRC corbels in this thesis are summarized in the following paragraphs.

In this thesis, experimental, finite element, stochastic and reliability analyses were carried out for steel fiber reinforced concrete (SFRC) corbels. Detailed research was implemented on SFRC corbels to clarify all uncertainties on the mechanical behavior and ultimate load carrying capacities. Since use of steel fiber reinforced concrete in structural elements is a new trend, there are no special measures for SFRC corbels. Moreover, because of its remarkable benefits, steel fiber reinforced concrete corbels can be considered in construction sector as an efficient solution. However, a detailed research is necessary to encourage the designers and engineers. Therefore, uncertainties about the mechanical outputs of SFRC corbels should be clarified.

Use of steel fibers in reinforced concrete corbels leads to considerable advantages. The most apparent benefits are to satisfy ductile behavior and to increase the load carrying capacity. These outputs prove that steel fibers can be used as secondary reinforcement instead of horizontal stirrups. However, use of steel fibers does not guarantee ductile behavior since this behavior is also dependent on shear span, reinforcement ratio and compressive strength of concrete. Therefore, if a designer designs a steel fiber reinforced concrete corbel, he or she has to be careful about selection of class of concrete, diameter of main reinforcement and shear span values as well as steel fiber percentage amount.

Experimental studies show that steel fiber reinforced concrete retards the failure of the corbel effectively. Moreover, the degradation in load carrying capacity of SFRC corbel is slower than that of reinforced concrete corbel. That is, the corbel fails completely in larger displacements. As a result, steel fiber is one of the most effective and inexpensive solution to prevent sudden and brittle failure in reinforced concrete corbels.

Another advantage of use of steel fiber in the corbel is about the crack widths. Crack widths of steel fiber reinforced concrete corbels are much smaller as compared to corbels without steel fiber. Reduction in crack widths leads to longer service life of corbels. Moreover, it facilitates effective and successful repairing operation in the case of a possible rehabilitation process.

Experimental results carried out on SFRC corbels show that compressive strength, tensile strength, steel fiber amount, reinforcement ratio and shear span are effective parameters on the load carrying capacities of SFRC corbels. Load carrying capacity and failure mode of SFRC corbel can be regulated by altering of these parameters.

The following inferences were recommended to designers and engineers about mechanical behavior corbels:

- Compressive strength increases the load carrying capacity of SFRC corbels. However, a designer has to be careful for selection of concrete class to achieve ductility in the corbel. For example, in lower compressive strength corbels fiber bridging effect is provided earlier as compared to higher compressive strength corbels. Therefore ductility can be achieved, even if in large reinforcement ratios (1.16%). While a designer should select lower reinforcement ratios (smaller than 1.16%) to achieve ductility for high compressive strength corbels.

- Whenever steel fiber amount increases, the load carrying capacity of SFRC corbels increases. However, the rate of increase decreases as the fiber amount becomes higher and higher.

- A designer has to be very careful about the selection of shear span because load carrying capacity decreases as the span increases.

- Concrete cover to main reinforcement should not be in high values (for example, it should not exceed 3 cm) to protect the shear strength of SFRC corbels.

- Steel reinforcement ratio is very important parameter to determine ductility and load carrying capacity of SFRC corbels. However, the effect of reinforcement ratio on load carrying capacity of the corbels becomes more apparent when the larger support region is achieved.

As a result of a detailed finite element analyses of SFRC corbels and a detailed literature research on SFRC corbels, failure and crack pattern prediction were proposed for SFRC corbels within the thesis studies. These predictions provide considerable advantages to designers and engineers. Necessary measures can be taken into account beforehand by these predictions. For instance, strengthening of SFRC corbel can be achieved successfully by the true prediction of crack regions. Moreover, design of SFRC corbels can be made by the consideration of possible failure scenarios and undesirable failure event can be prevented. According to failure mode analyses, critical value for compressive strength is nearly 35 MPa and for tensile strength is nearly 6 MPa. Therefore, classification of failure modes was made based on these values. Reinforcement ratio was also considered during classification process. It was also extracted that shear span is not as effective as the tensile strength, compressive strength and reinforcement ratio. Its little effect on alteration of crack pattern is also stated in the failure mode prediction table in Chapter 4.

Comparison of experimental and FE results of SFRC corbels showed an excellent correlation which proved the accuracy of the FE modeling process. Not only ultimate load capacity, but also crack patterns of SFRC corbels were accurately captured when compared with actual test results. Afterwards, reliability analyses of SFRC corbels were carried out via a specialized stochastic analysis module of the finite element software used in this study. Based on results of stochastic finite element based reliability analyses, probabilistic, statistical parameters (probability distribution functions, coefficient of variation and bias factor values) and resistance factor were proposed considering uncertainties in SFRC mechanical properties.

As a result of stochastic finite element analyses of SFRC corbels, it can be concluded that there is a close relationship between the uncertainty of load capacity and shear span to effective depth ratio of SFRC corbels. If the standard deviation values of SFRC corbels are analyzed in a general perspective, it can be seen that the smaller the shear span to effective depth ratio is, the higher the uncertainty (higher standard deviation and higher coefficient of variation) of the corbel. Also the uncertainty of short span corbels increases when effective depth becomes smaller, even if a/d ratio is high. Thus, analysis of SFRC corbels with short spans is found to be more critical and during design process, a designer should be more careful. As a result of stochastic FE analyses, *"Lognormal 3 parameter"* type distribution was recommended as probability distribution function (PDF) for the load carrying capacity of SFRC corbels. Lognormal type probability distribution function is one of the most suitable probability distribution functions for the properties which cannot take negative value (for example, load carrying capacity).

According to reliability analysis results and reliability index versus load ratio graphs, it was concluded that recommended statistical parameters (bias factor = 1.04 and COV = 0.074) and strength reduction factor (ϕ = 0.85) can be used safely for load combinations stated in most of the design codes (Eurocode, ACI, ASCE, TS 500). The proposed parameters achieve the reliability requirements of the codes (β is commonly between 3.5 and 4.7).

As a consequence of the study, a general formulation was produced for ultimate load capacity of steel fiber reinforced concrete corbels. The model is simpler and more practical as compared to other formulations used in the literature and its statistical outputs allow to be used for obtaining the ultimate load safely.

When the formulation was analyzed in detail, it is observed that splitting tensile strength of concrete is efficient on the ultimate load. This situation can be expected due to improvement of tensile properties of the concrete by addition of steel fibers. Since corbels are short and deep structural members, they are usually characterized by their shear span to depth ratios. The proposed formulation also includes the reciprocal of this important ratio for the corbel. Therefore, the empirical formulation proposed in this study can be effectively used to calculate ultimate load capacity of steel fiber reinforced concrete corbels.

In the current study, parametric analysis of the proposed formula for the ultimate load capacity of steel fiber reinforced corbels was carried out. As a consequence of the study, it was concluded that geometry of the corbel, tensile strength of fibrous concrete, amount of reinforcement and effective depth to span ratio are effective parameters for ultimate load capacity of SFRC corbels. When main plots, interaction plots and 3D plots of the input parameters are analyzed, it can be concluded that there are no extreme and contradictory cases which prevent the effectiveness of the formulation. Therefore, the proposed formulation can be effectively and safely used to obtain ultimate load capacity of SFRC corbels in practical applications.

7.2 Recommendations for Future Research

Providing secondary reinforcement with new techniques other than horizontal stirrups has become a challenging trend. However, this replacement has to provide both the same mechanical effect and easier applicability. Therefore, steel fiber is a good option for use as secondary reinforcement in reinforced concrete corbels.

However, replacement of horizontal stirrups by other types of fiber can be researched in future works. For instance, use of basalt fibers, glass fibers in corbels can be tried experimentally and their performance as a secondary reinforcement can be observed. Main steel reinforcement can also be replaced by new type main reinforcements in reinforced concrete corbels. Since corbel is a connection part between the girder and column or wall, ultimate strength is much critical for them and so main reinforcements whose ultimate strength are higher than steel can be tried on corbels.

Since corbels are significant structural elements in industrial buildings and industrial buildings are likely to exposure to fire. Fire performance of reinforced concrete and steel fiber reinforced concrete can be researched and necessary measures can be taken into account before a possible fire by strengthening and rehabilitation processes.

REFERENCES

Abdel-Hafez, A. M., Ahmed, M. M., Diab, H., Drar, A. A. M. (2012). Shear Behaviour of high strength fiber reinforced concrete corbels. *Journal of Engineering Sciences*. **40(4)**, 969-987.

Abdul-Wahab, H. M. (1989). Strength of reinforced concrete corbels with fibers. *ACI Structural Journal*. **86(1)**. 60-66.

ACI. American Concrete Institute. (1999). Static flexural analysis of beams containing bars and fibers, Design considerations for steel fiber reinforced concrete. ACI Committee 544, Detroit.

ACI. American Concrete Institute. (1999). Building code requirements for structural concrete (ACI 318-99) and commentary (318R-99), Farmington Hills, Michigan.

ACI. American Concrete Institute. (2002). State-of-the-Art Report on Fiber Reinforced Concrete. ACI 544.1R-96.

Alameer, M. (2004). Effects of fibres and headed bars on the response of concrete corbels. M.Sc. Thesis. McGill University, Montreal, Canada.

ASCE. American Society of Civil Engineers. (1998). Minimum design load for buildings and other structures. ASCE 7-98. Washington, D. C., 352 pp.

Asensio E. C. (2012). On Shear Behavior of Structural Elements Made of Steel Fiber Reinforced Concrete. Ph.D. Thesis. Universitat Politecnica De Valencia.

Banzhaf, W., Nordin, R., Keller, R. E., Francone, F.D. (1998). Genetic programming: An introduction. Morgan Kaufmann Publishers.

Bekaert. (2014). Steel wire transformation and coating company. http://www.bekaert.com.

Bergmeister, K., Novak, D., Pukl, R. and Cervenka, V. (2009). Structural assessment and reliability analysis for existing engineering structures, theoretical background. *Structure and Infrastructure Engineering*. **5(4)**, 267-275.

Campione G., Mendola L. L., Papia M. (2005). Flexural behavior of concrete corbels containing steel fibers or wrapped with FRP sheets. Materials and Structures. **38**, 617-625.

Campione, G., Mendola, L. L. and Mangiavillano, M. L. (2007). Steel fiber-reinforced concrete corbels: experimental behavior and shear strength prediction. *ACI Structural Journal*. **104(59)**, 570-579.

Campione, G. (2009a). Flexural response of FRC corbels. *Cement and Concrete Composites*. **31(3)**, 204-210.

Campione, G. (2009b). Performance of steel fibrous reinforced concrete corbels subjected to vertical and horizontal loads. *Journal of Structural Engineering*. **135(5)**, 519-529.

Cervenka, V. and Papanikolaou, V. K. (2008). Three dimensional combined fracture-plastic material model for concrete. *International Journal of Plasticity*. **24(2008)**, 2192-2220.

Cervenka, V., Jendele, L. and Cervenka J. (2013). ATENA Program Documentation – Theory, Cervenka Consulting.

Cevik, A., Gulsan., M. E. (2013). Modelling ultimate load capacity of steel fibre reinforced concrete corbels: Part1. Formulation. *Fibre Concrete*, Cezech Republic, Prague.

De Borst, R. (1986). Nonlinear analysis of frictional materials. Ph.D. Thesis. Delft University of Technology.

Deluce J. R. (2011). Cracking behaviour of steel fibre reinforced concrete containing conventional steel reinforcement. M.Sc. Thesis. University of Toronto.

Ellingwood, B., Galambos, T. V., MacGregor, J. G. and Cornell, C. A. (1980). Development of a probability based load criterion for American National Standard A58. NBS Special Report 577. U.S. Department of Commerce, National Bureau of Standards, p. 222.

El-Reedy M. A. (2013). Reinforced Concrete Structural Reliability. CRC Press, (Taylor&Francis Group).

Ersoy, U., Özcebe, G. and Tankut, T. (2006). Reinforced concrete. Ankara: Middle East Technical University Press.

Fanella, D. A., Naaman, A. E. (1985). Stress-strain properties of fiber reinforced mortar in compression. *ACI Journal Proceedings*. **82(4)**, 475-483.

Fattuhi, N. I. (1987). Sfrc corbel tests. *ACI Structural Journal*. **84(2)**, 119-123.

Fattuhi, N. I. and Hughes, B. P. (1989b). Ductility of reinforced concrete corbels containing either steel fibers or stirrups. *ACI Structural Journal*. **86(6)**, 644-651.

Fattuhi, N. I. and Hughes, B. P. (1989c). Reinforced steel fiber concrete corbel with various shear span-to- depth ratios. *ACI Material Journal*. **86(6)**, 590–596.

Fattuhi, N. I. (1990a). Column-load effect on reinforced concrete corbels. *Journal of Structural Engineering*. **116(1)**, 188-197.

Fattuhi, N. I. (1990b). Strength of SFRC corbels subjected to vertical load. *Journal of Structural Engineering*. **116(3)**, 701–718.

Fattuhi, N. I. (1994a). Strength of FRC corbels in flexure. *Journal of Structural Engineering*. **120(2)**, 360-377.

Fattuhi, N. I. (1994b). Reinforced corbels with plain and fibrous concretes. *ACI Structural Journal*. **91(5)**, 530-536.

Fattuhi, N. I. (1994c). Reinforced corbels made with high strength concrete and various secondary reinforcements. *ACI Structural Journal*. **91(4)**, 376-383.

Gulsan, M. E. (2013). Modelling ultimate load capacity of steel fibre reinforced concrete corbels: Part 2. Parametric study. *Fibre Reinforced Concrete*. Czech Republic, Prague.

Gulsan, M. E., Cevik, A., Kurtoglu A. E. (2015). Stochastic finite element based reliability analysis of steel fiber reinforced concrete (SFRC) corbels. *Computers and Concrete*. **15(2)**, 279-304.

Haido J. H. (2012). Investigation of SFRC corbel performance using a developed nine-noded lagrangian elements. *ARPN Journal of Engineering and Applied Sciences*. **7(8)**, 963-970.

Hasofer, A. M., Lind, N. C. (1974). Exact and invariant second-moment code format. *Journal of Engineering Mechanics Division (ASCE)*. **100**, 111-121.

Holland, J. (1975). Adaptation in natural and artificial systems. University of Michigan Press.

Hughes, B. P. and Fattuhi, N. I. (1989a). Reinforced steel and polypropylene fiber concrete corbel tests. *The Structural Engineer London*, **67(4)**, 68–72.

Kabele, P. (2002). Equivalent continuum model of multiple cracking. *Engineering Mechanics (Association for Engineering Mechanics, Cezech Republic)*. **9(1/2)**, 75-90.

Kleiber, M., Hien, T. D. (1992). The stochastic finite element method. John Willey & Sons.

Koza, J. R. (1992). Genetic programming: On the programming of computers by means of natural selection. Cambridge, USA: MIT Press.

Kumar, S. (2004). Shear strength of reinforced steel fibrous concrete corbels without shear reinforcement. *Journal of Institution of Engineers*. **85**, 202-212.

Kumar, S., Barai, S. V. (2010). Neural networks modeling of shear strength of SFRC corbels without stirrups. *Applied Soft Computing*. **10**, 135-148.

Menetrey, P., William, K. J. (1995). Triaxial failure criterion for concrete and its generalization. *ACI Structural Journal*. **92(3)**, 311-318.

Mordini, A. (2006). Three–dimensional numerical modeling of reinforced concrete behavior. Ph.D. Thesis. University of Parma.

Muhammad, A.H. (1998). Behavior and strength of high-strength fiber reinforced concrete subjected to monotonic and cyclic (repeated) loading. Ph.D. Thesis. University of Technology, Baghdad.

Novak, D., Teply, B., (1991). Statistical analysis of random behavior of RC beams. *Kniznice odbor a ved spisu*. **51**, 127-136.

Novak, D., Teply, B., Kersner, Z. (1998). The role of Latin Hypercube Sampling method inreliability engineering. *7th International Conference on Structural Safety and Reliability* (ICOSSAR). **97**, 403-409.

Novak. D., Teply, B., Kersner, Z. and Vorechovsky, M. (2002). SARA Program Documentation – Theory. Cervenka Consulting, Prague.

Novak, D., Vorechovsky, M. and Teply, B. (2014). FReET: Software for the statistical and reliability analysis of engineering problems and great D: Degradation module. *Advances in Engineering Software*. **72**, 179-192.

Nowak, S. and Collins, R. (2000). Reliability of structures. USA: McGraw-Hill Press.

Ridha, M. M. S. (2005). Nonlinear finite element analysis of high strength fiber reinforced concrete corbels. *Engineering & Technology*. **26**, 1-15.

Strauss, A., Mordini, A. and Bergmeister, K. (2006). Nonlinear finite element analysis of reinforced concrete corbels at both deterministic and probabilistic levels. *Computers and Concrete*, **3(2/3)**, 123-144.

Szerszen, M. M. and Nowak, A. S. (2003). Calibration of design code for buildings (ACI 318): part 2 – reliability analysis and resistance factors. *ACI Structural Journal*, **100(3)**, 383-391.

Thomas, J. and Ramaswamy, A. (2007). Mechanical properties of steel fiber-reinforced concrete. *ASCE Journal of Materials in Civil Engineering*. **19(5)**, 385-392.

TSE. Turkish Standart Institute. (2000). Design and construction rules for reinforced concrete structures. TSE 500, Ankara.

Van Mier, J. G. M. (1986). Multi-axial Strain-softening of Concrete, Part I: fracture, *Materials and Structures*, **19(111)**, 179-190.

Vanmarcke, E., Shinozuka, M., Nakagiri, S., Schueller, G. I., Grigoriu, M. (1986). Random fields and stochastic finite elements. *Structural Safety*. **3**, 143-166.

Vladislavleva, E. J., Smits, G. F. and Den Hertog D. (2009). Order of nonlinearity as a complexity measure for models generated by symbolic regression via pareto genetic programming. *IEEE Transactions on Evolutionary Computation*. **13.2**, 333-349.

Vorechovsky, M., Novak, D. (2003). Statistical correlation in stratified sampling. *Proceedings of 9th International Conference on Applications of Statistics and Probability in Civil Engineering (ICASP)*. **9**, 119-124.

Vorechovsky, M. (2004). Stochastic fracture mechanics and size effect. Ph.D. Thesis. Bruno University of Technology.

Waschbeton. (2013). Precast structures company. http://www.waschbeton.com.

Yamazaki, F., Shinozuka, M., Dasgupta, G. (1988). Neumann expansion for stochastic finite element analysis. *Journal of Engineering Mechanics*. **114(8)**, 1335-1354.

Yang, J. M., Lee, J. H., Shin, H. O., Yoon, Y. S. (2009). Enhancing the performance of high-strength concrete corbels using steel fibers and headed bars. *Journal of the Korea Concrete Institute*. **21(6)**. 697-703.

Yang, J. M., Lee, J. H., Yoon, Y. S., Cook, W. D. and Mitchell, D. (2012). Influence of steel fibers and headed bars on the serviceability of high-strength concrete corbels. *Journal of Structural Engineering*. **138(1)**, 123-129.

APPENDIX A

Table A.1 Comparison of Experimental and Finite Element Model Results for SFRC Corbels

References	Corbel Number	Shear Span	Width	Effec. depth	Height	Reinfor. Ratio	Comp. Strength	Sp. Ten. Strength	V_{exp} (kN)	V_{NLFEA} (kN)	V_{NLFEA}/V_{exp}
		a **(mm)**	***b*** **(mm)**	***d*** **(mm)**	***h*** **(mm)**	A_s/bh **(%)**	f_c **(MPa)**	f_{ct} **(MPa)**			
Fattuhi and Hughes (1989)	C2	125	152	120	147,5	0,700	43,34	4,37	84,5	87,80	1,039
	C3	125	152	119	146	0,710	42,61	5,45	92,9	92,21	0,993
	C4	125	151	123	149,5	0,700	41,63	4,79	91,8	97,32	1,060
	C5	125	152	119	146	0,710	41,39	5,36	96,0	97,19	1,012
	C6	125	156	117	146,5	0,690	32,48	3,19	75,2	90,21	1,200
Fattuhi and Hughes (1989)	C27	52,5	153	121	148,5	0,450	38,31	4,64	125,8	130,10	1,034
	C28	89	151	124	148	0,450	45,12	6,09	88,2	88,87	1,008
	C29	125	153	130	149	0,440	45,12	6,09	65,9	67,99	1,032
	C30	52,5	154	121,5	146,5	0,700	41,63	4,79	171,0	190,60	1,115
	C31	64,5	153	118	146	1,020	46,17	5,05	179,0	194,90	1,089
	C32	125	153	118	148	1,000	38,31	4,64	110,1	112,30	1,020
Fattuhi and Hughes (1989)	T3	89	152	122	148	0,700	38,80	4,66	133,0	132,50	0,996
	T4	89	151	123	147	0,710	45,28	6,19	142,5	145,10	1,018
	T5	89	152	123	147	0,700	46,49	9,28	143,0	151,40	1,059
	T10	89	151	117	147	1,020	38,80	4,66	138,0	149,90	1,086
	T11	89	152	121	146	1,020	45,28	6,19	160,2	171,9	1,073
	T12	89	152	121	147	1,020	46,49	9,28	171,2	176,8	1,033
Fattuhi (1990)	1	80	152,5	123	149	1	33,53	5,84	153,0	159,40	1,042
	2	80	155	124	150	0,98	35,15	5,44	160,0	164,00	1,025
	3	80	152,5	126	150	0,44	34,02	4,86	91,2	98,29	1,078
	4	80	155	125	149	0,44	32,89	5,30	93,0	98,97	1,064
	5	140	155	123	149	0,98	32,81	5,46	103,0	100,90	0,980

Table A.1 (Continued)

	Corbel Number	Shear Span a (mm)	Width b (mm)	Effec. depth d (mm)	Height h (mm)	Reinfor. Ratio A_s/bh (%)	Comp. Strength f_c (MPa)	Sp. Ten. Strength f_{ct} (MPa)	V_{exp} (kN)	V_{NLFEA} (kN)	V_{NLFEA}/V_{exp}
	6	140	154,5	124	150	0,98	30,78	5,35	95,7	100,20	1,047
	7	140	153	126	150	0,44	27,38	3,89	53,3	54,13	1,016
	8	140	153	125,5	149,5	0,44	29,89	3,72	53,1	53,78	1,013
	9	80	152,5	123	149	1	27,95	5,29	152,9	153,30	1,003
	10	140	155,5	123	149	0,98	30,05	5,24	102,9	99,10	0,963
	11	140	153	126	150	0,44	29,00	3,76	56,0	53,84	0,961
	12	80	154	125	149	0,44	30,78	3,89	92,0	89,41	0,972
	13	110	154,7	123	149	0,99	27,54	5,04	111,7	121,30	1,086
	14	110	153,5	125	149	0,44	29,57	4,24	68,3	67,38	0,987
	15	110	152,5	126	150	0,44	31,59	3,92	67,2	70,21	1,045
	16	110	154,5	123,5	149,5	0,98	30,54	4,94	114,3	127,50	1,115
	18	89	154	124,5	150,5	0,99	26,41	4,98	119,0	141,70	1,191
Fattuhi (1990)	20	110	153	123,5	149,5	0,99	31,27	5,43	126,0	128,00	1,016
	21	110	156	122	148	0,98	29,97	4,73	118,0	123,5	1,047
	22	100	153	123	149	0,69	29,97	4,73	108,5	107,1	0,987
	23	110	153	122,5	148,5	1,000	27,38	5,12	126,5	125,7	0,994
	24	80	153	124	150	0,69	27,38	5,12	131,5	134,4	1,022
	27	80	153,5	123,5	149,5	0,99	34,26	6,29	171,5	178	1,038
	28	60	154	124	150	0,68	34,26	6,29	173,5	178	1,026
	29	75	151,5	122,5	148,5	0,45	30,21	4,42	100,0	98,12	0,981
	30	120	153,9	120,2	146,2	0,7	30,21	4,42	86,5	85,95	0,994
	31	135	154,5	124	150	1,19	32,89	5,50	119,5	128,7	1,077
	32	120	154	120,2	146,2	1,23	32,89	5,50	132,5	137,1	1,035

Table A.1 (Continued)

	Corbel Number	**Shear Span** a **(mm)**	**Width** b **(mm)**	**Effec. depth** d **(mm)**	**Height** h **(mm)**	**Reinfor. Ratio** A_s/bh **(%)**	**Comp. Strength** f_c **(MPa)**	**Sp. Ten. Strength** f_{ct} **(MPa)**	V_{exp} **(kN)**	V_{NLFEA} **(kN)**	V_{NLFEA}/V_{exp}
	35	135	155,1	122,5	148,5	1,48	31,35	4,91	124,5	132,7	1,066
	36	60	154,8	122	148	0,44	31,35	4,91	123,5	122,5	0,992
	37	135	153,8	123,1	149,1	1,49	32,08	5,72	140,0	143,1	1,022
	38	110	152,2	124	150	0,44	32,08	5,72	74,0	81,58	1,102
	39	110	153,5	124	150	1,2	31,35	5,64	144,5	150,90	1,044
	40	125	155,5	122,8	148,8	1,47	31,35	5,64	142,0	152,00	1,070
	44	135	153,8	122,6	148,6	1,21	28,67	4,85	109,5	118,80	1,085
	45	135	153	122,3	148,3	1,5	28,19	4,37	120,0	118,50	0,988
	46	75	154,5	92	146	0,45	28,19	4,37	74,5	76,84	1,031
	48	80	155,5	93,2	148,2	0,68	28,92	5,16	100,0	104,50	1,045
	49	80	154,1	122,1	148,2	1,000	30,46	5,81	164,5	169,60	1,031
Fattuhi (1994)	51	110	153,4	132,3	148,3	1,000	31,27	5,83	130,5	138,20	1,059
	52	110	152,2	94	150	1,000	31,27	5,83	99,0	100,20	1,012
	53	135	153,6	133,6	149,6	1,480	33,29	5,68	144,5	150,80	1,044
	54	135	151,7	93,8	149,8	1,490	33,29	5,68	101,5	109,50	1,079
	55	75	153,7	135,3	149,3	0,440	29,89	4,06	104,0	106,40	1,023
	56	75	152,9	115,8	149,8	0,440	29,89	4,06	95,5	93,44	0,978
	57	80	152,2	135,1	150,1	0,690	31,43	5,92	138,5	143,40	1,035
	58	80	152,8	113,3	148,3	0,690	31,43	5,92	121,5	127,60	1,050
	59	135	153	114	150	0,990	29,32	5,37	97,5	97,87	1,004
	60	110	152,8	112,6	148,6	1,490	29,32	5,37	142,0	142,20	1,001
	61	60	152,6	95	149	0,440	29,40	4,82	98,5	100,60	1,021
	62	135	153	114,1	150,1	1,200	29,40	4,82	109,5	110,40	1,008

Table A.1 (Continued)

	Corbel Number	**Shear Span**	**Width**	**Effec. depth**	**Height**	**Reinfor. Ratio**	**Comp. Strength**	**Sp. Ten. Strength**	V_{exp} **(kN)**	V_{NLFEA} **(kN)**	V_{NLFEA}/V_{exp}
		***a* (mm)**	***b* (mm)**	***d* (mm)**	***h* (mm)**	A_s/bh **(%)**	f_c **(MPa)**	f_{ct} **(MPa)**			
	63	80	153	94	150	0,680	30,94	5,94	101,8	111,20	1,092
	64	60	152,6	92,5	147,5	1,000	30,94	5,94	170,0	170,10	1,001
	75	75	154,3	125,9	149,9	0,440	25,11	4,05	94,8	96,41	1,017
	76	75	154,5	94,8	148,8	0,440	25,11	4,05	73,5	75,66	1,029
	77	110	153,1	122,3	148,3	1,000	26,89	4,96	114,5	120,2	1,050
	78	135	153,1	121,7	147,7	1,500	26,89	4,96	120,0	122,3	1,019
	79	135	153,2	123,4	149,4	1,480	27,38	5,26	128,0	130,6	1,020
	80	110	154	122,1	148,1	1,000	27,38	5,26	120,8	124,7	1,032
	81	135	153,6	121,6	147,6	1,220	28,67	5,04	110,8	122,2	1,103
	82	110	154	92	148	1,000	28,67	5,04	98,0	96,66	0,986
	83	135	150,4	111,9	147,9	1,530	28,27	4,96	115,3	118,6	1,029
	84	135	152,4	91,7	147,7	1,510	28,27	4,96	94,0	99,29	1,056
	85	110	154,2	112,5	148,5	0,990	28,43	5,17	123,3	116,2	0,942
	86	135	153,2	113,9	149,9	1,480	28,43	5,17	115,5	125,8	1,089
	87	60	152,9	93,5	148,5	0,690	29,32	6,01	139,8	141,8	1,014
	88	80	153,1	93,1	149,1	1,000	29,32	6,01	138,8	132,2	0,952
Gulsan (2015)	50-1-10-100	100	150	120	150	0,698	40,00	3,70	110,58	106,90	0,967
	50-1-10-130	130	150	124	150	0,698	40,00	3,70	78,80	79,82	1,013
	50-1-12-100	100	150	122	150	1,005	38,00	3,60	121,78	124,30	1,021
	50-1-12-130	130	150	122	150	1,005	38,00	3,60	89,18	87,05	0,976
	50-1,5-10-100	100	150	123	150	0,698	42,50	4,50	125,13	114,7	0,917
	50-1,5-10-130	130	150	125	150	0,698	42,50	4,50	86,58	87,66	1,012
	50-1,5-12-100	100	150	124	150	1,005	42,50	4,20	127,54	135,9	1,066

Table A.1 (Continued)

Corbel Number	**Shear Span**	**Width**	**Effec. depth**	**Height**	**Reinfor. Ratio**	**Comp. Strength**	**Sp. Ten. Strength**	V_{exp} **(kN)**	V_{NLFEA} **(kN)**	V_{NLFEA}/V_{exp}
	a **(mm)**	b **(mm)**	d **(mm)**	h **(mm)**	A_s/bh **(%)**	f_c **(MPa)**	f_{ct} **(MPa)**			
50-1,5-12-130	130	150	125	150	1,005	42,50	4,20	89,13	94,21	1,057
30-1-10-100	100	150	124	150	0,698	22,3	2,5	71,00	79,95	1,126
30-1-10-130	130	150	124	150	0,698	22,3	2,5	52,60	55,61	1,057
30-1-12-100	100	150	124	150	1,005	22,3	2,3	73,39	85,53	1,165
30-1-12-130	130	150	127	150	1,005	22,3	2,3	56,15	58,77	1,047
30-1,5-10-100	100	150	122	150	0,698	25,50	3,10	79,66	84,96	1,066
30-1,5-10-130	130	150	123	150	0,698	25,50	3,10	58,35	59,05	1,012
30-1,5-12-100	100	150	127	150	1,005	25,50	3,10	87,01	95,77	1,101
30-1,5-12-130	130	150	124	150	1,005	25,50	3,10	59,79	64,54	1,079
									Mean	1,036
									Std. Dev.	0,048
									COV	0,047
									Highest V.	1,200

Table A.2 Stochastic Finite Element Results of SFRC Corbels

Corbel Number	*a* (mm)	*a/d*	Standard Deviation (kN)	COV of Resistance	Stochastic Analysis Resistance (kN)			Distribution Type
					R_{min}	R_{mean}	R_{max}	
C2	125	1,04	0,73	0,008	85,40	87,51	88,90	Lognormal 3 parameter
C3	125	1,05	2,33	0,025	87,43	93,17	96,69	Rayleigh negative
C4	125	1,02	2,14	0,022	91,74	96,68	99,94	Rayleigh negative
C5	125	1,05	2,63	0,027	90,96	97,49	103,10	Logistic
C6	125	1,07	1,64	0,018	85,08	89,57	91,85	Half-normal negative
C27	52,5	0,43	5,26	0,041	118,72	127,65	136,66	Beta
C28	89	0,72	4,67	0,053	79,81	88,37	98,93	Lognormal 3 parameter
C29	125	0,96	3,77	0,056	58,99	67,71	73,93	Triangular
C30	52,5	0,43	3,83	0,020	184,88	191,31	199,01	Weibull min. 3 parameter
C31	64,5	0,55	4,92	0,025	184,29	193,57	203,48	Rayleigh negative
C32	125	1,06	1,93	0,017	107,83	111,35	114,22	Beta
T3	89	0,73	4,55	0,035	122,10	130,92	137,08	Half-normal negative
T4	89	0,72	5,55	0,038	129,07	145,20	155,45	Lognormal 3 parameter
T5	89	0,72	6,77	0,045	132,73	150,86	161,79	Lognormal 3 parameter
T10	89	0,76	4	0,027	139,14	149,34	156,26	Half-normal negative
T11	89	0,74	5,72	0,033	153,95	171,08	179,52	Beta
T12	89	0,74	7,43	0,042	157,08	176,17	188,91	Weibull max. 3 parameter
1	80	0,65	4,3	0,027	147,09	159,48	166,80	Gamma negative 3 parameter
2	80	0,65	4,8	0,029	149,55	163,01	169,06	Beta
3	80	0,63	5,93	0,061	81,98	97,42	107,61	Lognormal 3 parameter
4	80	0,64	6,08	0,063	83,00	97,27	108,44	Rayleigh negative
5	140	1,14	2,58	0,026	93,46	100,39	104,96	Logistic
6	140	1,13	2,3	0,023	93,00	99,64	103,36	Lognormal 3 parameter

Table A.2 (Continued)

Corbel Number	*a* (mm)	*a/d*	Standard Deviation (kN)	COV of Resistance	Stochastic Analysis Resistance (kN)			Distribution Type
					R_{min}	R_{mean}	R_{max}	
7	140	1,11	2,94	0,054	46,67	54,05	59,23	Lognormal 3 parameter
8	140	1,12	2,84	0,053	46,82	53,69	58,54	Lognormal 3 parameter
9	80	0,65	3,78	0,025	143,09	152,33	160,68	Gumbel max. EV I
10	140	1,14	2,09	0,021	94,18	98,65	102,17	Gumbel min. EV I
11	140	1,11	2,85	0,053	46,85	53,72	58,50	Weibull min. 3 parameter
12	80	0,64	4,67	0,052	79,05	90,01	98,44	Gumbel min. EV I
13	110	0,89	2,6	0,022	113,22	119,74	123,38	Beta
14	110	0,88	3,44	0,051	59,10	67,24	73,31	Weibull max. 3 parameter
15	110	0,87	3,54	0,051	60,95	69,89	75,89	Weibull min. 2 parameter
16	110	0,89	3,4	0,027	116,54	125,87	132,76	Weibull min. 3 parameter
18	89	0,71	3,51	0,025	129,03	140,43	145,41	Gumbel min. EV I
20	110	0,89	3,52	0,028	118,60	127,72	132,11	Beta
21	110	0,90	2,83	0,023	115,71	123,21	127,39	Beta
22	100	0,81	3,78	0,035	96,06	106,65	113,47	Lognormal 3 parameter
23	110	0,90	3,35	0,027	117,73	125,97	131,44	Normal
24	80	0,65	5,39	0,040	119,10	133,83	144,90	Rayleigh negative
27	80	0,65	5,83	0,033	159,94	177,29	185,46	Rayleigh negative
28	60	0,48	7,88	0,045	157,26	176,70	193,02	Rayleigh negative
29	75	0,61	5,11	0,052	86,16	97,86	107,03	Rayleigh negative
30	120	1,00	2,73	0,032	78,92	85,76	90,68	Weibull max. 3 parameter
31	135	1,09	3,24	0,025	119,35	128,43	133,92	Lognormal 3 parameter
32	120	1,00	3,31	0,024	128,75	136,41	142,70	Normal
35	135	1,10	4,65	0,035	121,73	131,10	141,28	Gumbel min. EV I

Table A.2 (Continued)

Corbel Number	***a* (mm)**	***a/d***	**Standard Deviation (kN)**	**COV of Resistance**	**Stochastic Analysis Resistance (kN)**			**Distribution Type**
					R_{min}	**R_{mean}**	**R_{max}**	
36	60	0,49	6,87	0,057	105,00	121,43	134,84	Gamma negative 3 parameter
37	135	1,10	5	0,035	125,97	142,35	150,92	Gumbel min. EV I
38	110	0,89	5,5	0,068	67,98	81,46	93,33	Logistic
39	110	0,89	3,85	0,026	138,97	150,26	156,88	Gumbel max. EV I
40	125	1,02	4,93	0,033	136,70	150,31	157,58	Rayleigh negative
44	135	1,10	3,38	0,029	109,96	117,98	122,34	Half-normal negative
45	135	1,10	4,87	0,041	103,09	118,35	125,83	Lognormal 3 parameter
46	75	0,82	5,2	0,068	64,24	76,57	86,95	Weibull min. 2 parameter
48	80	0,86	5,5	0,052	92,34	105,15	115,60	Triangular
49	80	0,66	5,17	0,031	153,79	168,56	176,73	Normal
51	110	0,83	3,48	0,025	127,41	137,80	142,67	Gumbel min. EV I
52	110	1,17	2,77	0,028	92,50	99,69	104,26	Weibull min. 2 parameter
53	135	1,01	5,39	0,036	133,25	150,41	157,60	Gamma negative 3 parameter
54	135	1,44	2,12	0,019	103,99	108,85	112,86	Rayleigh negative
55	75	0,55	5,41	0,051	92,54	106,03	114,03	Weibull max. 3 parameter
56	75	0,65	5,6	0,060	78,64	93,31	103,01	Gamma negative 3 parameter
57	80	0,59	5,9	0,041	128,30	143,17	151,49	Beta
58	80	0,71	6,54	0,052	110,45	126,55	137,18	Beta
59	135	1,18	2,52	0,026	91,46	97,68	101,78	Lognormal 3 parameter
60	110	0,98	5,49	0,039	125,85	141,73	153,37	Lognormal 3 parameter
61	60	0,63	7,36	0,074	83,87	99,92	113,06	Triangular
62	135	1,18	2,38	0,022	102,06	109,64	113,03	Beta
63	80	0,85	6,34	0,057	96,64	111,43	123,45	Lognormal 3 parameter

Table A.2 (Continued)

Corbel Number	*a* (mm)	*a/d*	Standard Deviation (kN)	COV of Resistance	Stochastic Analysis Resistance (kN)			Distribution Type
					R_{min}	R_{mean}	R_{max}	
64	60	0,65	6,01	0,036	151,69	168,12	179,01	Weibull min 3 para
75	75	0,60	5,03	0,052	84,21	96,25	104,52	Weibull max. 3 parameter
76	75	0,79	4,36	0,058	63,31	74,81	82,54	Weibull min. 2 parameter
77	110	0,90	2,93	0,024	110,50	120,19	124,08	Lognormal 3 parameter
78	135	1,11	5,12	0,042	104,33	120,88	129,74	Weibull min. 2 parameter
79	135	1,09	4,9	0,038	119,12	130,16	138,14	Lognormal 2 para
80	110	0,90	3,25	0,026	117,40	124,93	132,81	Weibull max. 3 parameter
81	135	1,11	3,29	0,027	109,57	120,67	127,74	Student-t
82	110	1,20	2,93	0,030	88,85	96,10	100,85	Half-normal negative
83	135	1,21	4,67	0,040	105,88	116,75	124,52	Logistic
84	135	1,47	3,67	0,038	85,53	97,68	103,00	Lognormal 3 parameter
85	110	0,98	3,78	0,033	107,53	115,97	121,57	Normal
86	135	1,19	3,87	0,031	114,61	124,77	132,44	Lognormal 3 parameter
87	60	0,64	7,6	0,054	119,77	140,37	152,03	Gamma negative 3 parameter
88	80	0,86	4,06	0,031	119,81	131,67	138,19	Normal

Table A.3 Results of Reliability Analyses of SFRC Corbels

Corbel No.	Std. Dev. of Res.	COV of Res.	Nominal Load (kN) ($D/(D+L)$=0.5)	Load Combination ($1.2D+1.6L$) (kN)	Nominal Resistance (R) (kN)				Bias Factors (λ)			
					Φ = 0,9	Φ = 0,85	Φ = 0,8	Φ = 0,75	Φ = 0,9	Φ = 0,85	Φ = 0,8	Φ = 0,75
C2	0,73	0,008	53,52	74,93	83,25	88,15	93,66	99,90	1,05	0,99	0,93	0,88
C3	2,33	0,025	56,06	78,48	87,20	92,33	98,11	104,65	1,07	1,01	0,95	0,89
C4	2,14	0,022	64,20	89,88	99,87	105,74	112,35	119,84	0,97	0,91	0,86	0,81
C5	2,63	0,027	58,49	81,89	90,98	96,34	102,36	109,18	1,07	1,01	0,95	0,89
C6	1,64	0,018	54,36	76,10	84,56	89,53	95,13	101,47	1,06	1,00	0,94	0,88
C27	5,26	0,041	74,41	104,17	115,75	122,56	130,22	138,90	1,10	1,04	0,98	0,92
C28	4,67	0,053	49,85	69,79	77,54	82,11	87,24	93,05	1,14	1,08	1,01	0,95
C29	3,77	0,056	37,84	52,98	58,86	62,32	66,22	70,63	1,15	1,09	1,02	0,96
C30	3,83	0,020	115,88	162,23	180,26	190,86	202,79	216,31	1,06	1,00	0,94	0,88
C31	4,92	0,025	116,41	162,97	181,08	191,73	203,72	217,30	1,07	1,01	0,95	0,89
C32	1,93	0,017	67,65	94,71	105,23	111,42	118,39	126,28	1,06	1,00	0,94	0,88
T3	4,55	0,035	77,44	108,42	120,46	127,55	135,52	144,55	1,09	1,03	0,97	0,91
T4	5,55	0,038	85,24	119,34	132,60	140,40	149,17	159,11	1,10	1,03	0,97	0,91
T5	6,77	0,045	87,12	121,97	135,52	143,49	152,46	162,62	1,11	1,05	0,99	0,93
T10	4	0,027	89,62	125,47	139,41	147,61	156,84	167,29	1,07	1,01	0,95	0,89
T11	5,72	0,033	101,46	142,04	157,83	167,11	177,56	189,39	1,08	1,02	0,96	0,90
T12	7,43	0,042	102,45	143,43	159,37	168,74	179,29	191,24	1,11	1,04	0,98	0,92
1	4,3	0,027	95,68	133,95	148,84	157,59	167,44	178,60	1,07	1,01	0,95	0,89
2	4,8	0,029	97,39	136,35	151,50	160,41	170,43	181,79	1,08	1,02	0,96	0,90
3	5,93	0,061	53,45	74,83	83,14	88,04	93,54	99,77	1,17	1,11	1,04	0,98
4	6,08	0,063	53,04	74,26	82,51	87,36	92,82	99,01	1,18	1,11	1,05	0,98
5	2,58	0,026	60,35	84,49	93,88	99,40	105,61	112,65	1,07	1,01	0,95	0,89

Table A.3 (Continued)

Corbel No.	**Std. Dev. of Res.**	**COV of Res.**	**Nominal Load (kN) (*D*/(*D*+*L*)=0.5)**	**Load Combination (1.2*D*+1.6*L*) (kN)**	**Nominal Resistance (*R*) (kN)**				**Bias Factors (λ)**			
					Φ = 0,9	**Φ = 0,85**	**Φ = 0,8**	**Φ = 0,75**	**Φ = 0,9**	**Φ = 0,85**	**Φ = 0,8**	**Φ = 0,75**
6	2,3	0,023	60,12	84,17	93,52	99,02	105,21	112,22	1,07	1,01	0,95	0,89
7	2,94	0,054	30,34	42,48	47,20	49,97	53,10	56,63	1,15	1,08	1,02	0,95
8	2,84	0,053	30,28	42,39	47,10	49,87	52,99	56,52	1,14	1,08	1,01	0,95
9	3,78	0,025	91,69	128,37	142,63	151,02	160,46	171,15	1,07	1,01	0,95	0,89
10	2,09	0,021	59,67	83,54	92,82	98,28	104,42	111,38	1,06	1,00	0,94	0,89
11	2,85	0,053	30,28	42,39	47,10	49,87	52,99	56,52	1,14	1,08	1,01	0,95
12	4,67	0,052	50,93	71,30	79,22	83,88	89,13	95,07	1,14	1,07	1,01	0,95
13	2,6	0,022	72,38	101,33	112,59	119,21	126,67	135,11	1,06	1,00	0,95	0,89
14	3,44	0,051	38,13	53,38	59,31	62,80	66,73	71,18	1,13	1,07	1,01	0,94
15	3,54	0,051	39,70	55,58	61,76	65,39	69,48	74,11	1,13	1,07	1,01	0,94
16	3,4	0,027	75,51	105,71	117,46	124,37	132,14	140,95	1,07	1,01	0,95	0,89
18	3,51	0,025	84,50	118,30	131,44	139,18	147,88	157,73	1,07	1,01	0,95	0,89
20	3,52	0,028	76,55	107,17	119,08	126,08	133,96	142,89	1,07	1,01	0,95	0,89
21	2,83	0,023	74,35	104,09	115,66	122,46	130,11	138,79	1,07	1,01	0,95	0,89
22	3,78	0,035	62,99	88,19	97,98	103,75	110,23	117,58	1,09	1,03	0,97	0,91
23	3,35	0,027	75,62	105,87	117,63	124,55	132,34	141,16	1,07	1,01	0,95	0,89
24	5,39	0,040	78,19	109,47	121,63	128,78	136,83	145,95	1,10	1,04	0,98	0,92
27	5,83	0,033	105,26	147,36	163,74	173,37	184,21	196,49	1,08	1,02	0,96	0,90
28	7,88	0,045	102,12	142,97	158,85	168,20	178,71	190,62	1,11	1,05	0,99	0,93
29	5,11	0,052	55,31	77,43	86,04	91,10	96,79	103,25	1,14	1,07	1,01	0,95
30	2,73	0,032	51,02	71,43	79,36	84,03	89,29	95,24	1,08	1,02	0,96	0,90
31	3,24	0,025	77,26	108,16	120,18	127,25	135,21	144,22	1,07	1,01	0,95	0,89
32	3,31	0,024	82,17	115,04	127,82	135,34	143,80	153,38	1,07	1,01	0,95	0,89

Table A.3 (Continued)

Corbel No.	**Std. Dev. of Res.**	**COV of Res.**	**Nominal Load (kN) (*D*/(*D*+*L*)=0.5)**	**Load Combination (1.2*D*+1.6*L*) (kN)**	**Nominal Resistance (*R*) (kN)**				**Bias Factors (λ)**			
					Φ **= 0,9**	Φ **= 0,85**	Φ **= 0,8**	Φ **= 0,75**	Φ **= 0,9**	Φ **= 0,85**	Φ **= 0,8**	Φ **= 0,75**
35	4,65	0,035	77,43	108,40	120,45	127,53	135,50	144,54	1,09	1,03	0,97	0,91
36	6,87	0,057	67,66	94,72	105,25	111,44	118,41	126,30	1,15	1,09	1,03	0,96
37	5	0,035	84,13	117,78	130,87	138,57	147,23	157,04	1,09	1,03	0,97	0,91
38	5,5	0,068	43,54	60,96	67,73	71,71	76,20	81,27	1,20	1,14	1,07	1,00
39	3,85	0,026	90,34	126,48	140,53	148,80	158,10	168,63	1,07	1,01	0,95	0,89
40	4,93	0,033	89,25	124,95	138,83	147,00	156,19	166,60	1,08	1,02	0,96	0,90
44	3,38	0,029	70,59	98,83	109,81	116,27	123,53	131,77	1,07	1,01	0,96	0,90
45	4,87	0,041	69,00	96,60	107,33	113,65	120,75	128,80	1,10	1,04	0,98	0,92
46	5,2	0,068	40,86	57,20	63,56	67,30	71,51	76,27	1,20	1,14	1,07	1,00
48	5,5	0,052	59,42	83,19	92,43	97,87	103,99	110,92	1,14	1,07	1,01	0,95
49	5,17	0,031	100,50	140,70	156,33	165,53	175,88	187,60	1,08	1,02	0,96	0,90
51	3,48	0,025	82,89	116,05	128,94	136,52	145,06	154,73	1,07	1,01	0,95	0,89
52	2,77	0,028	59,73	83,62	92,91	98,38	104,53	111,50	1,07	1,01	0,95	0,89
53	5,39	0,036	88,76	124,26	138,07	146,19	155,33	165,69	1,09	1,03	0,97	0,91
54	2,12	0,019	65,98	92,37	102,64	108,67	115,47	123,16	1,06	1,00	0,94	0,88
55	5,41	0,051	60,16	84,22	93,58	99,09	105,28	112,30	1,13	1,07	1,01	0,94
56	5,6	0,060	51,36	71,90	79,89	84,59	89,88	95,87	1,17	1,10	1,04	0,97
57	5,9	0,041	83,46	116,84	129,83	137,46	146,06	155,79	1,10	1,04	0,98	0,92
58	6,54	0,052	71,65	100,31	111,46	118,01	125,39	133,75	1,14	1,07	1,01	0,95
59	2,52	0,026	58,71	82,19	91,33	96,70	102,74	109,59	1,07	1,01	0,95	0,89
60	5,49	0,039	83,11	116,35	129,28	136,89	145,44	155,14	1,10	1,04	0,97	0,91
61	7,36	0,074	51,98	72,77	80,86	85,61	90,97	97,03	1,24	1,17	1,10	1,03
62	2,38	0,022	66,27	92,78	103,09	109,15	115,97	123,70	1,06	1,00	0,95	0,89

Table A.3 (Continued)

Corbel No.	**Std. Dev. of Res.**	**COV of Res.**	**Nominal Load (kN) (*D*/(*D*+*L*)=0.5)**	**Load Combination (1.2*D*+1.6*L*) (kN)**	**Nominal Resistance (*R*) (kN)**				**Bias Factors (λ)**			
					Φ = 0,9	**Φ = 0,85**	**Φ = 0,8**	**Φ = 0,75**	**Φ = 0,9**	**Φ = 0,85**	**Φ = 0,8**	**Φ = 0,75**
63	6,34	0,057	62,02	86,83	96,48	102,15	108,54	115,77	1,16	1,09	1,03	0,96
64	6,01	0,036	99,23	138,92	154,36	163,44	173,65	185,23	1,09	1,03	0,97	0,91
75	5,03	0,052	54,40	76,16	84,62	89,60	95,20	101,55	1,14	1,07	1,01	0,95
76	4,36	0,058	41,44	58,02	64,46	68,25	72,52	77,35	1,16	1,10	1,03	0,97
77	2,93	0,024	72,39	101,35	112,61	119,23	126,68	135,13	1,07	1,01	0,95	0,89
78	5,12	0,042	70,26	98,36	109,29	115,72	122,96	131,15	1,11	1,04	0,98	0,92
79	4,9	0,038	76,51	107,11	119,02	126,02	133,89	142,82	1,09	1,03	0,97	0,91
80	3,25	0,026	75,06	105,08	116,76	123,63	131,36	140,11	1,07	1,01	0,95	0,89
81	3,29	0,027	72,36	101,30	112,56	119,18	126,63	135,07	1,07	1,01	0,95	0,89
82	2,93	0,030	57,31	80,23	89,15	94,39	100,29	106,98	1,08	1,02	0,96	0,90
83	4,67	0,040	68,26	95,56	106,18	112,43	119,46	127,42	1,10	1,04	0,98	0,92
84	3,67	0,038	57,43	80,40	89,34	94,59	100,50	107,20	1,09	1,03	0,97	0,91
85	3,78	0,033	68,89	96,45	107,16	113,47	120,56	128,59	1,08	1,02	0,96	0,90
86	3,87	0,031	74,34	104,08	115,64	122,44	130,10	138,77	1,08	1,02	0,96	0,90
87	7,6	0,054	78,85	110,39	122,66	129,87	137,99	147,19	1,14	1,08	1,02	0,95
88	4,06	0,031	78,48	109,87	122,08	129,26	137,34	146,50	1,08	1,02	0,96	0,90
							Mean		1,10	1,04	0,98	0,92
							Biggest Value		1,24	1,17	1,10	1,03

Table A.4 Comparison of Experimental Results and Fattuhi's Model (V_{model}) and Proposed Models for Load Carrying Capacity of SFRC Corbels

Corbel Number	V_{exp} (kN)	V_{model} (kN)	$V_{proposed-1}$ (kN)	$V_{proposed-2}$ (kN)	V_{exp}/V_{model}	$V_{exp}/V_{proposed-1}$	$V_{exp}/V_{proposed-2}$
C2	84,5	86,43	80,16	78,68	0,98	1,054	1,074
C3	92,9	91,98	85,54	85,48	1,01	1,086	1,087
C4	91,8	93,74	84,95	84,00	0,98	1,081	1,093
C5	96,0	91,85	85,07	84,89	1,05	1,128	1,131
C6	75,2	80,92	71,40	68,32	0,93	1,053	1,101
C27	125,8	130,81	132,35	129,99	0,96	0,950	0,968
C28	88,2	90,91	93,78	94,15	0,97	0,940	0,937
C29	65,9	67,64	74,01	74,29	0,97	0,890	0,887
C30	171,0	181,17	173,00	171,04	0,94	0,988	1,000
C31	179,0	179,16	179,04	178,38	1,00	1,000	1,003
C32	110,1	101,47	100,54	99,48	1,09	1,095	1,107
T3	133,0	119,46	110,54	109,05	1,11	1,203	1,220
T4	142,5	135,42	121,76	122,92	1,05	1,170	1,159
T5	143,0	145,61	139,17	145,13	0,98	1,028	0,985
T10	138,0	134,19	131,55	130,23	1,03	1,049	1,060
T11	160,2	145,15	148,72	150,63	1,10	1,077	1,064
T12	171,2	169,24	171,45	179,41	1,01	0,999	0,954
1	153,0	149,00	163,52	164,81	1,03	0,936	0,928
2	160,0	169,49	162,54	162,86	0,94	0,984	0,982
3	91,2	96,25	97,28	95,89	0,95	0,937	0,951
4	93,0	98,86	100,44	99,69	0,94	0,926	0,933
5	103,0	95,86	100,78	101,02	1,07	1,022	1,020
6	95,7	91,76	101,13	101,20	1,04	0,946	0,946
7	53,3	53,70	56,86	55,06	0,99	0,937	0,968
8	53,1	52,18	55,65	53,69	1,02	0,954	0,989
9	152,9	143,78	158,20	158,18	1,06	0,967	0,967
10	102,9	90,66	99,73	99,64	1,14	1,032	1,033
11	56,0	51,74	56,22	54,29	1,08	0,996	1,032
12	92,0	86,68	89,98	87,12	1,06	1,022	1,056
13	111,7	110,50	120,42	119,94	1,01	0,928	0,931
14	68,3	68,52	70,82	69,05	1,00	0,964	0,989
15	67,2	66,99	69,45	67,29	1,00	0,968	0,999
16	114,3	111,58	119,55	118,87	1,02	0,956	0,962
18	119,0	132,41	145,31	144,58	0,90	0,819	0,823
20	126,0	122,29	122,93	123,17	1,03	1,025	1,023
21	118,0	109,76	116,58	115,51	1,08	1,012	1,022
22	108,5	102,44	102,00	100,73	1,06	1,064	1,077

Table A.4 (Continued)							
Corbel Number	**V_{exp} (kN)**	**V_{model} (kN)**	**$V_{proposed-1}$ (kN)**	**$V_{proposed-2}$ (kN)**	**V_{exp}/V_{model}**	**$V_{exp}/V_{proposed-1}$**	**$V_{exp}/V_{proposed-2}$**
23	126,5	119,28	119,63	119,31	1,06	1,057	1,060
24	131,5	120,21	127,81	127,03	1,09	1,029	1,035
27	171,5	172,37	168,86	171,20	0,99	1,016	1,002
28	173,5	181,73	173,60	175,38	0,95	0,999	0,989
29	100,0	99,21	96,81	94,72	1,01	1,033	1,056
30	86,5	82,03	83,66	82,19	1,05	1,034	1,052
31	119,5	108,78	117,98	118,54	1,10	1,013	1,008
32	132,5	116,09	125,62	126,25	1,14	1,055	1,050
35	124,5	119,86	127,10	126,80	1,04	0,980	0,982
36	123,5	127,31	120,92	119,28	0,97	1,021	1,035
37	140,0	132,23	134,25	135,59	1,06	1,043	1,033
38	74,0	73,42	77,61	77,52	1,01	0,953	0,955
39	144,5	129,20	140,86	141,82	1,12	1,026	1,019
40	142,0	130,33	142,31	143,55	1,09	0,998	0,989
44	109,5	103,59	111,60	111,02	1,06	0,981	0,986
45	120,0	115,05	121,22	119,81	1,04	0,990	1,002
46	74,5	81,20	76,19	74,48	0,92	0,978	1,000
48	100,0	104,37	100,59	100,03	0,96	0,994	1,000
49	164,5	147,55	163,06	164,28	1,11	1,009	1,001
51	130,5	121,22	133,37	134,41	1,08	0,978	0,971
52	99,0	96,11	100,71	101,50	1,03	0,983	0,975
53	144,5	133,34	143,10	144,44	1,08	1,010	1,000
54	101,5	94,18	105,85	106,86	1,08	0,959	0,950
55	104,0	105,72	102,88	99,95	0,98	1,011	1,041
56	95,5	93,94	90,22	87,65	1,02	1,059	1,090
57	138,5	144,80	143,44	144,24	0,96	0,966	0,960
58	121,5	124,69	122,89	123,58	0,97	0,989	0,983
59	97,5	87,89	96,94	97,06	1,11	1,006	1,005
60	142,0	129,81	143,30	144,00	1,09	0,991	0,986
61	98,5	107,51	96,85	95,40	0,92	1,017	1,032
62	109,5	97,30	104,90	104,29	1,13	1,044	1,050
63	101,8	108,63	105,75	106,36	0,94	0,963	0,957
64	170,0	172,90	163,27	164,78	0,98	1,041	1,032
75	94,8	102,97	97,59	94,79	0,92	0,971	1,000
76	73,5	83,72	76,60	74,40	0,88	0,960	0,988
77	114,5	108,96	118,12	117,51	1,05	0,969	0,974
78	120,0	114,45	125,52	125,34	1,05	0,956	0,957
79	128,0	117,70	130,04	130,44	1,09	0,984	0,981
80	120,8	110,32	120,84	120,78	1,09	1,000	1,000
81	110,8	103,01	111,92	111,68	1,08	0,990	0,992

Table A.4 (Continued)							
Corbel Number	***V_{exp}* (kN)**	***V_{model}* (kN)**	***$V_{proposed-1}$* (kN)**	***$V_{proposed-2}$* (kN)**	***V_{exp}/V_{model}***	***$V_{exp}/V_{proposed-1}$***	***$V_{exp}/V_{proposed-2}$***
82	98,0	91,08	94,06	93,70	1,08	1,042	1,046
83	115,3	105,73	116,49	116,35	1,09	0,990	0,991
84	94,0	86,68	99,11	98,98	1,08	0,948	0,950
85	123,3	110,73	112,02	111,80	1,11	1,101	1,103
86	115,5	109,63	121,35	121,57	1,05	0,952	0,950
87	139,8	144,34	134,01	134,92	0,97	1,043	1,036
88	138,8	131,39	131,54	132,89	1,06	1,055	1,044
50-1-10-100	110,58	111,18	91,46	88,57	0,99	1,209	1,248
50-1-10-130	78,80	88,23	75,56	73,17	0,89	1,043	1,077
50-1-12-100	121,78	126,19	113,95	110,47	0,97	1,069	1,102
50-1-12-130	89,18	100,70	91,59	88,80	0,89	0,974	1,004
50-1,5-10-100	125,13	116,40	99,68	98,06	1,08	1,255	1,276
50-1,5-10-130	86,58	87,11	81,21	79,89	0,99	1,066	1,084
50-1,5-12-100	127,54	131,57	121,61	119,37	0,97	1,049	1,068
50-1,5-12-130	89,13	105,51	98,41	96,60	0,84	0,906	0,923
30-1-10-100	71,00	96,06	82,45	77,36	0,74	0,861	0,918
30-1-10-130	52,60	77,07	66,27	62,19	0,68	0,794	0,846
30-1-12-100	73,39	111,67	99,43	92,98	0,66	0,738	0,789
30-1-12-130	56,15	92,68	81,53	76,24	0,61	0,689	0,736
30-1,5-10-100	79,66	99,26	87,40	83,44	0,80	0,911	0,955
30-1,5-10-130	58,35	79,83	70,74	67,54	0,73	0,825	0,864
30-1,5-12-100	87,01	121,08	112,07	107,35	0,72	0,776	0,811
30-1,5-12-130	59,79	95,56	88,31	84,60	0,63	0,677	0,707

Table A.5 Values of Cumulative Distribution Function (CDF) Φ(β) for the Standard Normal Probability Distribution

β	**Second Number after Decimal Point**									
	0	**0,01**	**0,02**	**0,03**	**0,04**	**0,05**	**0,06**	**0,07**	**0,08**	**0,09**
0	5,00E-01	4,96E-01	4,92E-01	4,88E-01	4,84E-01	4,80E-01	4,76E-01	4,72E-01	4,68E-01	4,64E-01
-0,1	4,60E-01	4,56E-01	4,52E-01	4,48E-01	4,44E-01	4,40E-01	4,36E-01	4,33E-01	4,29E-01	4,25E-01
-0,2	4,21E-01	4,17E-01	4,13E-01	4,09E-01	4,05E-01	4,01E-01	3,97E-01	3,94E-01	3,90E-01	3,86E-01
-0,3	3,82E-01	3,78E-01	3,74E-01	3,71E-01	3,67E-01	3,63E-01	3,59E-01	3,56E-01	3,52E-01	3,48E-01
-0,4	3,45E-01	3,41E-01	3,37E-01	3,34E-01	3,30E-01	3,26E-01	3,23E-01	3,19E-01	3,16E-01	3,12E-01
-0,5	3,09E-01	3,05E-01	3,02E-01	2,98E-01	2,95E-01	2,91E-01	2,88E-01	2,84E-01	2,81E-01	2,78E-01
-0,6	2,74E-01	2,71E-01	2,68E-01	2,64E-01	2,61E-01	2,58E-01	2,55E-01	2,51E-01	2,48E-01	2,45E-01
-0,7	2,42E-01	2,39E-01	2,36E-01	2,33E-01	2,30E-01	2,27E-01	2,24E-01	2,21E-01	2,18E-01	2,15E-01
-0,8	2,12E-01	2,09E-01	2,06E-01	2,03E-01	2,00E-01	1,98E-01	1,95E-01	1,92E-01	1,89E-01	1,87E-01
-0,9	1,84E-01	1,81E-01	1,79E-01	1,76E-01	1,74E-01	1,71E-01	1,69E-01	1,66E-01	1,64E-01	1,61E-01
-1	1,59E-01	1,56E-01	1,54E-01	1,52E-01	1,49E-01	1,47E-01	1,45E-01	1,42E-01	1,40E-01	1,38E-01
-1,1	1,36E-01	1,33E-01	1,31E-01	1,29E-01	1,27E-01	1,25E-01	1,23E-01	1,21E-01	1,19E-01	1,17E-01
-1,2	1,15E-01	1,13E-01	1,11E-01	1,09E-01	1,07E-01	1,06E-01	1,04E-01	1,02E-01	1,00E-01	9,85E-02
-1,3	9,68E-02	9,51E-02	9,34E-02	9,18E-02	9,01E-02	8,85E-02	8,69E-02	8,53E-02	8,38E-02	8,23E-02
-1,4	8,08E-02	7,93E-02	7,78E-02	7,64E-02	7,49E-02	7,35E-02	7,21E-02	7,08E-02	6,94E-02	6,81E-02
-1,5	6,68E-02	6,55E-02	6,43E-02	6,30E-02	6,18E-02	6,06E-02	5,94E-02	5,82E-02	5,71E-02	5,59E-02
-1,6	5,48E-02	5,37E-02	5,26E-02	5,16E-02	5,05E-02	4,95E-02	4,85E-02	4,75E-02	4,65E-02	4,55E-02
-1,7	4,46E-02	4,36E-02	4,27E-02	4,18E-02	4,09E-02	4,01E-02	3,92E-02	3,84E-02	3,75E-02	3,67E-02
-1,8	3,59E-02	3,51E-02	3,44E-02	3,36E-02	3,29E-02	3,22E-02	3,14E-02	3,07E-02	3,01E-02	2,94E-02
-1,9	2,87E-02	2,81E-02	2,74E-02	2,68E-02	2,62E-02	2,56E-02	2,50E-02	2,44E-02	2,39E-02	2,33E-02
-2	2,28E-02	2,22E-02	2,17E-02	2,12E-02	2,07E-02	2,02E-02	1,97E-02	1,92E-02	1,88E-02	1,83E-02
-2,1	1,79E-02	1,74E-02	1,70E-02	1,66E-02	1,62E-02	1,58E-02	1,54E-02	1,50E-02	1,46E-02	1,43E-02
-2,2	1,39E-02	1,36E-02	1,32E-02	1,29E-02	1,25E-02	1,22E-02	1,19E-02	1,16E-02	1,13E-02	1,10E-02
-2,3	1,07E-02	1,04E-02	1,02E-02	9,90E-03	9,64E-03	9,39E-03	9,14E-03	8,89E-03	8,66E-03	8,42E-03

Table A.5 (Continued)

β	Second Number after Decimal Point									
	0	**0,01**	**0,02**	**0,03**	**0,04**	**0,05**	**0,06**	**0,07**	**0,08**	**0,09**
-2,4	8,20E-03	7,98E-03	7,76E-03	7,55E-03	7,34E-03	7,14E-03	6,95E-03	6,76E-03	6,57E-03	6,39E-03
-2,5	6,21E-03	6,04E-03	5,87E-03	5,70E-03	5,54E-03	5,39E-03	5,23E-03	5,08E-03	4,94E-03	4,80E-03
-2,6	4,66E-03	4,53E-03	4,40E-03	4,27E-03	4,15E-03	4,02E-03	3,91E-03	3,79E-03	3,68E-03	3,57E-03
-2,7	3,47E-03	3,36E-03	3,26E-03	3,17E-03	3,07E-03	2,98E-03	2,89E-03	2,80E-03	2,72E-03	2,64E-03
-2,8	2,56E-03	2,48E-03	2,40E-03	2,33E-03	2,26E-03	2,19E-03	2,12E-03	2,05E-03	1,99E-03	1,93E-03
-2,9	1,87E-03	1,81E-03	1,75E-03	1,69E-03	1,64E-03	1,59E-03	1,54E-03	1,49E-03	1,44E-03	1,39E-03
-3	1,35E-03	1,31E-03	1,26E-03	1,22E-03	1,18E-03	1,14E-03	1,11E-03	1,07E-03	1,04E-03	1,00E-03
-3,1	9,68E-04	9,35E-04	9,04E-04	8,74E-04	8,45E-04	8,16E-04	7,89E-04	7,62E-04	7,36E-04	7,11E-04
-3,2	6,87E-04	6,64E-04	6,41E-04	6,19E-04	5,98E-04	5,77E-04	5,57E-04	5,38E-04	5,19E-04	5,01E-04
-3,3	4,83E-04	4,66E-04	4,50E-04	4,34E-04	4,19E-04	4,04E-04	3,90E-04	3,76E-04	3,62E-04	3,49E-04
-3,4	3,37E-04	3,25E-04	3,13E-04	3,02E-04	2,91E-04	2,80E-04	2,70E-04	2,60E-04	2,51E-04	2,42E-04
-3,5	2,33E-04	2,24E-04	2,16E-04	2,08E-04	2,00E-04	1,93E-04	1,85E-04	1,78E-04	1,72E-04	1,65E-04
-3,6	1,59E-04	1,53E-04	1,47E-04	1,42E-04	1,36E-04	1,31E-04	1,26E-04	1,21E-04	1,17E-04	1,12E-04
-3,7	1,08E-04	1,04E-04	9,96E-05	9,57E-05	9,20E-05	8,84E-05	8,50E-05	8,16E-05	7,84E-05	7,53E-05
-3,8	7,23E-05	6,95E-05	6,67E-05	6,41E-05	6,15E-05	5,91E-05	5,67E-05	5,44E-05	5,22E-05	5,01E-05
-3,9	4,81E-05	4,61E-05	4,43E-05	4,25E-05	4,07E-05	3,91E-05	3,75E-05	3,59E-05	3,45E-05	3,30E-05
-4	3,17E-05	3,04E-05	2,91E-05	2,79E-05	2,67E-05	2,56E-05	2,45E-05	2,35E-05	2,25E-05	2,16E-05
-4,1	2,07E-05	1,98E-05	1,89E-05	1,81E-05	1,74E-05	1,66E-05	1,59E-05	1,52E-05	1,46E-05	1,39E-05
-4,2	1,33E-05	1,28E-05	1,22E-05	1,17E-05	1,12E-05	1,07E-05	1,02E-05	9,77E-06	9,34E-06	8,93E-06
-4,3	8,54E-06	8,16E-06	7,80E-06	7,46E-06	7,12E-06	6,81E-06	6,50E-06	6,21E-06	5,93E-06	5,67E-06
-4,4	5,41E-06	5,17E-06	4,94E-06	4,71E-06	4,50E-06	4,29E-06	4,10E-06	3,91E-06	3,73E-06	3,56E-06
-4,5	3,40E-06	3,24E-06	3,09E-06	2,95E-06	2,81E-06	2,68E-06	2,56E-06	2,44E-06	2,32E-06	2,22E-06
-4,6	2,11E-06	2,01E-06	1,92E-06	1,83E-06	1,74E-06	1,66E-06	1,58E-06	1,51E-06	1,43E-06	1,37E-06
-4,7	1,30E-06	1,24E-06	1,18E-06	1,12E-06	1,07E-06	1,02E-06	9,68E-07	9,21E-07	8,76E-07	8,34E-07

Table A.5 (Continued)

β	Second Number after Decimal Point									
	0	**0,01**	**0,02**	**0,03**	**0,04**	**0,05**	**0,06**	**0,07**	**0,08**	**0,09**
-4,8	7,93E-07	7,55E-07	7,18E-07	6,83E-07	6,49E-07	6,17E-07	5,87E-07	5,58E-07	5,30E-07	5,04E-07
-4,9	4,79E-07	4,55E-07	4,33E-07	4,11E-07	3,91E-07	3,71E-07	3,52E-07	3,35E-07	3,18E-07	3,02E-07
-5	2,87E-07	2,72E-07	2,58E-07	2,45E-07	2,33E-07	2,21E-07	2,10E-07	1,99E-07	1,89E-07	1,79E-07
-5,1	1,70E-07	1,61E-07	1,53E-07	1,45E-07	1,37E-07	1,30E-07	1,23E-07	1,17E-07	1,11E-07	1,05E-07
-5,2	9,96E-08	9,44E-08	8,95E-08	8,48E-08	8,03E-08	7,60E-08	7,20E-08	6,82E-08	6,46E-08	6,12E-08
-5,3	5,79E-08	5,48E-08	5,19E-08	4,91E-08	4,65E-08	4,40E-08	4,16E-08	3,94E-08	3,72E-08	3,52E-08
-5,4	3,33E-08	3,15E-08	2,98E-08	2,82E-08	2,66E-08	2,52E-08	2,38E-08	2,25E-08	2,13E-08	2,01E-08
-5,5	1,90E-08	1,79E-08	1,69E-08	1,60E-08	1,51E-08	1,43E-08	1,35E-08	1,27E-08	1,20E-08	1,14E-08
-5,6	1,07E-08	1,01E-08	9,55E-09	9,01E-09	8,50E-09	8,02E-09	7,57E-09	7,14E-09	6,73E-09	6,35E-09
-5,7	5,99E-09	5,65E-09	5,33E-09	5,02E-09	4,73E-09	4,46E-09	4,21E-09	3,96E-09	3,74E-09	3,52E-09
-5,8	3,32E-09	3,12E-09	2,94E-09	2,77E-09	2,61E-09	2,46E-09	2,31E-09	2,18E-09	2,05E-09	1,93E-09
-5,9	1,82E-09	1,71E-09	1,61E-09	1,51E-09	1,43E-09	1,34E-09	1,26E-09	1,19E-09	1,12E-09	1,05E-09
-6	9,87E-10	9,28E-10	8,72E-10	8,20E-10	7,71E-10	7,24E-10	6,81E-10	6,40E-10	6,01E-10	5,65E-10
-6,1	5,30E-10	4,98E-10	4,68E-10	4,39E-10	4,13E-10	3,87E-10	3,64E-10	3,41E-10	3,21E-10	3,01E-10
-6,2	2,82E-10	2,65E-10	2,49E-10	2,33E-10	2,19E-10	2,05E-10	1,92E-10	1,81E-10	1,69E-10	1,59E-10
-6,3	1,49E-10	1,40E-10	1,31E-10	1,23E-10	1,15E-10	1,08E-10	1,01E-10	9,45E-11	8,85E-11	8,29E-11
-6,4	7,77E-11	7,28E-11	6,81E-11	6,38E-11	5,97E-11	5,59E-11	5,24E-11	4,90E-11	4,59E-11	4,29E-11
-6,5	4,02E-11	3,76E-11	3,52E-11	3,29E-11	3,08E-11	2,88E-11	2,69E-11	2,52E-11	2,35E-11	2,20E-11
-6,6	2,06E-11	1,92E-11	1,80E-11	1,68E-11	1,57E-11	1,47E-11	1,37E-11	1,28E-11	1,19E-11	1,12E-11
-6,7	1,04E-11	9,73E-12	9,09E-12	8,48E-12	7,92E-12	7,39E-12	6,90E-12	6,44E-12	6,01E-12	5,61E-12
-6,8	5,23E-12	4,88E-12	4,55E-12	4,25E-12	3,96E-12	3,69E-12	3,44E-12	3,21E-12	2,99E-12	2,79E-12
-6,9	2,60E-12	2,42E-12	2,26E-12	2,10E-12	1,96E-12	1,83E-12	1,70E-12	1,58E-12	1,48E-12	1,37E-12
-7	1,28E-12	1,19E-12	1,11E-12	1,03E-12	9,61E-13	8,95E-13	8,33E-13	7,75E-13	7,21E-13	6,71E-13
-7,1	6,24E-13	5,80E-13	5,40E-13	5,02E-13	4,67E-13	4,34E-13	4,03E-13	3,75E-13	3,49E-13	3,24E-13

Table A.5 (Continued)

β	**Second Number after Decimal Point**									
	0	**0,01**	**0,02**	**0,03**	**0,04**	**0,05**	**0,06**	**0,07**	**0,08**	**0,09**
-7,2	3,01E-13	2,80E-13	2,60E-13	2,41E-13	2,24E-13	2,08E-13	1,94E-13	1,80E-13	1,67E-13	1,55E-13
-7,3	1,44E-13	1,34E-13	1,24E-13	1,15E-13	1,07E-13	9,91E-14	9,20E-14	8,53E-14	7,91E-14	7,34E-14
-7,4	6,81E-14	6,31E-14	5,86E-14	5,43E-14	5,03E-14	4,67E-14	4,33E-14	4,01E-14	3,72E-14	3,44E-14
-7,5	3,19E-14	2,96E-14	2,74E-14	2,54E-14	2,35E-14	2,18E-14	2,02E-14	1,87E-14	1,73E-14	1,60E-14
-7,6	1,48E-14	1,37E-14	1,27E-14	1,17E-14	1,09E-14	1,00E-14	9,30E-15	8,60E-15	7,95E-15	7,36E-15
-7,7	6,80E-15	6,29E-15	5,82E-15	5,38E-15	4,97E-15	4,59E-15	4,25E-15	3,92E-15	3,63E-15	3,35E-15
-7,8	3,10E-15	2,86E-15	2,64E-15	2,44E-15	2,25E-15	2,08E-15	1,92E-15	1,77E-15	1,64E-15	1,51E-15
-7,9	1,39E-15	1,29E-15	1,19E-15	1,10E-15	1,01E-15	9,33E-16	8,60E-16	7,93E-16	7,32E-16	6,75E-16
-8	6,22E-16	5,74E-16	5,29E-16	4,87E-16	4,49E-16	4,14E-16	3,81E-16	3,51E-16	3,24E-16	2,98E-16
-8,1	2,75E-16	2,53E-16	2,33E-16	2,15E-16	1,98E-16	1,82E-16	1,68E-16	1,54E-16	1,42E-16	1,31E-16
-8,2	1,20E-16	1,11E-16	1,02E-16	9,36E-17	8,61E-17	7,92E-17	7,28E-17	6,70E-17	6,16E-17	5,66E-17
-8,3	5,21E-17	4,79E-17	4,40E-17	4,04E-17	3,71E-17	3,41E-17	3,14E-17	2,88E-17	2,65E-17	2,43E-17
-8,4	2,23E-17	2,05E-17	1,88E-17	1,73E-17	1,59E-17	1,46E-17	1,34E-17	1,23E-17	1,13E-17	1,03E-17
-8,5	9,48E-18	8,70E-18	7,98E-18	7,32E-18	6,71E-18	6,15E-18	5,64E-18	5,17E-18	4,74E-18	4,35E-18
-8,6	3,99E-18	3,65E-18	3,35E-18	3,07E-18	2,81E-18	2,57E-18	2,36E-18	2,16E-18	1,98E-18	1,81E-18
-8,7	1,66E-18	1,52E-18	1,39E-18	1,27E-18	1,17E-18	1,07E-18	9,76E-19	8,93E-19	8,17E-19	7,48E-19
-8,8	6,84E-19	6,26E-19	5,72E-19	5,23E-19	4,79E-19	4,38E-19	4,00E-19	3,66E-19	3,34E-19	3,06E-19
-8,9	2,79E-19	2,55E-19	2,33E-19	2,13E-19	1,95E-19	1,78E-19	1,62E-19	1,48E-19	1,35E-19	1,24E-19

APPENDIX B

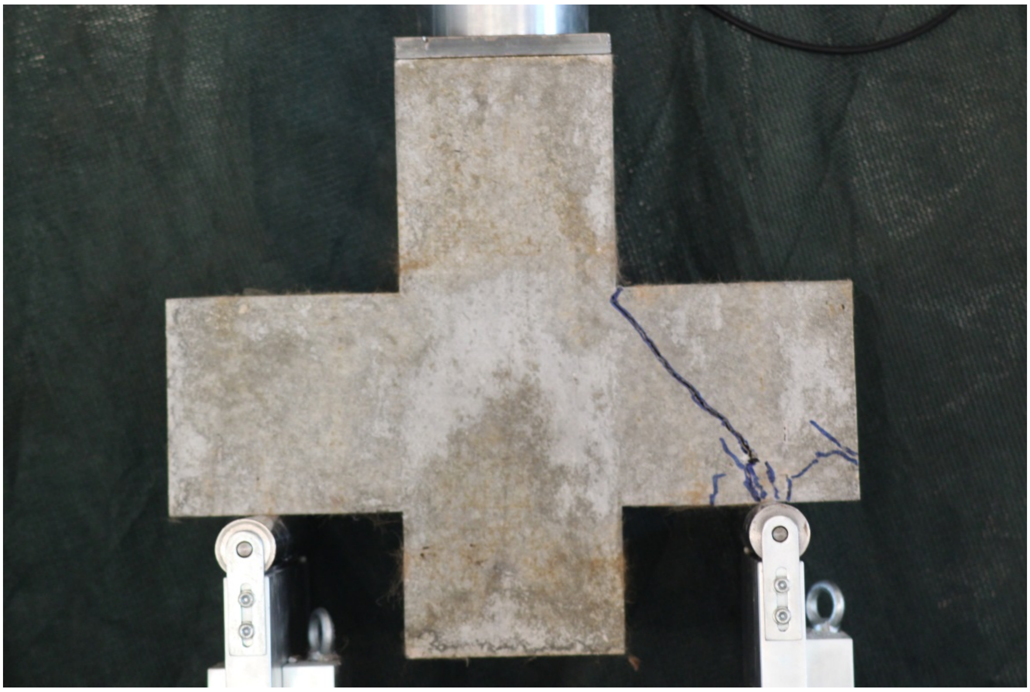

Figure B.1 Crack Pattern of 30-0-10-100 at Failure

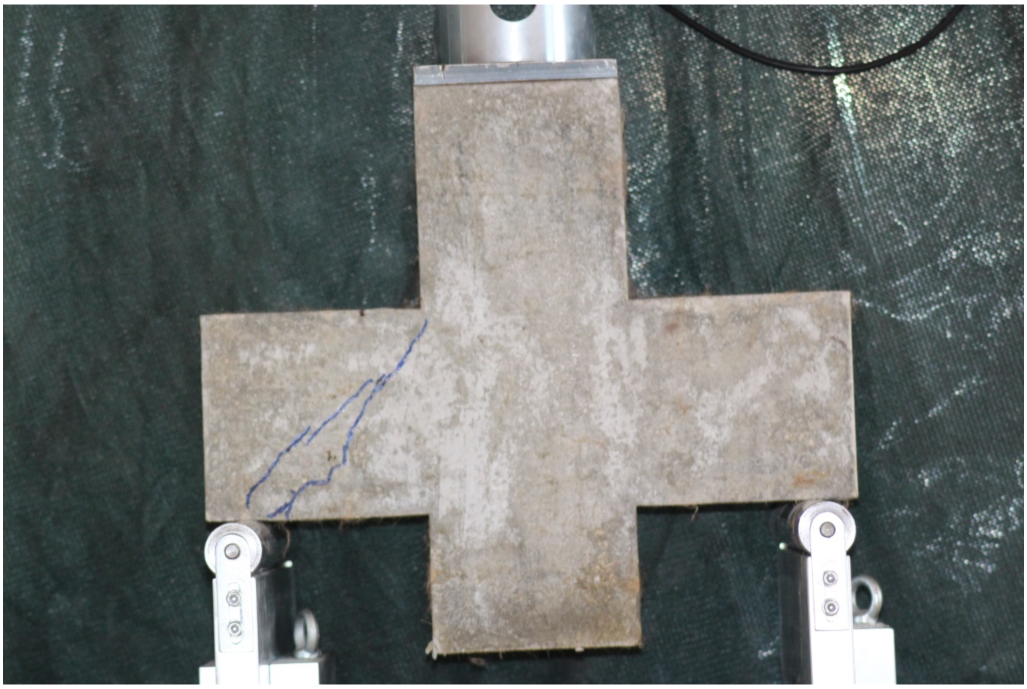

Figure B.2 Crack Pattern of 30-0-10-130 at Failure

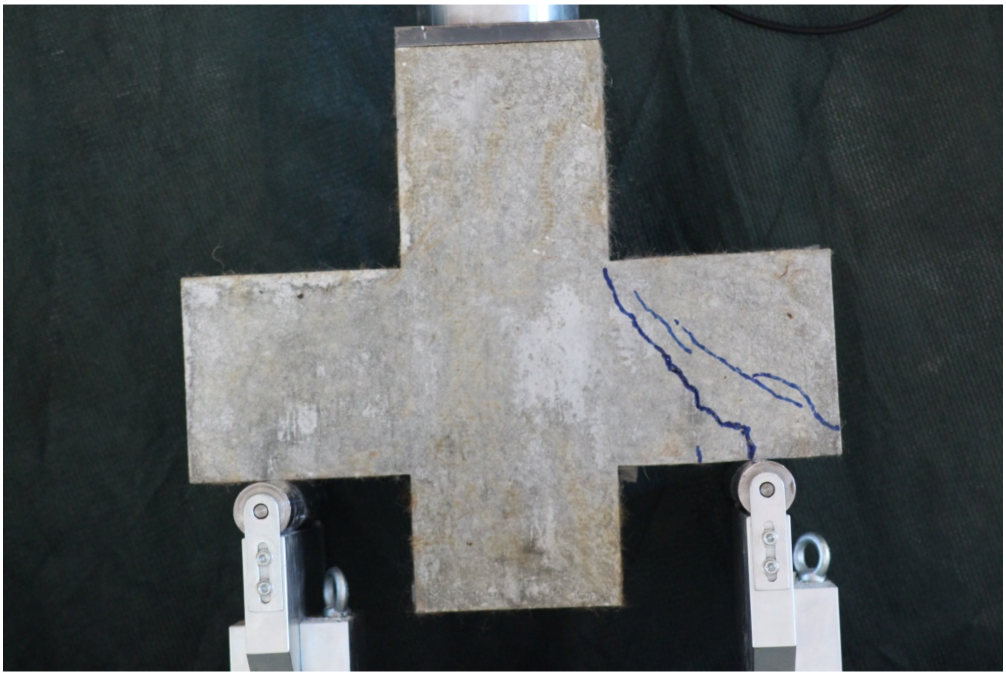
Figure B.3 Crack Pattern of 30-0-12-100 at Failure

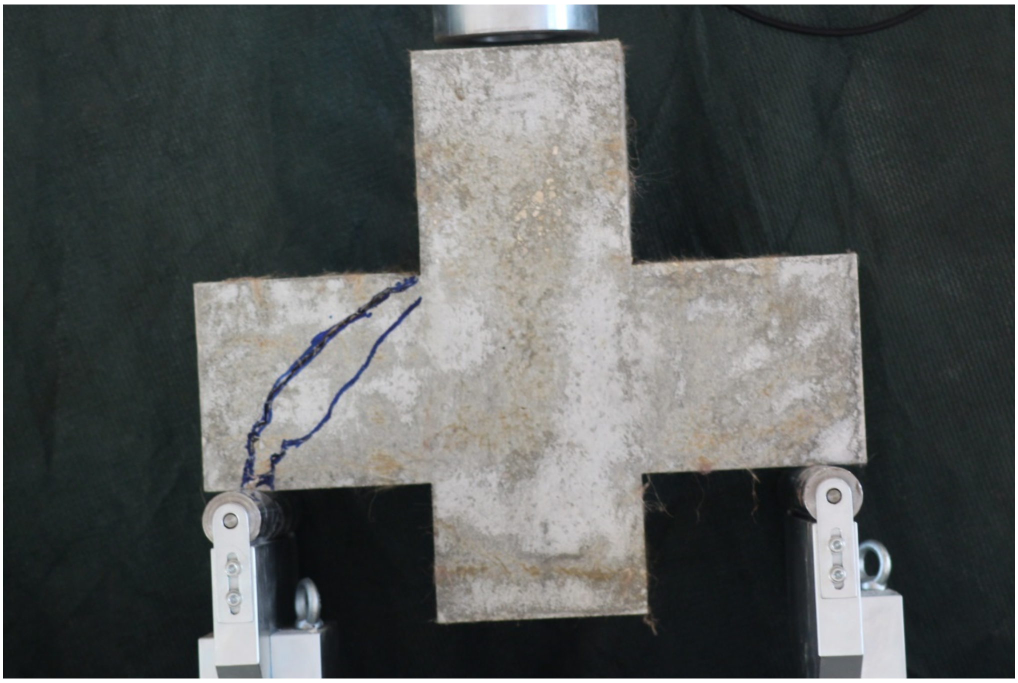
Figure B.4 Crack Pattern of 30-0-12-130 at Failure

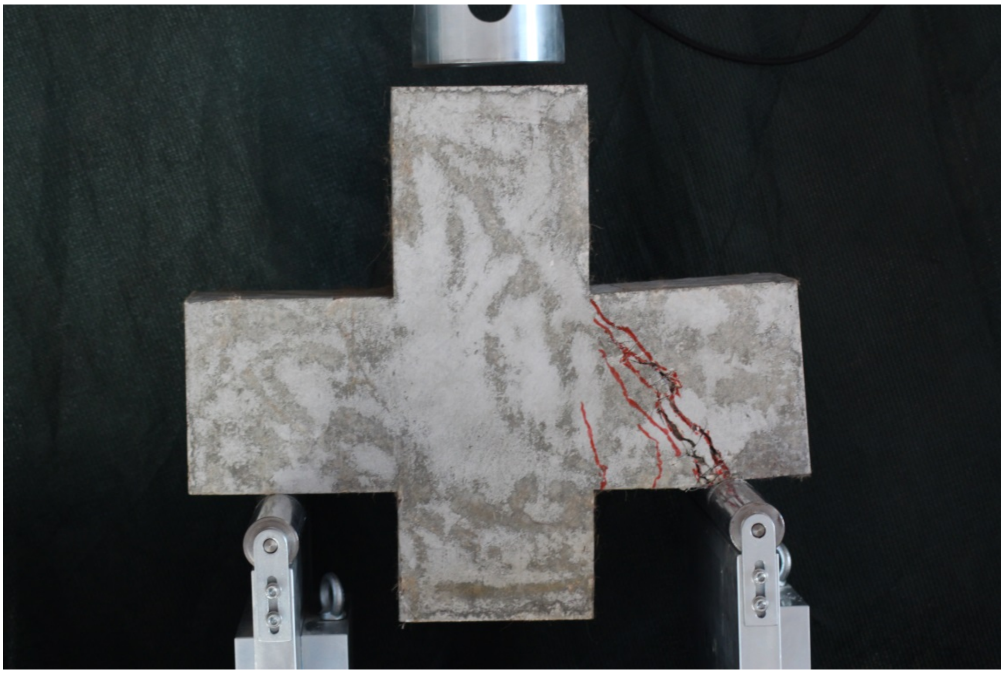

Figure B.5 Crack Pattern of 30-1-10-100 at Failure

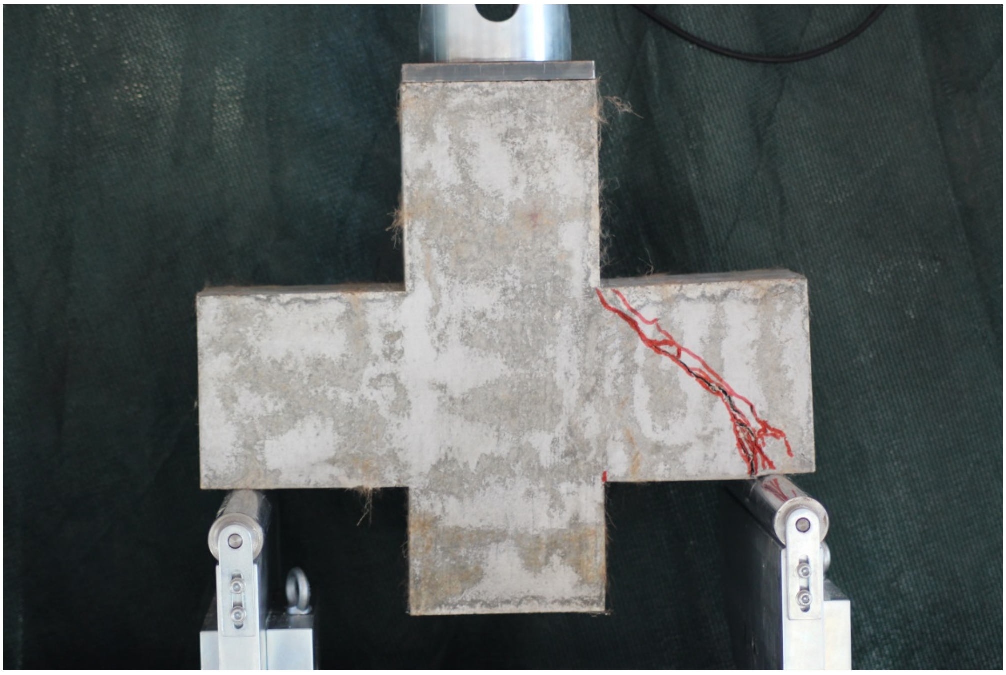

Figure B.6 Crack Pattern of 30-1-10-130 at Failure

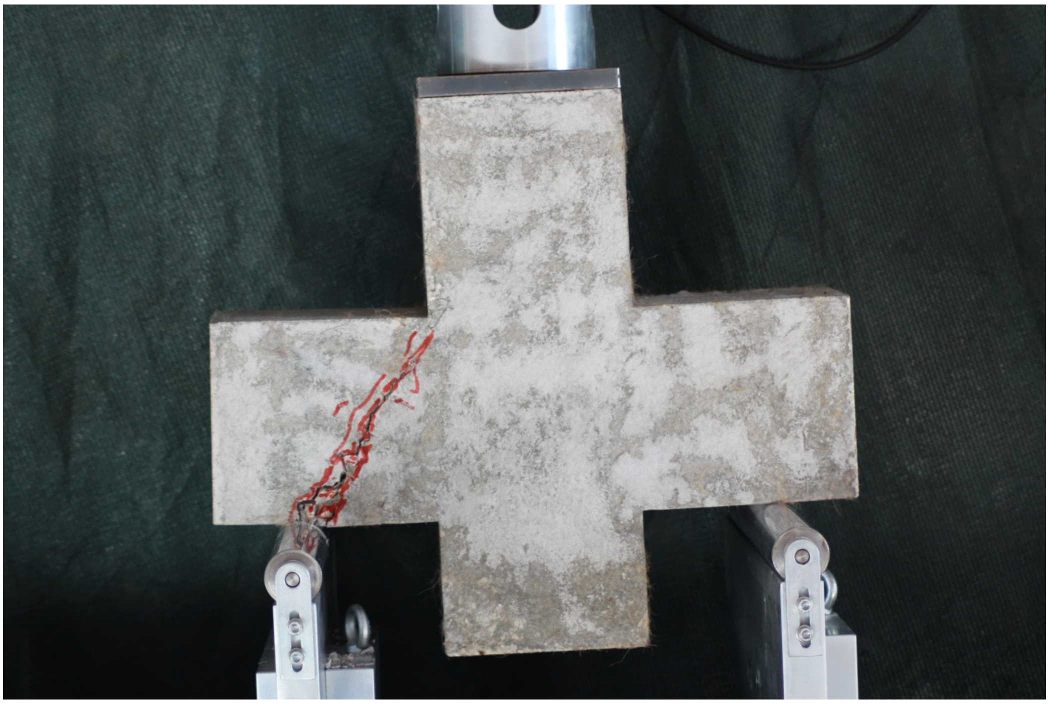

Figure B.7 Crack Pattern of 30-1-12-100 at Failure

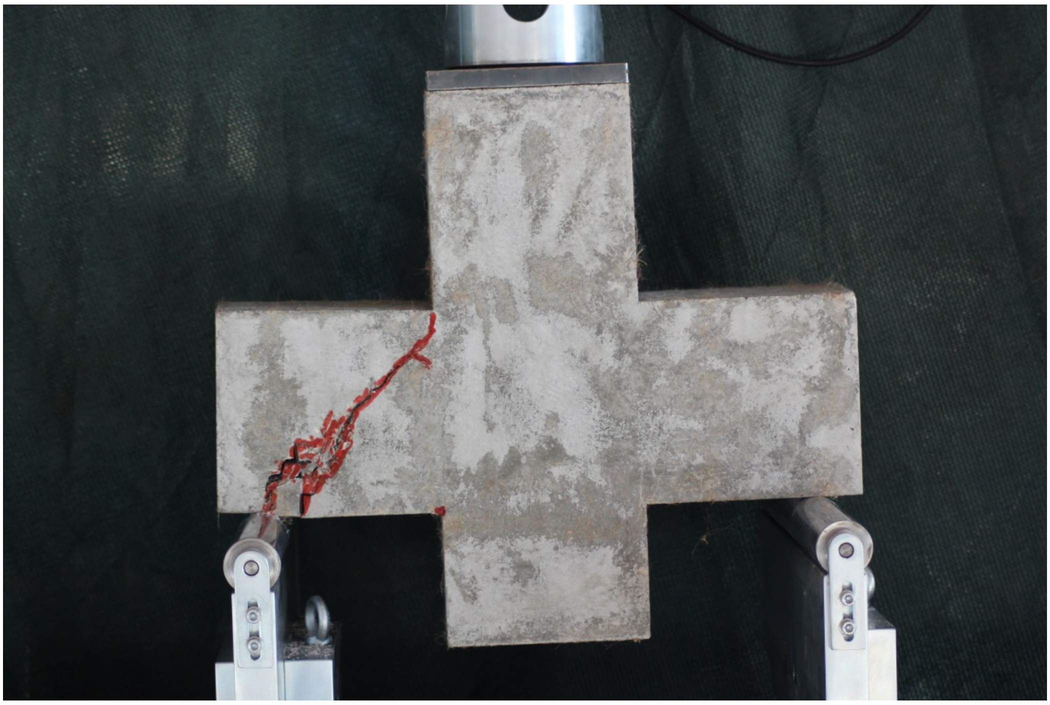

Figure B.8 Crack Pattern of 30-1-12-130 at Failure

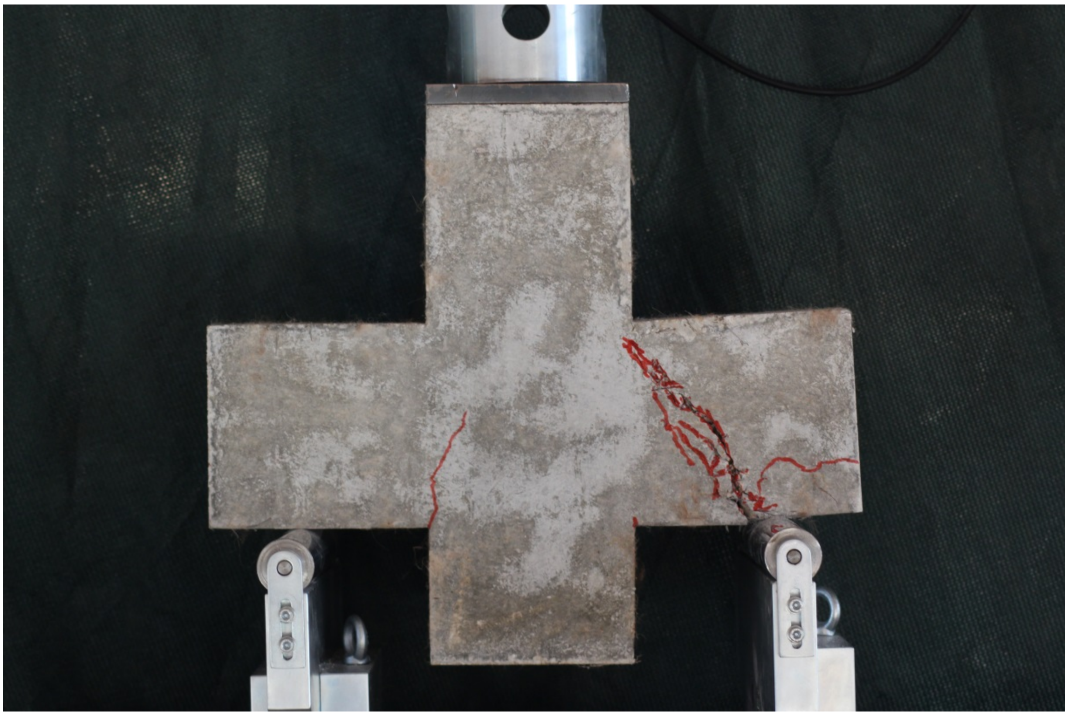

Figure B.9 Crack Pattern of 30-1.5-10-100 at Failure

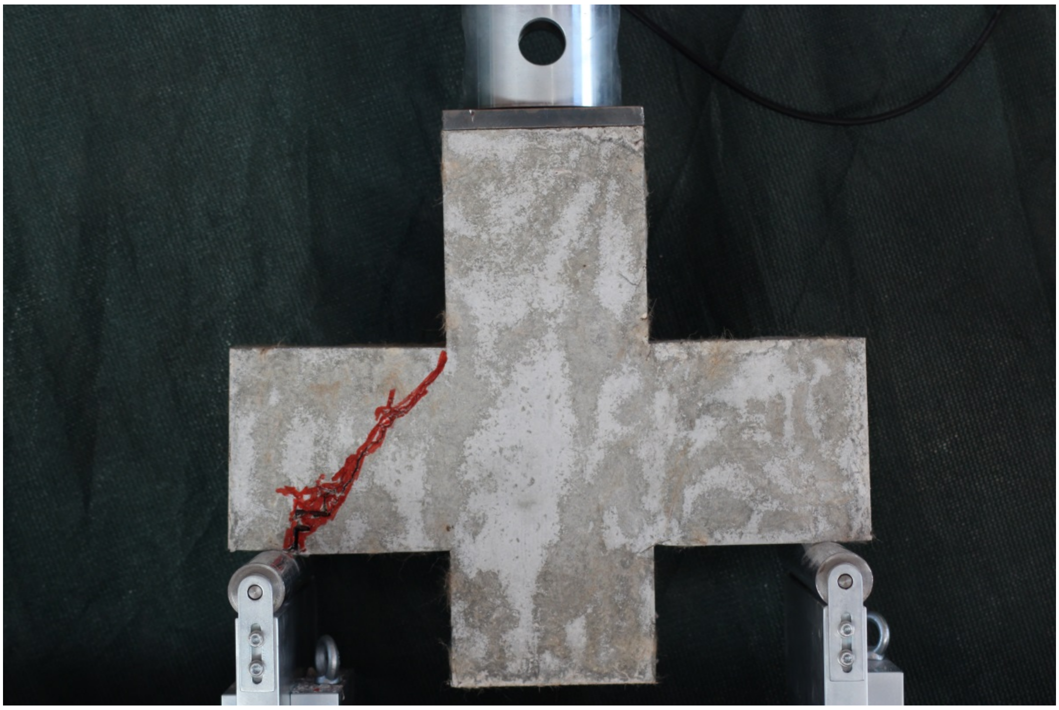

Figure B.10 Crack Pattern of 30-1.5-10-130 at Failure

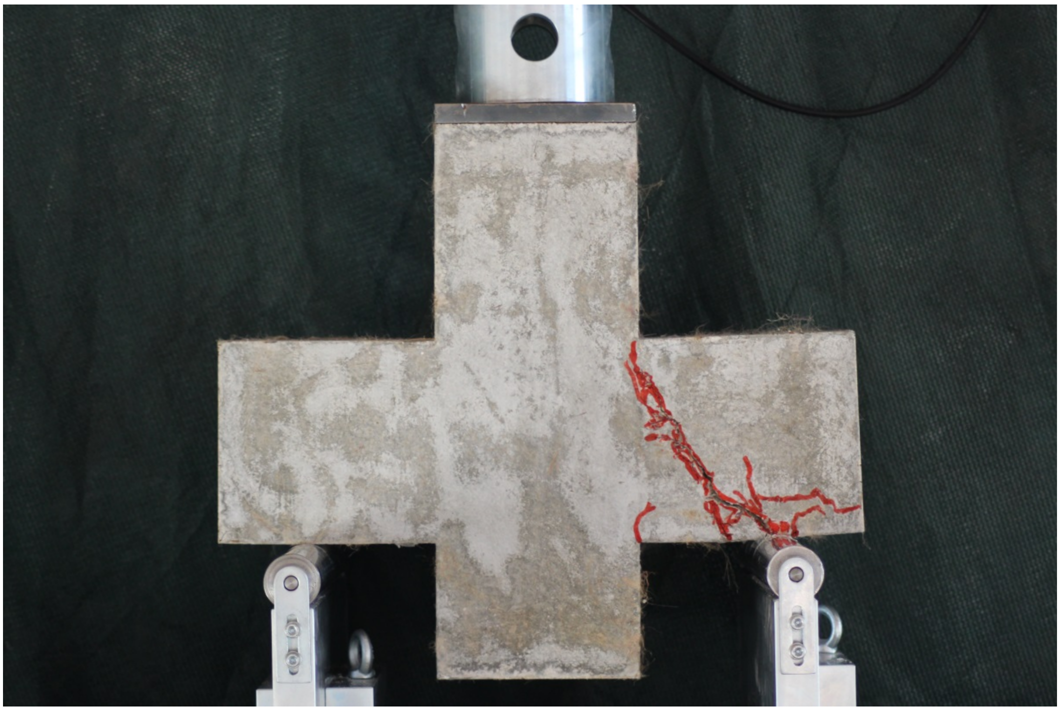

Figure B.11 Crack Pattern of 30-1.5-12-100 at Failure

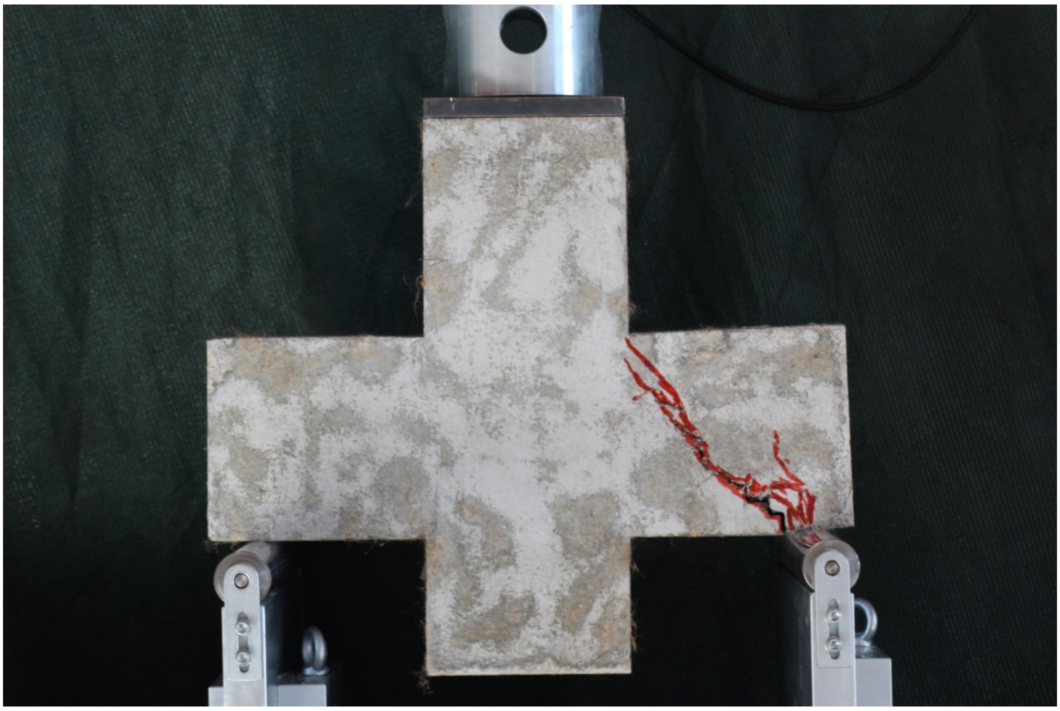

Figure B.12 Crack Pattern of 30-1.5-12-130 at Failure

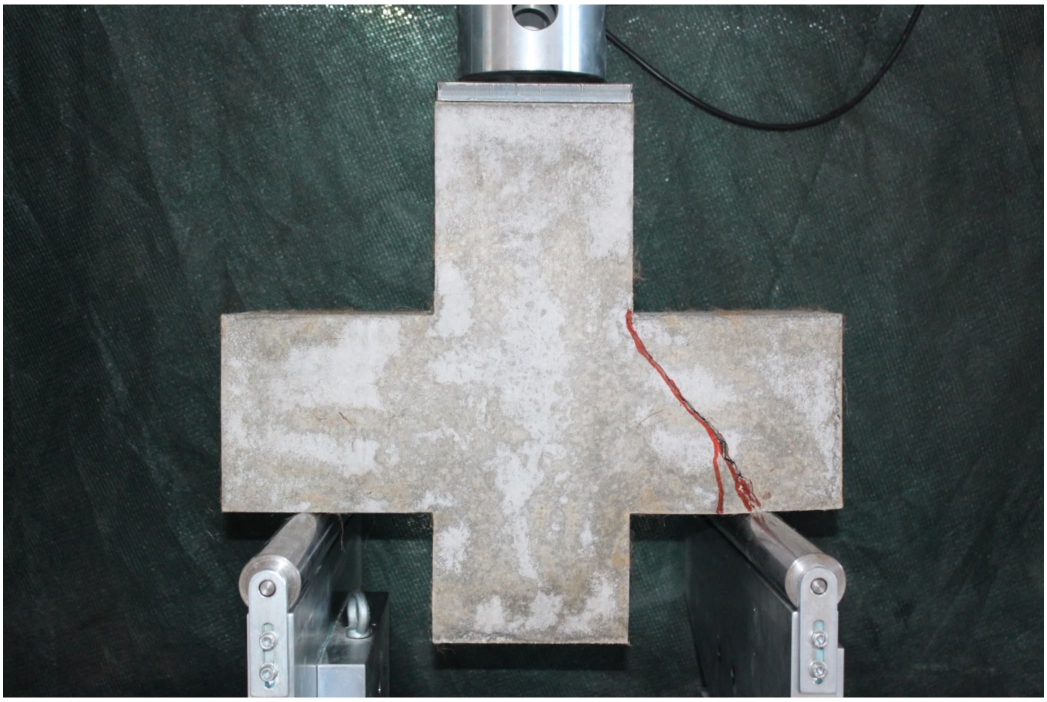

Figure B.13 Crack Pattern of 50-0-10-100 at Failure

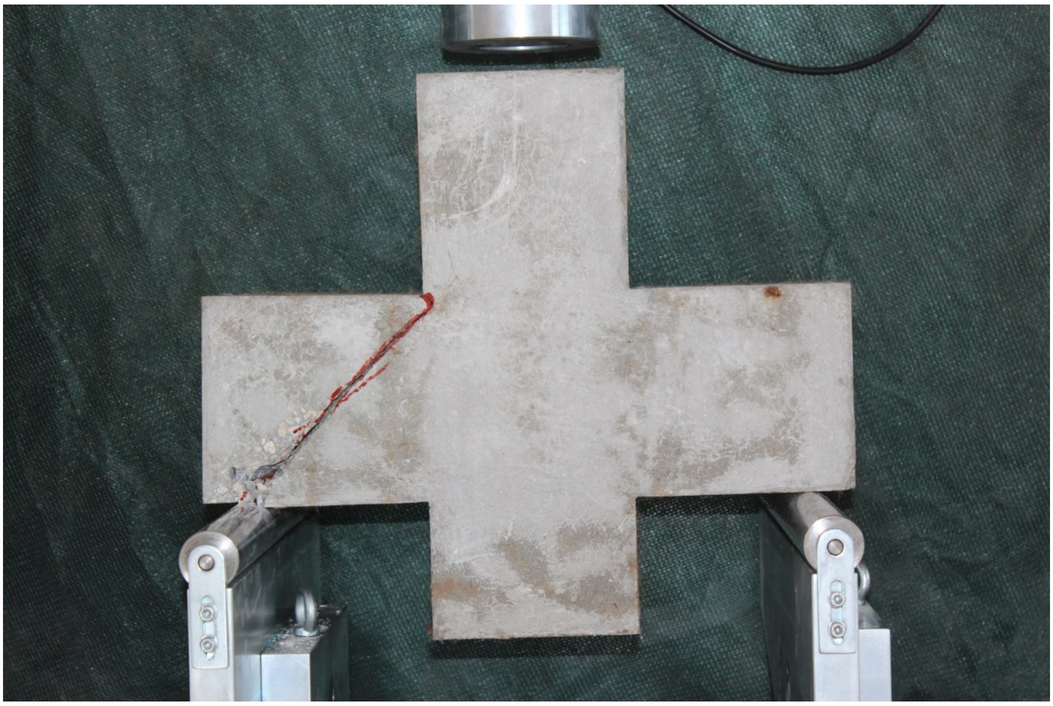

Figure B.14 Crack Pattern of 50-0-10-130 at Failure

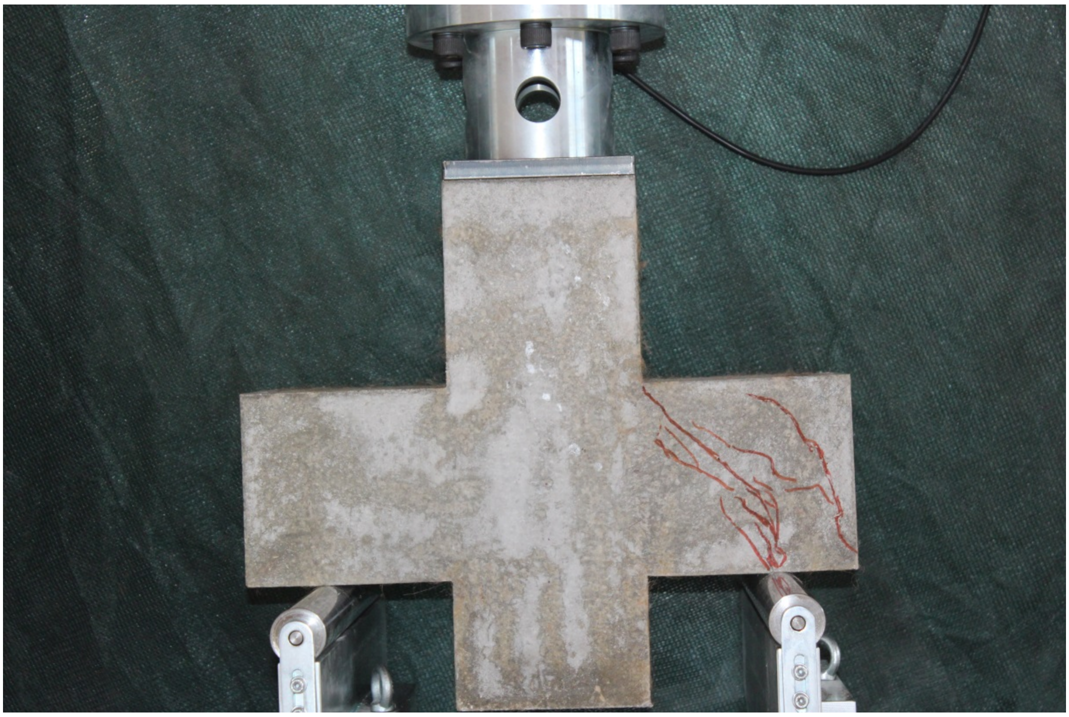
Figure B.15 Crack Pattern of 50-0-12-100 at Failure

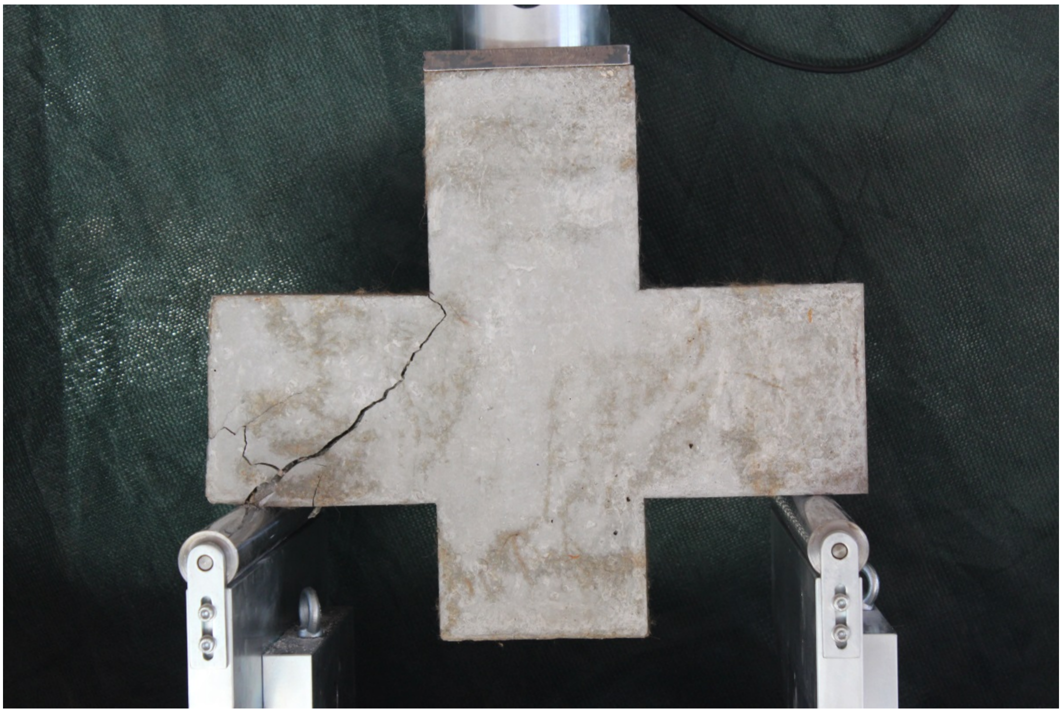
Figure B.16 Crack Pattern of 50-0-12-130 at Failure

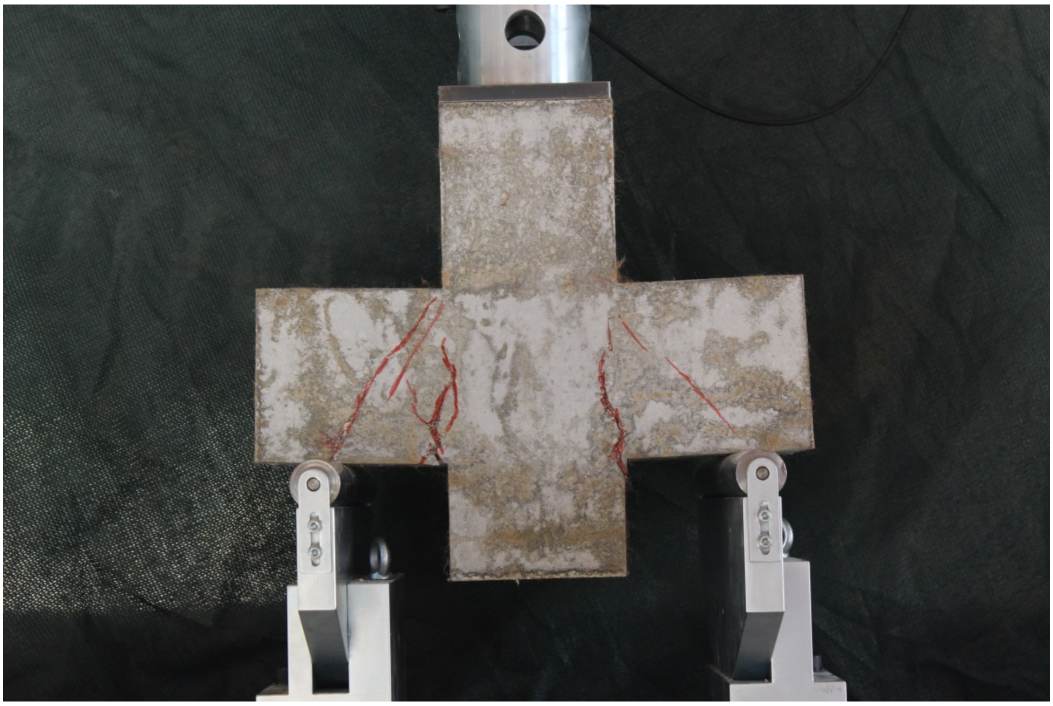

Figure B.17 Crack Pattern of 50-1-10-100 at Failure

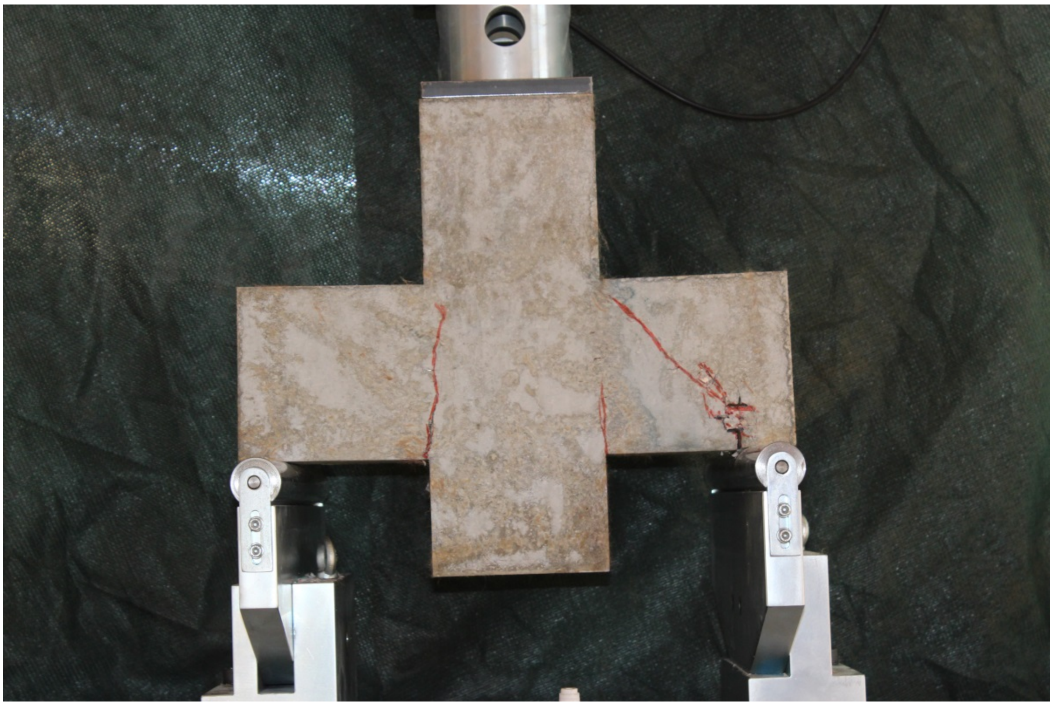

Figure B.18 Crack Pattern of 50-1-10-130 at Failure

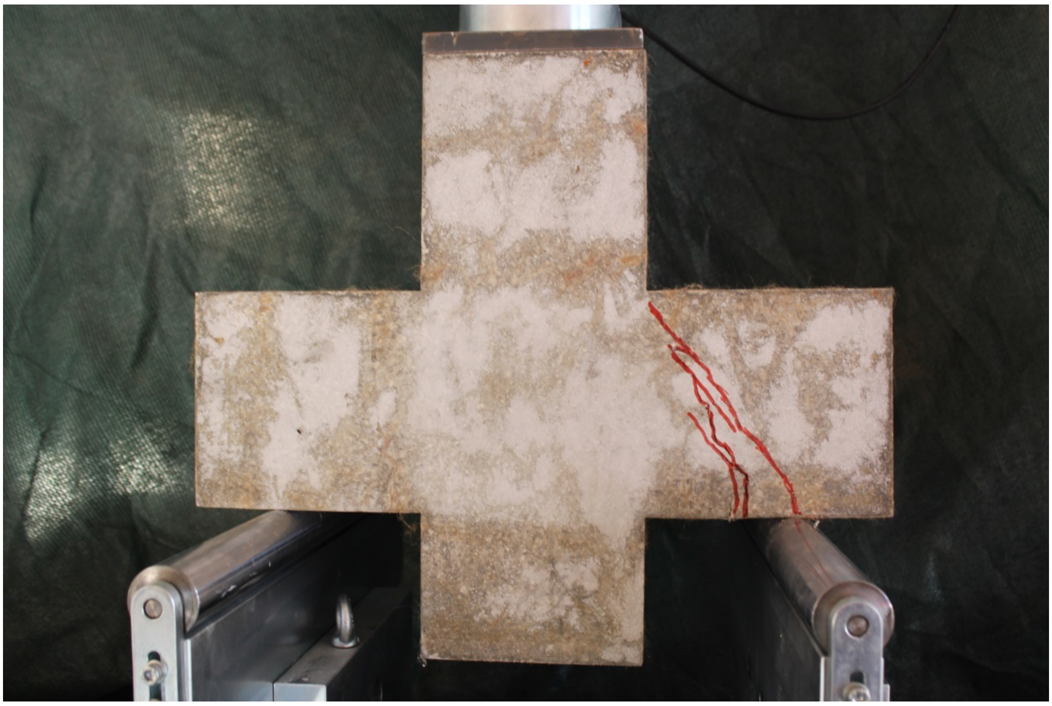
Figure B.19 Crack Pattern of 50-1-12-100 at Failure


Figure B.20 Crack Pattern of 50-1-12-130 at Failure

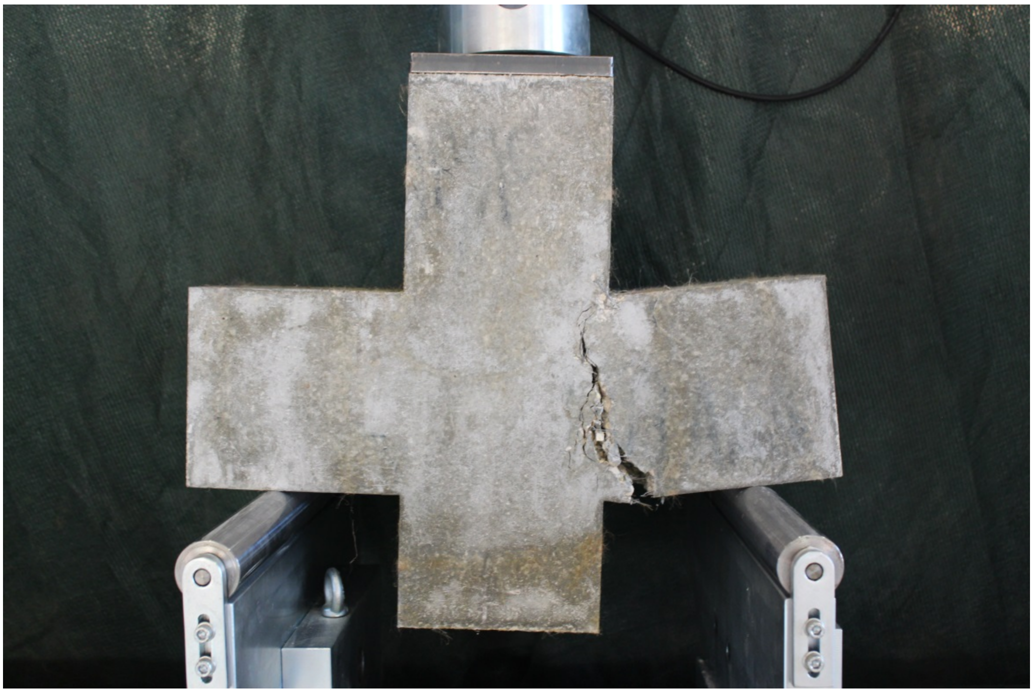

Figure B.21 Crack Pattern of 50-1.5-10-100 at Failure

Figure B.22 Crack Pattern of 50-1.5-10-130 at Failure

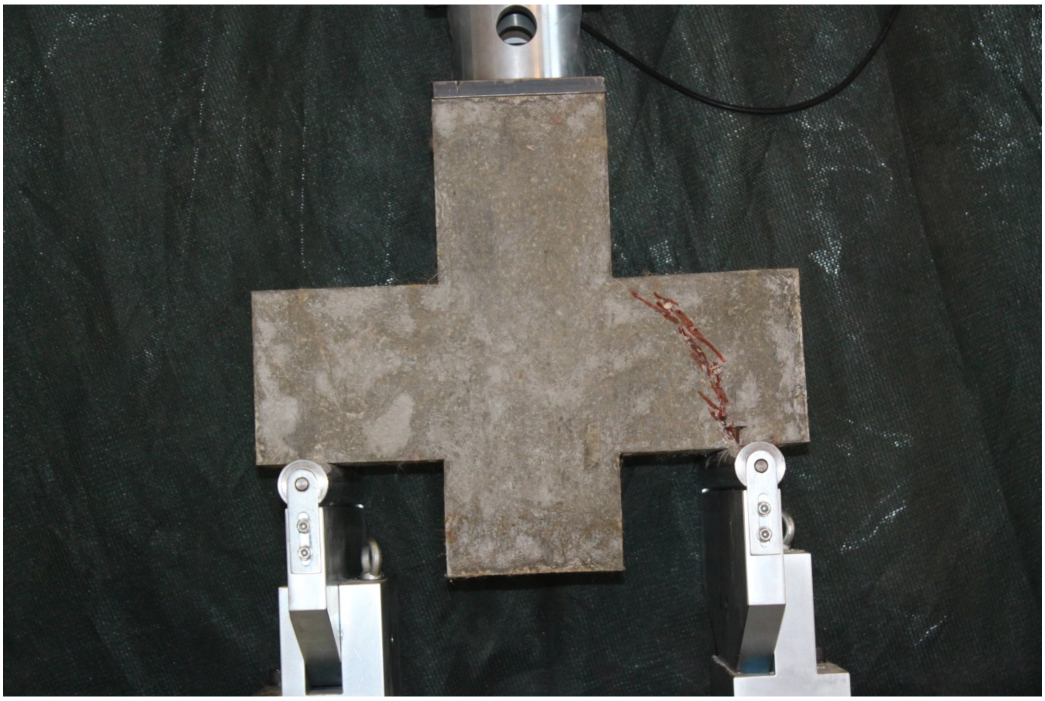

Figure B.23 Crack Pattern of 50-1.5-12-100 at Failure

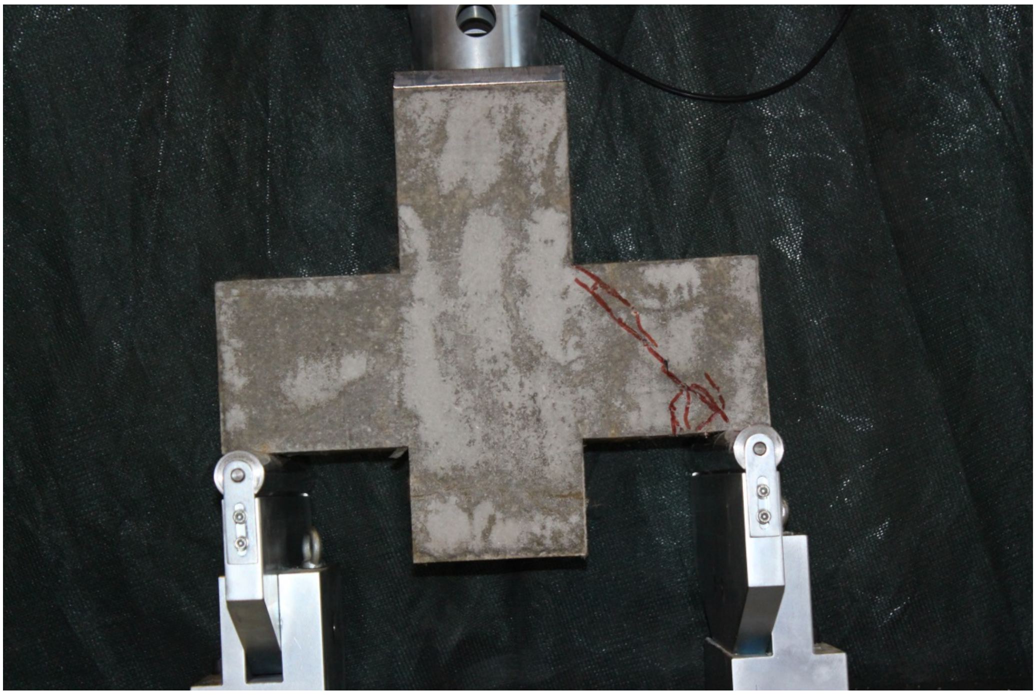

Figure B.24 Crack Pattern of 50-1.5-12-130 at Failure

CURRICULUM VITAE

PERSONAL INFORMATION

Name and Surname: Mehmet Eren GÜLŞAN

Nationality: Republic of Turkey

Place and Date of Birth: Gaziantep – 01.07.1986

Marital Status: Single

GSM: 0536 213 11 33

E-mail: gulsan@gantep.edu.tr

EDUCATIONAL INFORMATION

B.Sc.	Mechanical Engineering (DMP)-Gaziantep University	2010
B.Sc.	Civil Engineering-Gaziantep University	2009
High School	Fitnat Nuri Tekerekoğlu Anatolian High School	2004

WORK EXPERIENCE

	Duty - Place
2010 (February)-2010 (June)	Mechanical Eng.- Şahinbey Municipality
2010-2012	Res. Assist. Hasan Kalyoncu Unıversity-Civil Eng.
2012-Continue	Res. Assist. Gaziantep University-Civil Eng.

PUBLICATIONS

Papers published in international refereed journals (SCI)

Tapkın, S., Cevik, A., Usar, U., Gulsan, M. E. (2013) Rutting prediction of asphalt mixtures modified by polypropylene fibers via repeated creep testing by utilising genetic programming. *Materials Research*. **16(2)**, 277-292

Cevik, A., Kurtoglu, A. E., Bilgehan, M., Gulsan, M. E., Albegmprli, H. M. (2014). Support vector machines in Structural Engineering: A review. *Journal of Civil Engineering and Management*. **21(3)**, 261-281.

Gulsan, M. E., Cevik, A., Kurtoglu, A.E. (2015). Stochastic finite element based reliability analysis of steel fiber reinforced concrete (SFRC) Corbels. *Computers and Concrete*. **15(2)**, 279-304.

Albegmprli, H. M, Cevik, A., Gulsan, M. E., Kurtoglu, A.E. (2015). Reliability analysis of reinforced concrete haunched beams shear capacity based on stochastic nonlinear FE analysis. *Computers and Concrete*. **15(2)**, 259-277.

Proceedings published in international conferences

Cevik, A., Gulsan., M. E. (2013). Modelling ultimate load capacity of steel fibre reinforced concrete corbels: Part1. Formulation. *Fibre Concrete*, Cezech Republic, Prague.

Gulsan, M. E. (2013). Modelling ultimate load capacity of steel fibre reinforced concrete corbels: Part 2. Parametric study. *Fibre Reinforced Concrete*. Czech Republic, Prague.

LANGUAGE SKILL

YDS (English) : 88.75

SOCIAL ACTIVITIES

Basketball, Cinema, Detective Stories